



The University of
Nottingham

UNITED KINGDOM • CHINA • MALAYSIA



University of Nottingham
Netherlands Aerospace Centre

THEORY MANUAL

SACAMOS: State of the Art Cable Models for Spice
Open Source Cable Models for EMI Simulations

AUTHORS

Christopher Smartt¹, David Thomas¹, Steve Greedy¹,
Jaco Verpoorte², Jesper Lansink Rotgerink² and Harmen Schippers²

This document is subject to the GNU Free Documentation License (version 2.0).

| | |
|-------------------|--------------------------|
| CONTRACT: | ESA 40000112765/14/NL/HK |
| DATE: | July 5, 2018 |
| DOCUMENT VERSION: | 1.2 |

¹University of Nottingham, contact: Chris.Smartt@nottingham.ac.uk

²Netherlands Aerospace Centre, contact: Jaco.Verpoorte@nlr.nl

Contents

| | | |
|----------|--|-----------|
| 1 | Introduction | 4 |
| 1.1 | Overview | 4 |
| 2 | Multi-Conductor Transmission line theory | 6 |
| 2.1 | Multi-Conductor Transmission line equations | 6 |
| 2.2 | Per-Unit-Length Parameters | 9 |
| 2.2.1 | The per-unit-length inductance matrix | 9 |
| 2.2.2 | The per-unit-length capacitance matrix | 9 |
| 2.2.3 | The per-unit-length resistance matrix | 10 |
| 2.2.4 | The per-unit-length conductance matrix | 10 |
| 2.2.5 | Exact analytic formulae for per-unit-length parameters | 11 |
| 2.2.6 | Approximate analytic formulae for per-unit-length parameters | 12 |
| 2.3 | Solution to the Multi-Conductor Transmission line equations | 15 |
| 2.3.1 | Solution of the transmission line equations by modal decomposition | 15 |
| 2.3.2 | Incorporating terminal conditions | 18 |
| 2.3.3 | Time domain solution of the transmission line equations | 19 |
| 2.4 | Incident Field Excitation Model | 20 |
| 3 | The Spice Cable Model | 24 |
| 3.1 | Spice cable bundle model structure | 26 |
| 3.1.1 | Terminology | 28 |
| 3.2 | Domain decomposition | 29 |
| 3.3 | Twisted Pair Model | 33 |
| 3.3.1 | Per-unit-length parameters for the twisted pair model | 34 |
| 3.3.2 | Per-unit-length parameters for the shielded twisted pair model | 34 |
| 3.4 | Modal decomposition | 36 |
| 3.5 | Method of characteristics | 41 |
| 3.6 | Approximate model for frequency dependent transmission lines | 43 |
| 3.6.1 | Frequency dependent dielectric models | 43 |
| 3.6.2 | Frequency dependent finite conductivity loss models | 43 |
| 3.6.3 | Single mode propagation correction | 45 |
| 3.6.4 | Multi-mode propagation correction | 47 |
| 3.7 | Transfer Impedance Model | 51 |

| | | |
|----------|--|------------|
| 3.7.1 | Multiple mode propagation | 55 |
| 3.7.2 | Spice circuit for Transfer Impedance model | 57 |
| 3.8 | Spice Incident Field Excitation Model | 61 |
| 3.8.1 | Spice circuit for Incident field excitation | 68 |
| 3.8.2 | Incident field excitation with a ground plane | 69 |
| 3.9 | Spice Incident Field Excitation Model for shielded cables | 72 |
| 3.9.1 | Incident field excitation with a ground plane | 76 |
| 3.9.2 | Multiple mode propagation | 76 |
| 3.9.3 | Spice circuit for direct transfer impedance incident field coupling model | 77 |
| 4 | Numerical computation of the per-unit-length MTL parameters using a FEM solver | 80 |
| 4.1 | Solving the capacitance matrix based on energy | 82 |
| 4.2 | Procedure capacitance matrix computation based on energy analysis | 83 |
| 4.2.1 | FEM Solver for the Open Boundary Electrostatic Field Problem | 84 |
| 4.2.2 | Computing the conductance matrix | 86 |
| 4.2.3 | Iterative solution of the Finite Element matrix equations | 87 |
| 5 | Frequency dependent transfer functions | 90 |
| 5.1 | Introduction | 90 |
| 5.2 | Filter fitting process for s-domain transfer functions | 90 |
| 6 | Cable models available | 94 |
| 6.1 | Frequency Dependent Cylindrical conductor with dielectric | 95 |
| 6.2 | Frequency Dependent Coaxial cable with transfer impedance and shield surface impedance loss | 96 |
| 6.3 | Frequency Dependent Twinax cable with transfer impedance and shield surface impedance loss | 98 |
| 6.4 | Frequency Dependent Twisted pair cable | 99 |
| 6.5 | Frequency Dependent Shielded twisted pair with transfer impedance and shield surface impedance loss | 100 |
| 6.6 | Frequency dependent spacewire with transfer impedance - high frequency model including shield surface impedance loss | 101 |
| 6.7 | Frequency Dependent Overshield with transfer impedance and surface impedance loss | 103 |
| 6.8 | Flex cable | 104 |
| 6.9 | D connector | 105 |
| 7 | Network synthesis for specified frequency dependent transfer functions | 106 |
| 7.1 | Overview | 106 |
| 7.2 | One port impedance models for positive-real transfer functions | 107 |
| 7.2.1 | Algorithm for impedance synthesis | 110 |
| 7.2.2 | Identification of series impedance branches | 110 |
| 7.2.3 | Identification of admittance branches | 115 |
| 7.2.4 | Brune Synthesis | 121 |

7.3 Synthesis of non-positive real transfer functions 122
7.4 Application of the network synthesis in Spice cable bundle models . . . 124

Chapter 1

Introduction

1.1 Overview

This manual describes the theory which underlies the Spice cable bundle modelling software SACAMOS. The SACAMOS software generates a Spice subcircuit which models the propagation of signals on multi-conductor transmission lines i.e. cables and bundles of cables. The models include the effects of crosstalk, transfer impedance coupling and incident field excitation as required by the user. The frequency dependence of the transmission line parameters is taken into account in the model. The resulting models take the form of Spice sub-circuits which may be linked to arbitrary termination circuits. The use of the SACAMOS software and the resulting cable models is described in the accompanying user guide [1].

The document is structured as follows:

Chapter 2 describes the multiconductor transmission line equations which form the basis for the Spice cable bundle model. The chapter includes a discussion of the per-unit-length parameters which characterise a multi-conductor transmission line, the solution of the transmission line equations and the inclusion of termination conditions into the solution. The method for including the effect of a plane wave incident field illuminating a transmission line into the multi-conductor transmission line equations is also described.

Following this review of the theory of multi-conductor transmission lines, the Spice multi-conductor transmission line model is derived in chapter 3. The chapter provides an overview of the Spice model structure before describing the different aspects of the Spice cable bundle model; the domain decomposition approach to deal with shielded cables, the model for twisted pairs, the implementation of modal decomposition and the propagation model using method of characteristics (the technique used to incorporate the frequency dependent propagation model) and finally the transfer impedance coupling and incident field excitation models.

The ways in which the per-unit-length parameters of multi-conductor cables are calculated using a Finite Element method are described in chapter 4. The 'filter fitting' process which is used to create s-domain transfer functions for frequency dependent

aspects of the model is described in chapter 5. Following this the types of cable implemented in the software are described and the approximations made for each cable type are described in chapter 6. Finally the implementation of frequency dependent transfer functions using passive circuit elements through a network synthesis process is described.

Chapter 2

Multi-Conductor Transmission line theory

In this chapter we present the multi-conductor transmission line equations which underly the models which are used in the SACAMOS project. The fundamental approximations applied throughout this document are that the models produced will obtain quasi TEM propagation on cables and that the cables are uniform along their length [2]. The only non-uniformity along the length of the transmission lines that will be considered involves twisting of wire pairs.

2.1 Multi-Conductor Transmission line equations

The electrical state of a multi-conductor cable bundle is described by the voltage and current on each of the conductors. We assume that a multi-conductor cable bundle (including the ground plane) carries no common mode current, i.e. at any cross section of the cable normal to the propagation direction, z and at any time, t :

$$\sum_{n=1}^{n_{conductors}} I_n(z, t) = 0. \quad (2.1)$$

We note that this assumption does not preclude the use of the current distribution on the conductors in 3D space from being used to provide an estimate of radiation from a cable bundle. The currents induced by external fields may be common mode on the cables but differential with respect to ground. Finally it is assumed that there is no field interaction between the circuit subsystems (i.e. the interconnect can be broken down into separate elements).

The differential mode voltage, V , and current, I , on the conductors of a z directed multi-conductor cable bundle in the absence of sources may be described in the time

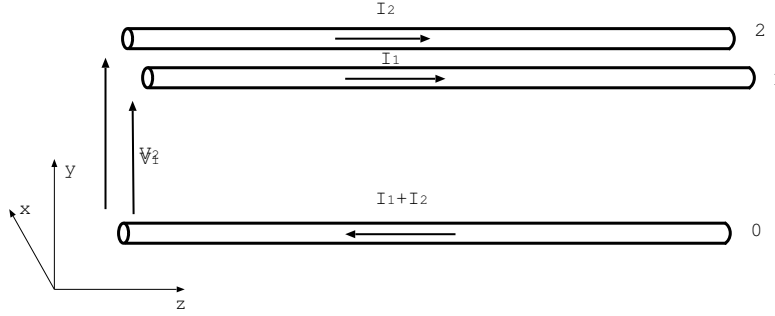


Figure 2.1 A multi-conductor cable showing the differential mode voltages and currents.

domain by the following equations:

$$\begin{aligned} \frac{\partial}{\partial z} (V(z, t)) &= -[R](I(z, t)) - [L] \frac{\partial}{\partial t} (I(z, t)) \\ \frac{\partial}{\partial z} (I(z, t)) &= -[G](V(z, t)) - [C] \frac{\partial}{\partial t} (V(z, t)). \end{aligned} \quad (2.2)$$

Here the cable bundle per-unit-length parameter matrices are inductance, $[L]$, capacitance, $[C]$, Resistance, $[R]$ and conductance, $[G]$. We have implicitly assumed for the purposes of this initial discussion that these matrices are constant. We note that this is not the case in practice and the cable properties are frequency dependent which implies a convolution process in the time domain. The discussion of the generalisation of this theory to more realistic situations will be described in subsequent sections of this document.

For an $n + 1$ conductor system the vectors and matrices are of dimension n where one of the conductors is chosen as a reference conductor. Typically the ground plane would be chosen as this reference. The voltage and current directions are shown in figure 2.1.

Values for these per-unit-length parameters can be obtained for some configurations by analytic expressions, such as for cylindrical conductors that are widely spaced (separation significantly larger than wire radius). In general these matrices can be obtained by numerical methods for the capacitance matrix, from which the other parameters can also be obtained. This involves the solution of the Laplace equation in the 2D cable cross section and can take account of dielectric materials including dielectric losses. This is described in chapter 4.

The frequency domain equations corresponding to equation (2.2) are expressed as:

$$\begin{aligned} \frac{d}{dz} (\tilde{V}(z)) &= -[R] (\tilde{I}(z)) - j\omega [L] (\tilde{I}(z)) \\ \frac{d}{dz} (\tilde{I}(z)) &= -[G] (\tilde{V}(z)) - j\omega [C] (\tilde{V}(z)). \end{aligned} \quad (2.3)$$

The resistance and inductance terms are conveniently combined into a single frequency dependent series impedance, similarly the capacitance and conductance terms

are combined into a single frequency dependent admittance term, this yields:

$$\begin{aligned}\frac{d}{dz} \left(\tilde{V}(z) \right) &= - \left[\tilde{Z} \right] \left(\tilde{I}(z) \right) \\ \frac{d}{dz} \left(\tilde{I}(z) \right) &= - \left[\tilde{Y} \right] \left(\tilde{V}(z) \right),\end{aligned}\tag{2.4}$$

where

$$\begin{aligned}\left[\tilde{Z} \right] &= [R] + j\omega [L] \\ \left[\tilde{Y} \right] &= [G] + j\omega [C].\end{aligned}\tag{2.5}$$

This matrix formulation of the multi-conductor transmission line equations in frequency domain will be used in the next chapters to solve for currents and voltages on each conductor. It is also used for generating the models with frequency dependent cable parameters.

2.2 Per-Unit-Length Parameters

The multi-conductor transmission line equations express the transmission line voltages and currents in terms of the inductance, capacitance, resistance and conductance matrices.

This chapter describes the per-unit-length parameters of the transmission lines and gives some formulae which may be used for their evaluation. A detailed discussion of the per-unit-length parameters may be found in [2]

2.2.1 The per-unit-length inductance matrix

The inductance matrix relates the total magnetic flux, Φ linking the i th circuit to the currents which produce it

$$\begin{pmatrix} \Phi_1 \\ \Phi_2 \\ \vdots \\ \Phi_n \end{pmatrix} = \begin{bmatrix} L_{1,1} & L_{1,2} & \dots & L_{1,n} \\ L_{2,1} & L_{2,2} & \dots & L_{2,n} \\ \vdots & \vdots & \ddots & \vdots \\ L_{n,1} & L_{n,2} & \dots & L_{n,n} \end{bmatrix} \begin{pmatrix} I_1 \\ I_2 \\ \vdots \\ I_n \end{pmatrix} \quad (2.6)$$

An element of the inductance matrix L_{ij} may be calculated by putting a current on conductor j and zero current on all other conductors then

$$L_{i,j} = \left. \frac{\Phi_i}{I_j} \right|_{I_{k \neq j} = 0} \quad (2.7)$$

2.2.2 The per-unit-length capacitance matrix

The capacitance matrix relates the charge, q , on conductors to the conductor voltages, V .

$$\begin{pmatrix} q_1 \\ q_2 \\ \vdots \\ q_n \end{pmatrix} = \begin{bmatrix} C_{1,1} & C_{1,2} & \dots & C_{1,n} \\ C_{2,1} & C_{2,2} & \dots & C_{2,n} \\ \vdots & \vdots & \ddots & \vdots \\ C_{n,1} & C_{n,2} & \dots & C_{n,n} \end{bmatrix} \begin{pmatrix} V_1 \\ V_2 \\ \vdots \\ V_n \end{pmatrix} \quad (2.8)$$

The capacitance matrix is commonly calculated from its inverse, the elements of the inverse capacitance matrix $[P] = [C]^{-1}$ are determined by placing a charge on conductor j and zero charge on all other conductors then

$$P_{i,j} = \left. \frac{V_i}{q_j} \right|_{I_{k \neq j} = 0} \quad (2.9)$$

then the capacitance matrix is found as

$$[C] = [P]^{-1} \quad (2.10)$$

In a homogeneous medium the capacitance matrix may be found from the inductance matrix using

$$[C] = \mu_0 \epsilon_0 \epsilon_r [L]^{-1} \quad (2.11)$$

2.2.3 The per-unit-length resistance matrix

The per-unit-length resistance matrix, $[R]$ incorporates the effects of conductor losses in the model i.e. the effects of the finite conductivity of the conductors. It relates the voltage drop along the transmission line to the currents on the conductors. The conductor resistance is a function of frequency due to the 'skin effect'. The calculation of the resistance of conductors, and the associated 'internal inductance' is discussed in section 3.6.2. The resistance matrix relates the conductor voltages and currents at zero frequency by

$$\frac{\partial}{\partial z} \begin{pmatrix} V_1 \\ V_2 \\ \vdots \\ V_n \end{pmatrix} = \begin{bmatrix} R_{1,1} & R_{1,2} & \dots & R_{1,n} \\ R_{2,1} & R_{2,2} & \dots & R_{2,n} \\ \vdots & \vdots & \ddots & \vdots \\ R_{n,1} & R_{n,2} & \dots & R_{n,n} \end{bmatrix} \begin{pmatrix} I_1 \\ I_2 \\ \vdots \\ I_n \end{pmatrix} \quad (2.12)$$

If a conductor i , $i = 1 \dots n$ has a resistance R_i and the reference conductor has resistance R_0 then the resistance matrix is given by

$$[R] = \begin{bmatrix} R_1 + R_0 & R_0 & \dots & R_0 \\ R_0 & R_2 + R_0 & \dots & R_0 \\ \vdots & \vdots & \ddots & \vdots \\ R_0 & R_0 & \dots & R_n + R_0 \end{bmatrix} \quad (2.13)$$

2.2.4 The per-unit-length conductance matrix

The per-unit-length conductance matrix, $[G]$ incorporates the effects of losses due to conductance of the medium in which the conductors are situated and also due to polarisation losses in dielectrics. The conductance loss will be assumed to be zero therefore the only contributions to the conductance matrix are due to lossy dielectrics. In this work the conductance matrix is calculated by generalising the capacitance matrix calculation to complex permittivities.

The admittance matrix is written as

$$[Y] = [G] + j\omega [C] = j\omega \left[C - \frac{j}{\omega} G \right] = j\omega [C'] \quad (2.14)$$

Thus if we determine the complex capacitance matrix $[[C']]$ then we can calculate the capacitance matrix and admittance matrices as

$$[C] = \Re \{ [C'] \} \quad (2.15)$$

and

$$[G] = -\omega \Im \{ [C'] \} \quad (2.16)$$

The calculation of the capacitance and conductance matrices for configurations with lossy inhomogeneous dielectrics is discussed in section 4.

2.2.5 Exact analytic formulae for per-unit-length parameters

Exact analytical formulae are available for the inductance and capacitance of some conductor configurations. There are also approximations which may be made which allow the derivation of approximate analytic formulae. Where possible these formulae are used in the SACAMOS software. The derivation of the formulae presented in the following sections may be found in [2].

Figure 2.2 shows a coaxial cable

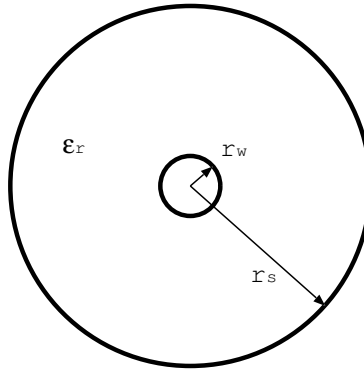


Figure 2.2 Coaxial cable

In SACAMOS, the inductance and capacitance of the coaxial cable is always calculated using the analytic formulae

$$L = \frac{\mu_0}{2\pi} \ln \left(\frac{r_s}{r_w} \right) \quad (2.17)$$

$$C = \frac{2\pi\epsilon_0\epsilon_r(j\omega)}{\ln \left(\frac{r_s}{r_w} \right)} \quad (2.18)$$

Figure 2.3 shows a two wire transmission line.

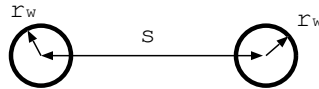


Figure 2.3 Two wire cable

The analytic formulae used to calculate the inductance and capacitance of the two wire transmission line are

$$C = \frac{\pi\epsilon_0}{\ln \left(\frac{s}{2r_w} + \sqrt{\frac{s^2}{4r_w^2} - 1} \right)} \quad (2.19)$$

$$L = \frac{\mu_0 \epsilon_0}{C} \quad (2.20)$$

These formulae are used for the calculation of the differential mode inductance and capacitance for twisted pairs.

2.2.6 Approximate analytic formulae for per-unit-length parameters

Approximate analytic formulae are available for multi-conductor configurations where the assumption made is that the conductor radii are small compared to the conductor separation. It is also assumed that the conductors are perfectly conducting and are situated in a homogeneous dielectric (free space here).

Figure 2.4 shows part of a multi-conductor configuration.

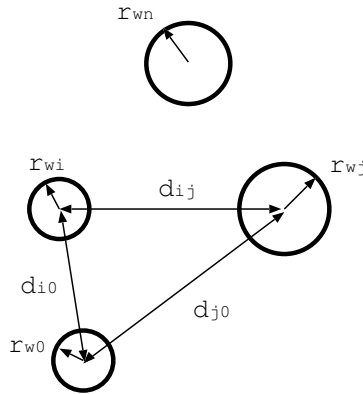


Figure 2.4 Multi-wire cable

The analytic formulae used to calculate the inductance and capacitance of the multi-wire transmission line are as follows:

For the diagonal elements of the inductance matrix

$$L_{ii} = \frac{\mu_0}{2\pi} \ln \left(\frac{d_{i0}^2}{r_{w0} r_{wi}} \right) \quad (2.21)$$

The off diagonal elements are given by

$$L_{ij} = \frac{\mu_0}{2\pi} \ln \left(\frac{d_{i0} d_{j0}}{d_{ij} r_{w0}} \right) \quad (2.22)$$

Since the conductors are in a homogeneous dielectric medium, the capacitance matrix is found from the inverse of the inductance matrix.

$$[C] = \mu_0 \epsilon_0 [L]^{-1} \quad (2.23)$$

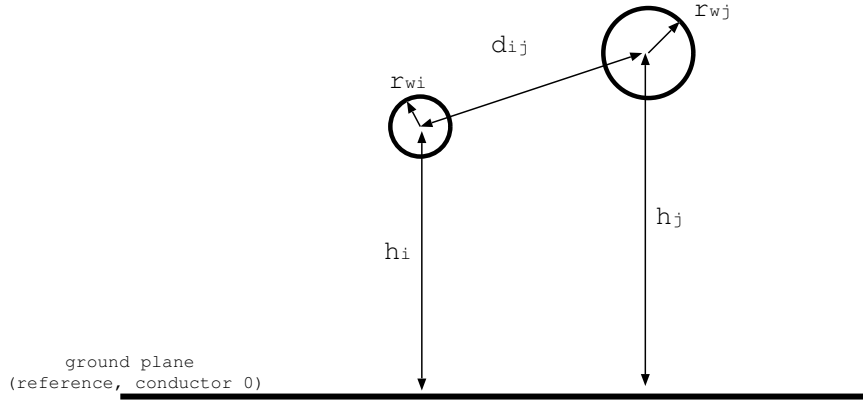


Figure 2.5 Multi-wire cable over a ground plane

Figure 2.5 shows part of a multi-conductor configuration above a ground plane. Here the ground plane is the reference conductor

For the diagonal elements of the inductance matrix

$$L_{ii} = \frac{\mu_0}{2\pi} \ln \left(\frac{2h_i}{r_{wi}} \right) \quad (2.24)$$

The off diagonal elements are given by

$$L_{ij} = \frac{\mu_0}{4\pi} \ln \left(1 + \frac{4h_i h_j}{d_{ij}^2} \right) \quad (2.25)$$

Since the conductors are in a homogeneous dielectric medium, the capacitance matrix may be found from the inverse of the inductance matrix.

$$[C] = \mu_0 \epsilon_0 [L]^{-1} \quad (2.26)$$

Figure 2.6 shows part of a multi-conductor configuration within a cylindrical shield. Here the shield is the reference conductor

For the diagonal elements of the inductance matrix

$$L_{ii} = \frac{\mu_0}{2\pi} \ln \left(\frac{r_s^2 - d_i^2}{r_s r_{wi}} \right) \quad (2.27)$$

The off diagonal elements are given by

$$L_{ij} = \frac{\mu_0}{2\pi} \ln \left(\frac{d_j}{r_s} \sqrt{\frac{(d_i^2 d_j^2 + r_s^4 - 2d_i d_j r_s^2 \cos(\theta_{ij}))}{d_i^2 d_j^2 + d_j^4 - 2d_i d_j^3 \cos(\theta_{ij})}} \right) \quad (2.28)$$

Since the conductors are in a homogeneous dielectric medium, the capacitance matrix is found from the inverse of the inductance matrix.

$$[C] = \mu_0 \epsilon_0 [L]^{-1} \quad (2.29)$$

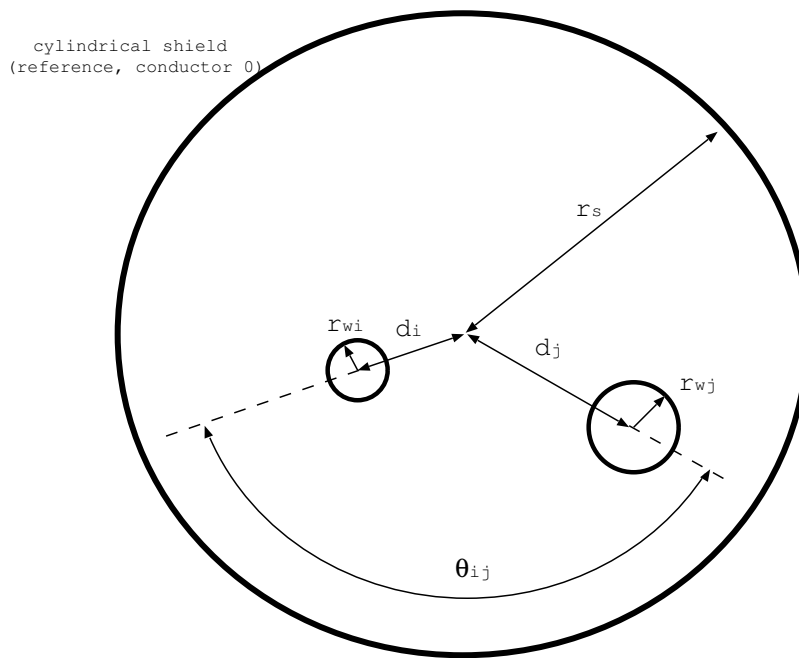


Figure 2.6 Multi-wire cable inside a cylindrical shield

2.3 Solution to the Multi-Conductor Transmission line equations

The SACAMOS software includes the ability to set up a validation test for the Spice transmission line models. In the validation test a resistive termination circuit with series voltage sources is specified and the solution for conductor voltages calculated with the Spice transmission line model can be compared with the solution obtained using the frequency domain analytic solution. The frequency domain analytic solution is calculated on the basis of the full dimension multi-conductor transmission line equations (i.e. no domain decomposition) and therefore includes the self consistent model of transfer impedance coupling. All the parameters in the analytic solution implemented are frequency dependent. The comparison between the Spice solution and the analytic solution therefore allows the effect of the approximations made in the derivation of the Spice model to be tested.

This section outlines the solution of the transmission line equations defined in section 2.1. A more complete discussion of the multi-conductor transmission line equations may be found in [2].

2.3.1 Solution of the transmission line equations by modal decomposition

The impedance and admittance matrices are given by:

$$\begin{aligned} [\tilde{Z}] &= [R] + j\omega [L] \\ [\tilde{Y}] &= [G] + j\omega [C]. \end{aligned} \quad (2.30)$$

We can derive a frequency domain solution to the transmission line equations using a modal analysis. Equation 2.4 can be re-written as an uncoupled second order equation in the following ways:

$$\begin{aligned} \frac{d^2}{dz^2} (\tilde{V}(z)) &= [\tilde{Z}] [\tilde{Y}] (\tilde{V}(z)) \\ \frac{d^2}{dz^2} (\tilde{I}(z)) &= [\tilde{Y}] [\tilde{Z}] (\tilde{I}(z)). \end{aligned} \quad (2.31)$$

A change of variables to modal quantities via a similarity transformation allows the decoupling (diagonalisation) of the matrix system. The conductor voltages and currents are related to their corresponding modal quantities by:

$$\begin{aligned} \tilde{V}(z) &= [\tilde{T}_V] (\tilde{V}_m(z)) \\ \tilde{I}(z) &= [\tilde{T}_I] (\tilde{I}_m(z)). \end{aligned} \quad (2.32)$$

The voltage modal transformation matrix, $[T_V]$ diagonalises the first equation given in (2.31):

$$\begin{aligned} \frac{d^2}{dz^2} \left(\tilde{V}_m(z) \right) &= \left[\tilde{T}_V \right]^{-1} \left[\tilde{Z} \right] \left[\tilde{Y} \right] \left[\tilde{T}_V \right] \left(\tilde{V}_m(z) \right) \\ &= \left[\gamma^2 \right] \left(\tilde{V}_m(z) \right), \end{aligned} \quad (2.33)$$

where $[\gamma^2]$ is a diagonal matrix with elements whose values are the squares of the mode propagation constants. The elements of the diagonal matrix $[\gamma^2]$ are found as the eigenvalues of the $[Z][Y]$ product and the columns of the matrix $[\tilde{T}_V]$ are the corresponding eigenvectors. (We note that when there are repeated eigenvalues which may originate from the symmetry of the cable cross section, then the diagonalisation is not unique. The eigenvectors corresponding to these eigenvalues are only required to span a certain subspace of the original matrix. In this situation the eigenvector solver for general complex matrices in Eispack ([12]) may on rare occasions return the same eigenvector for more than one eigenvalue. In order to avoid this in practice we perturb the matrix by a very small amount in a manner which prevents this degeneracy).

In the lossless case the impedance matrices and admittance matrices are imaginary and symmetric, and the $[Z][Y]$ product is real and symmetric. The modal transformation matrices are real and are independent of frequency and the diagonal $[\gamma^2]$ matrix has negative, real values of the form $-\frac{\omega^2}{v^2}$, where v is the mode velocity. Modal decomposition for a lossless transmission line will be important in the derivation of the Spice multi-conductor transmission line model derived in section 3.

The solution for the modal voltages at any point z on the multi-conductor transmission line may be written in terms of modes travelling in the $+z$ and $-z$ directions as:

$$\tilde{V}_m(z) = [e^{-\gamma z}] \left(\tilde{V}_m^+ \right) + [e^{+\gamma z}] \left(\tilde{V}_m^- \right). \quad (2.34)$$

The general solution for the actual conductor voltages is then:

$$\tilde{V}(z) = \left[\tilde{T}_V \right] \left([e^{-\gamma z}] \left(\tilde{V}_m^+ \right) + [e^{+\gamma z}] \left(\tilde{V}_m^- \right) \right). \quad (2.35)$$

Similarly, the current modal transformation matrix $[T_I]$ diagonalises the second equation in (2.31):

$$\begin{aligned} \frac{d^2}{dz^2} \left(\tilde{I}_m(z) \right) &= \left[\tilde{T}_I \right]^{-1} \left[\tilde{Y} \right] \left[\tilde{Z} \right] \left[\tilde{T}_I \right] \left(\tilde{I}_m(z) \right) \\ &= \left[\gamma^2 \right] \left(\tilde{I}_m(z) \right). \end{aligned} \quad (2.36)$$

It can be shown [2] that the voltage and current modal transformation matrices can be related by:

$$\left[\tilde{T}_I \right]^T = \left[\tilde{T}_V \right]^{-1}. \quad (2.37)$$

The solution for the modal currents at any point z on the multi-conductor transmission line may be written in terms of modes travelling in the $+z$ and $-z$ directions as:

$$\tilde{I}_m(z) = [e^{-\gamma z}] \left(\tilde{I}_m^+ \right) - [e^{+\gamma z}] \left(\tilde{I}_m^- \right). \quad (2.38)$$

The general solution for the actual conductor currents is then:

$$\tilde{I}(z) = [\tilde{T}_I] \left([e^{-\gamma z}] \left(\tilde{I}_m^+ \right) - [e^{+\gamma z}] \left(\tilde{I}_m^- \right) \right). \quad (2.39)$$

The conductor voltage vector may be written in terms of the modal current vectors as:

$$\tilde{V}(z) = [\tilde{Z}_C] [\tilde{T}_I] \left([e^{-\gamma z}] \left(\tilde{I}_m^+ \right) + [e^{+\gamma z}] \left(\tilde{I}_m^- \right) \right), \quad (2.40)$$

where $[Z_C]$ is the characteristic impedance matrix defined as:

$$[\tilde{Z}_C] = [\tilde{Y}]^{-1} [\tilde{T}_I] [\gamma] [\tilde{T}_I]^{-1} = [\tilde{Z}] [\tilde{T}_I] [\gamma]^{-1} [\tilde{T}_I]^{-1}. \quad (2.41)$$

2.3.2 Incorporating terminal conditions

The solution in terms of voltages and currents of the MTL equations are given by (2.39) and (2.40). These expressions allow computing the state, i.e. current and voltage, of each conductor at any point of the transmission line, after determining the constants \tilde{I}_m^+ and \tilde{I}_m^- . Therefore the terminal conditions have to be incorporated, which can be done via the generalised Thévenin equivalent:

$$\begin{aligned} [\tilde{V}(0)] &= [\tilde{V}_S] - [\tilde{Z}_S] (\tilde{I}(0)) \\ [\tilde{V}(L)] &= [\tilde{V}_L] + [\tilde{Z}_L] (\tilde{I}(L)), \end{aligned} \quad (2.42)$$

where $[\tilde{Z}_S]$ and $[\tilde{Z}_L]$ are the matrices with termination impedances on respectively the source and load side of the multi conductor transmission line, i.e. respectively at $z = 0$ and $z = L$. \tilde{V}_S and \tilde{V}_L are the vectors containing the voltage sources on respectively source and load side of the transmission line.

By evaluating equations (2.39) and (2.40) at $z = 0$ and $z = L$ and substituting this into the Thevenin equivalent given by equation 2.42, we obtain:

$$\begin{bmatrix} ([\tilde{Z}_C] + [\tilde{Z}_S]) [\tilde{T}_I] & ([\tilde{Z}_C] - [\tilde{Z}_S]) [\tilde{T}_I] \\ ([\tilde{Z}_C] - [\tilde{Z}_L]) [\tilde{T}_I] e^{-\gamma L} & ([\tilde{Z}_C] + [\tilde{Z}_L]) [\tilde{T}_I] e^{\gamma L} \end{bmatrix} \begin{pmatrix} \tilde{I}_m^+ \\ \tilde{I}_m^- \end{pmatrix} = \begin{pmatrix} \tilde{V}_S \\ \tilde{V}_L \end{pmatrix} \quad (2.43)$$

This matrix equation is readily solved for the current waves, \tilde{I}_m^+ and \tilde{I}_m^- and then equations (2.39) and (2.40) lead to a final solution for the conductor voltages and currents.

The detail of the solution as it is implemented in the SACAMOS software is described here. In order to keep the solution clear, these equations are rewritten as

$$\begin{bmatrix} [\tilde{M}_{11}] & [\tilde{M}_{12}] \\ [\tilde{M}_{21}] & [\tilde{M}_{22}] \end{bmatrix} \begin{pmatrix} \tilde{I}_m^+ \\ \tilde{I}_m^- \end{pmatrix} = \begin{pmatrix} \tilde{V}_S \\ \tilde{V}_L \end{pmatrix} \quad (2.44)$$

These equations are solved for \tilde{I}_m^+ and \tilde{I}_m^- first by eliminating \tilde{I}_m^- to give

$$\left[[\tilde{M}_{11}] - [\tilde{M}_{12}] [\tilde{M}_{22}]^{-1} [\tilde{M}_{21}] \right] (\tilde{I}_m^+) = (\tilde{V}_S) - [\tilde{M}_{12}] [\tilde{M}_{22}]^{-1} (\tilde{V}_L) \quad (2.45)$$

Thus

$$(\tilde{I}_m^+) = \left[[\tilde{M}_{11}] - [\tilde{M}_{12}] [\tilde{M}_{22}]^{-1} [\tilde{M}_{21}] \right]^{-1} \left((\tilde{V}_S) - [\tilde{M}_{12}] [\tilde{M}_{22}]^{-1} (\tilde{V}_L) \right) \quad (2.46)$$

\tilde{I}_m^- may then be found as

$$(\tilde{I}_m^-) = [\tilde{M}_{22}]^{-1} \left((\tilde{V}_L) \right) - [\tilde{M}_{21}] (\tilde{I}_m^+) \quad (2.47)$$

substituting these expressions in equations (2.39) and (2.40) leads to a final solution for the conductor voltages and currents along the entire length of the multi conductor transmission line.

2.3.3 Time domain solution of the transmission line equations

The frequency domain solution of the transmission line equations may be used as the basis for calculating the time domain solution by the Inverse Fourier Transform (IFT) method. If we assume that we have specified termination source voltages as a function of time $V_S(t)$ and $V_L(t)$ then we wish to calculate the time response of the conductor voltages $V(0, t)$, $V(L, t)$.

The solution proceeds by finding the Fourier Transform of the source voltage functions

$$\tilde{V}_S(j\omega) = \int_{-\text{inf}}^{\text{inf}} V_S(t) e^{j\omega t} dt \quad (2.48)$$

$$\tilde{V}_L(j\omega) = \int_{-\text{inf}}^{\text{inf}} V_L(t) e^{j\omega t} dt \quad (2.49)$$

The Frequency domain solution is then obtained for the transmission line current waves (equations 2.46, 2.47) and then the termination voltages and currents using equations 2.40 2.39.

The time domain solution for the transmission line voltages and currents may then be calculated by the inverse Fourier Transform

$$\tilde{V}(z, t) = \frac{1}{2\pi} \int_{-\text{inf}}^{\text{inf}} V(z, j\omega) e^{-j\omega t} d\omega \quad (2.50)$$

$$\tilde{I}(z, t) = \frac{1}{2\pi} \int_{-\text{inf}}^{\text{inf}} I(z, j\omega) e^{-j\omega t} d\omega \quad (2.51)$$

In practice we use the Fast Fourier Transform (FFT) algorithm to transform between the time and frequency domains [11]. The FFT algorithm assumes that the time response is discrete in time and periodic with period T i.e. we have a finite number of samples of the time response. These assumptions also make the frequency response periodic and discrete thus the analysis outlined above may be performed at a discrete set of frequencies. We assume that the time response may be adequately sampled at a sampling rate of δt and the period for the time response is chosen to be $T = n\delta t$ where n is conveniently chosen to be an integer power of 2. It is important that the period T is chosen to be long enough such that the time response of the transmission line has decayed to an insignificant level, otherwise the solution will be affected by aliasing i.e. the time response within a period T is corrupted by the response from adjacent periods.

2.4 Incident Field Excitation Model

An electromagnetic field illuminating a transmission line can couple energy onto the line and therefore be a cause of interference. The effect of an incident field excitation may be included in the transmission line equations by distributed forcing functions I_F and V_F in the transmission line equations as described in references [3], [2] thus the transmission line equations with incident field excitation are written as

$$\begin{aligned}\frac{\partial}{\partial z}(V(z,t)) &= -[R](I(z,t)) - [L]\frac{\partial}{\partial t}(I(z,t)) + V_F(z,t) \\ \frac{\partial}{\partial z}(I(z,t)) &= -[G](V(z,t)) - [C]\frac{\partial}{\partial t}(V(z,t)) + I_F(z,t).\end{aligned}\quad (2.52)$$

Assuming that the conductors are widely separated, the time domain forcing functions may be written in terms of the incident electric field as

$$V_F(z,t) = -\frac{\partial}{\partial z}E_T(z,t) + E_L(z,t) \quad (2.53)$$

where for the i -th conductor

$$E_L(z,t)_i = E_z^{inc}(i\text{th conductor}, z,t) - E_z^{inc}(\text{reference conductor}, z,t) \quad (2.54)$$

and

$$E_T(z,t)_i = \int_{ref}^{conductor\ i} E^{inc}(z,t) \cdot dl \quad (2.55)$$

and

$$I_F(z,t) = -[G](E_T(z,t)) - [C]\frac{\partial}{\partial t}(E_T(z,t)) \quad (2.56)$$

Reference [3] notes the following assumptions made in the derivation of this model for incident field excitation:

1. The propagation is transverse magnetic
2. The sum of the induced currents in any cross section, including the reference conductor is zero
3. $\frac{\partial E_z^s}{\partial z}$ is small compared with $\nabla_t \dot{E}_t$
4. The conductivity of the medium surrounding the conductors is homogeneous.

A solution may be obtained in the frequency domain by the use of chain parameter matrices [2] which relate the voltages and currents at one end of the transmission line to the voltages and currents at the other. In the absence of distributed forcing functions we can write

$$\begin{aligned}V(L) &= \Phi_{11}(L)V(0) + \Phi_{12}(L)I(0) \\ I(L) &= \Phi_{21}(L)V(0) + \Phi_{22}(L)I(0)\end{aligned}\quad (2.57)$$

where

$$\begin{aligned}
 \Phi_{11}(L) &= [Y]^{-1} [T] [\cosh(\gamma L)] [T]^{-1} [Y] \\
 \Phi_{12}(L) &= -[Y]^{-1} [T] [\gamma \sinh(\gamma L)] [T]^{-1} \\
 &= -[Z_C] [T] [\sinh(\gamma L)] [T]^{-1} \\
 \Phi_{21}(L) &= -[T] [\sinh(\gamma L) \gamma^{-1}] [T]^{-1} [Y] \\
 &= -[T] [\sinh(\gamma L)] [T]^{-1} [Y_C] \\
 \Phi_{22}(L) &= [T] [\cosh(\gamma L)] [T]^{-1}
 \end{aligned} \tag{2.58}$$

The distributed sources in equation 2.52 launch waves in the $\pm z$ directions. The cumulative effect of these waves may be calculated using the chain parameters for the transmission line and by this means, the effect of the incident field excitation on the transmission line may be included as lumped voltage and current sources at one end of the transmission line

$$\begin{aligned}
 V(L) &= \Phi_{11}(L) V(0) + \Phi_{12}(L) I(0) + V_{FT}(L) \\
 I(L) &= \Phi_{21}(L) V(0) + \Phi_{22}(L) I(0) + I_{FT}(L)
 \end{aligned} \tag{2.59}$$

where the incident field contribution appears as lumped voltage and current sources at the line termination $z = L$. These lumped source terms are given by the convolutions

$$\begin{aligned}
 V_{FT}(L) &= \int_0^L \Phi_{11}(L-z) V_F(z) + \Phi_{12}(L-z) I_F(z) dz \\
 I_{FT}(L) &= \int_0^L \Phi_{21}(L-z) V_F(z) + \Phi_{22}(L-z) I_F(z) dz
 \end{aligned} \tag{2.60}$$

The source and load may be represented using Thévenin equivalent termination conditions:

$$\begin{aligned}
 (\tilde{V}(0)) &= (\tilde{V}_S) - [\tilde{Z}_S] (\tilde{I}(0)) \\
 (\tilde{V}(L)) &= (\tilde{V}_L) + [\tilde{Z}_L] (\tilde{I}(L)),
 \end{aligned} \tag{2.61}$$

An equivalent circuit model of the incident field excitation is shown in figure 2.7 In the second part of the figure the incident field sources have been combined into the termination Thévenin equivalent circuit where

$$\begin{aligned}
 [\tilde{Z}'_L] &= [\tilde{Z}_L] \\
 (V'_S) &= (V_S) + [\tilde{Z}_L] (I_{FT}) - (V_{FT})
 \end{aligned} \tag{2.62}$$

Thus the solution may be found as for the unexcited transmission line for the termination voltages with one variation. The solution for the termination voltage in the lower

part of figure 2.7 includes V_{FT} so to determine the actual transmission line voltages we have

$$(V(L)) = (V'(L)) - (V_{FT}) \quad (2.63)$$

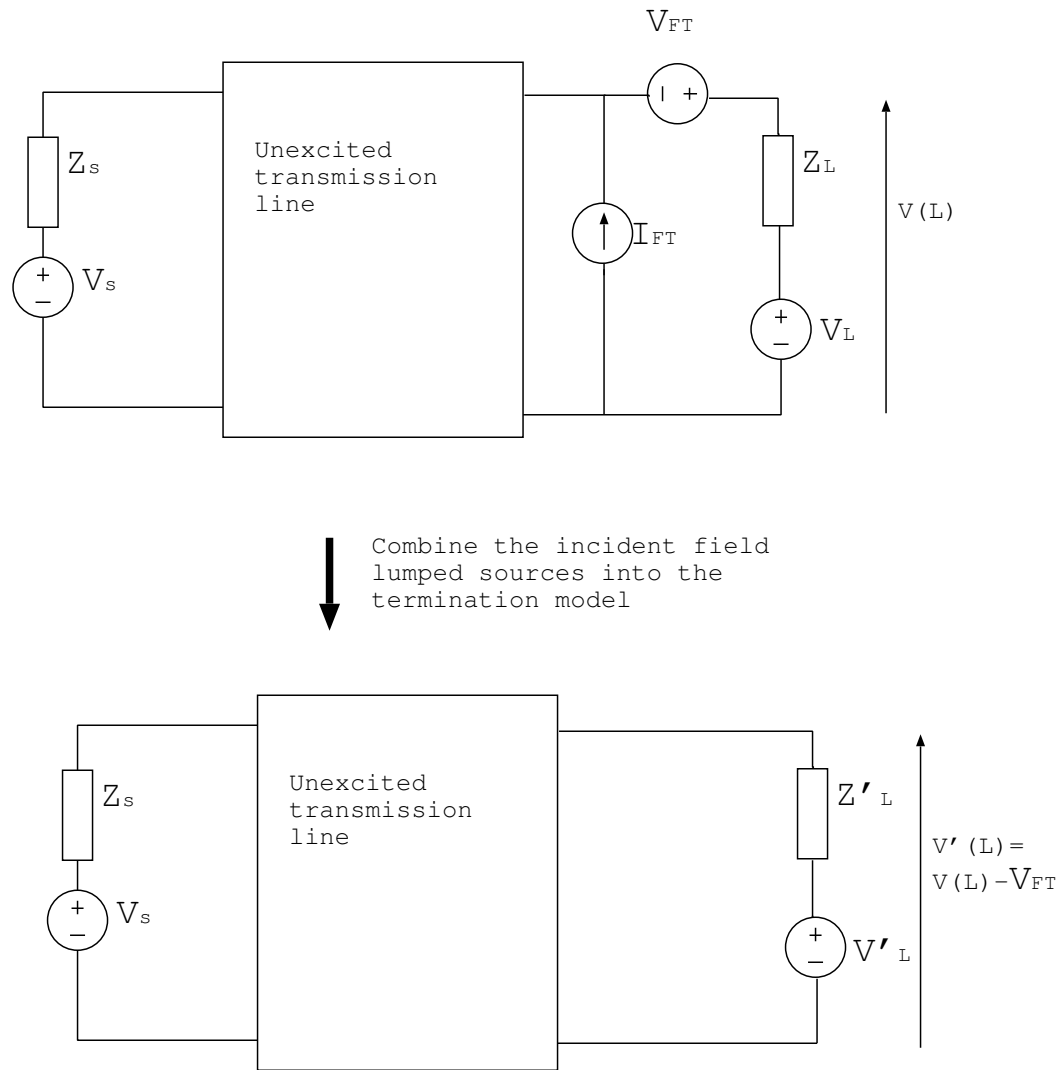


Figure 2.7 Equivalent circuit for the incident field excitation solution

Chapter 3

The Spice Cable Model

In this chapter we describe how the transmission line theory discussed in the previous chapter may be implemented using circuit elements and implemented as a Spice model.

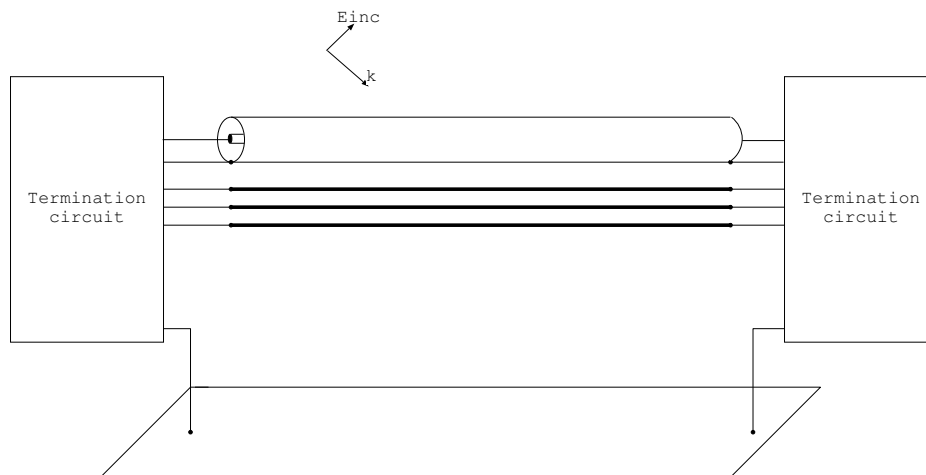


Figure 3.1 Multi-conductor cable modelling scenario with shielded conductors and incident field excitation

The scenario which we are aiming to model is illustrated in Figure 3.1. The termination circuits are arbitrary and to be specified by the user. The proposed Spice model being considered here concerns the transmission line only, though we note that connectors, ground plane bonding straps, pigtailed etc could be modelled as short lengths of transmission line cascaded with the main transmission line.

The model has been developed so as to include frequency dependent cable parameters arising from the finite conductivity of conductors, frequency dependent dielectrics and frequency dependent transfer impedance effects. This is a challenging requirement as in general the modal decomposition used in the analysis of the previous chapter

is a function of frequency. It is shown in section 3.6 that if the d.c. resistance of the conductors is lumped at the cable terminations then the modal decomposition becomes a weak function of frequency. Simulations show that the frequency dependence of the modal decomposition can be neglected and the decomposition based on lossless high frequency inductance and capacitance matrices can be used provided that the propagation of the individual modes is corrected for the propagation loss.

The spice model of the scenario depicted is based on a number of different parts these are:

- Domain decomposition: we model shielded conductor systems as separate domains, in which the electrical quantities are referenced the shielding conductor, plus the external domain consisting of the ground plane, unshielded conductors and the exterior surface of shields.
- Modal decomposition: Signal propagation on the multi-conductor system within each domain is analysed by a modal decomposition method i.e. we diagonalise the transmission line equations within each domain and propagate the modes on 'modal transmission lines'
- Method of characteristics. The propagation of each mode is treated using the method of characteristics [2] i.e. modes are propagated in the +z and -z directions and the state of the transmission line is the combination of these +z and -z propagating modes.
- Frequency dependent propagation characteristics are dealt with using an approximate model in which the d.c. resistance is extracted and lumped at the ends of each transmission line and the frequency dependence of the propagation is dealt with by applying a frequency dependent propagation correction to the +z and -z propagating modes at the ends of the transmission lines.
- Incident field excitation is assumed to be a plane wave, in this model appropriate controlled source terms lumped at the cable terminations take account of the incident field excitation.
- Coupling through imperfect shields is modelled with transfer impedance terms and implemented in a weak form i.e. source and victim conductors are identified and one way coupling is implemented using appropriate controlled source terms
- The twisted pair model is derived on the assumption that there is no coupling between the differential mode and the other conductors within the bundle (or the shield for a shielded twisted pair) although coupling to the common mode is included. This model does however allow coupling from the common mode to the differential mode and vice versa, through unbalanced terminations.

In the subsequent sections each of these stages is treated in turn and theoretical model derivations and associated circuit diagrams will be presented.

3.1 Spice cable bundle model structure

Figure 3.2 shows the structure of the spice cable bundle model with a termination network. The termination network is an arbitrary network to be constructed by the user and does not concern us here. The spice cable bundle model consists of a number of cascaded elements. The major elements are (in order from the model terminals inwards)

1. d.c. conductor resistance
2. Domain decomposition network
3. Modal decomposition network
4. Sources to include transfer impedance and incident field excitation
5. Method of characteristics delay lines
6. Transfer impedance delay lines
7. Incident field delay lines

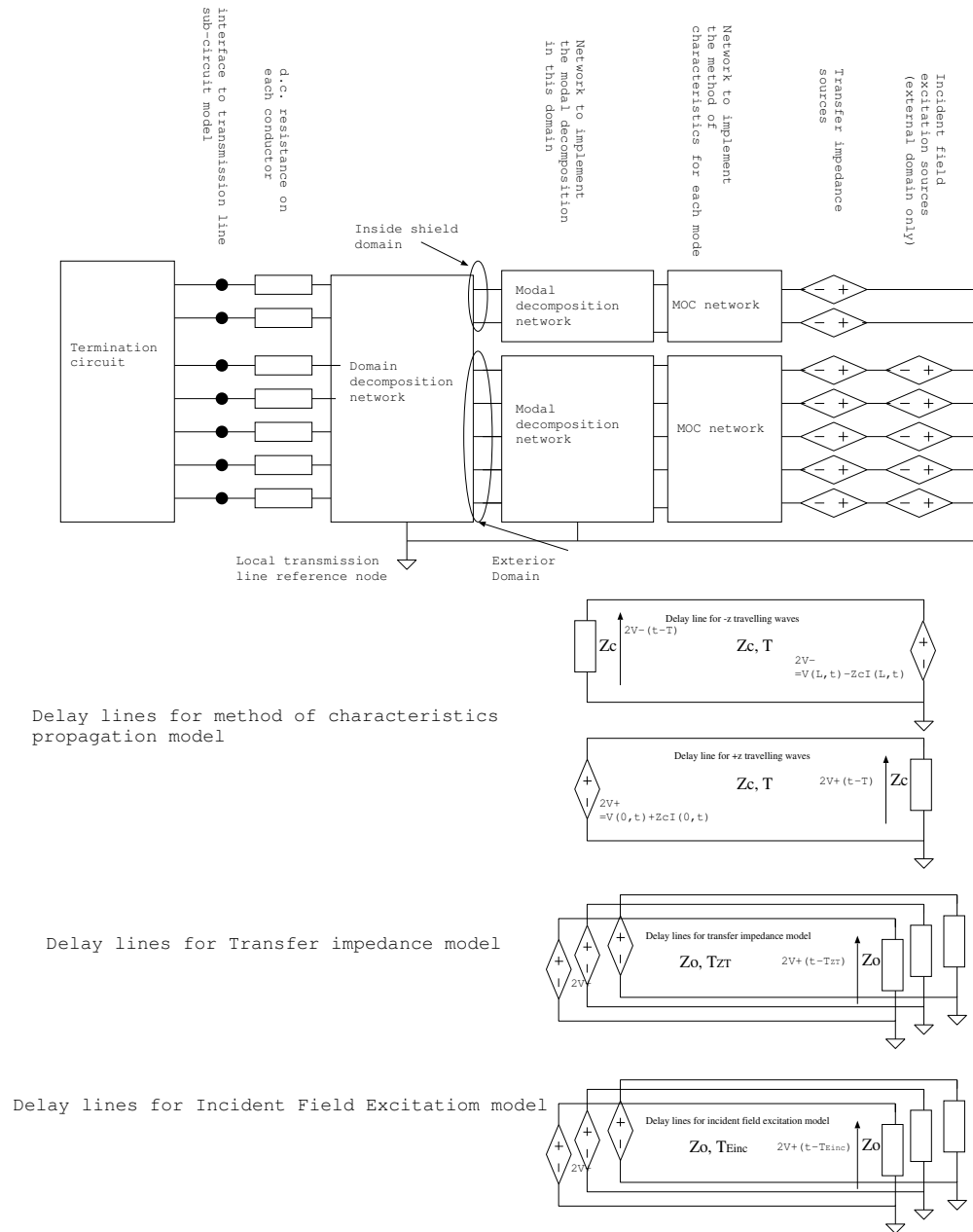


Figure 3.2 Structure of the spice cable bundle model

3.1.1 Terminology

In discussing the spice cable bundle model we require a clear terminology so as to allow unambiguous reference to particular sections of the model.

Cable numbering always relates to the numbering of the cables within a bundle and is specified by the order in which they are included in the cable_spec file.

Within a cable there is a local numbering system for cables and domains within a cable e.g for a coaxial cable the inner wire is local_conductor 1 and the shield is local conductor 2. Similarly the inner coaxial domain is domain 1 and the external domain is domain 2.

Once a cable bundle is built a global numbering is introduced.

We adopt the terminology in table 3.1 both in this document and in the software itself:

| Name | parameters | Description |
|---------------------------|---------------------------------|---|
| global terminal conductor | conductor number | The global conductor number in the cable bundle |
| global domain conductor | domain number, conductor number | The global conductor number in a particular domain |
| local cable conductor | cable number | The local conductor number in a particular cable. This is fixed for each cable type |
| global cable conductor | cable number, conductor number | The global conductor number in a particular cable |
| local cable domain | cable number | The local domain number in a particular cable. This is fixed for each cable type |
| global cable domain | cable number, conductor number | The global domain number in a particular cable |

Table 3.1 Spice cable bundle model terminology

3.2 Domain decomposition

The basis for computation of the systems being addressed in this work is the multi-conductor cable bundle. A bundle consists of multiple individual cables. These cables may consist of shielded and/ or un-shielded conductors perhaps with the addition of over-shielding and a ground plane (satellite panel).

The spice cable bundle model decomposes the transmission line system into domains. The domains consist of an external domain whose conductors are exposed to the external EM environment and internal domains in which conductors are shielded from the external environment. These domains are assumed to be only weakly coupled through transfer impedance terms.

The domain decomposition method along with the weak coupling assumption leads to a smaller system of coupled equations and has the advantage of removing one of the strong frequency dependent effects, that of transfer impedance coupling, from the main propagation model.

In an internal domain the natural reference conductor is the shield enclosing the domain. The model allows for multiple levels of shielding hence an internal domain may contain conductors which are themselves the shields of other domains as seen in Figure 3.3. In the case of imperfect shielding these domains are coupled through transfer impedance and admittance terms. In this work we assume that the coupling through transfer admittance may be neglected.

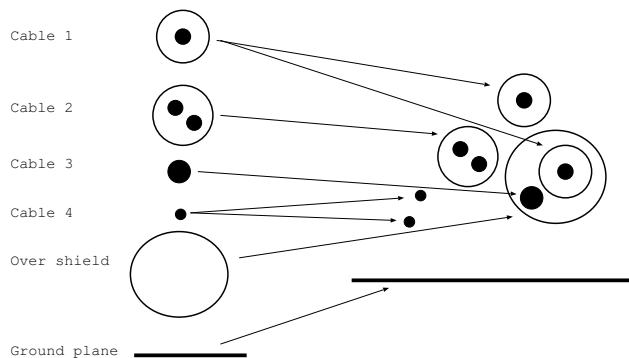


Figure 3.3 Illustration of a cable bundle built with multiple layers of shielding

When applying this decomposition technique the voltages on shielded cables are naturally referenced to their respective shields and the current return is also assumed to be on the inside of the shield. This can aid the propagation analysis and also the analysis of coupling from an external illuminating field. The internal and external propagation problems can be coupled by transfer impedance and admittance terms. We note that there may be more than one level of shielding in a particular cable installation and we must be able to take this into account in our analysis. Figure 3.4 shows a shielded cable with voltages and currents reference to their natural (local) references in blue on the right hand side and with voltages and currents referenced to the ground plane (global reference) on the right hand side.

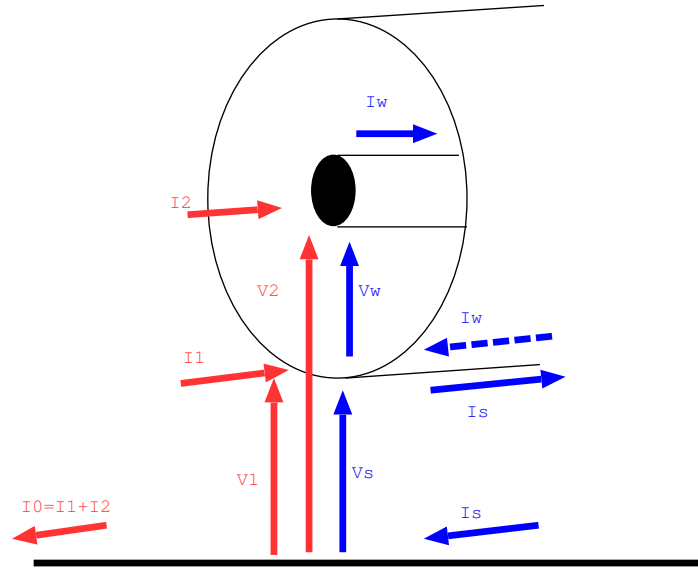


Figure 3.4 A shielded cable with alternative voltage and current definitions

We can define a domain decomposition matrix which transforms conductor voltages referenced to their local reference (shield for shielded conductors, ground for external conductors) and voltages referenced to the global reference (ground).

$$(V_{local}) = [M_V](V_{global}) \quad (3.1)$$

For the coaxial cable pictured

$$\begin{aligned} V_w &= V_2 - V_1 \\ V_s &= V_1 \end{aligned} \quad (3.2)$$

therefore

$$\begin{pmatrix} V_w \\ V_s \end{pmatrix} = \begin{bmatrix} -1 & 1 \\ 1 & 0 \end{bmatrix} \begin{pmatrix} V_1 \\ V_2 \end{pmatrix} \quad (3.3)$$

Similarly we can define a domain decomposition matrix which transforms conductor currents whose return path is their local reference (shield for shielded conductors, ground for external conductors) and total conductor currents with reference to the global ground.

$$(I_{local}) = [M_I](I_{global}) \quad (3.4)$$

For the coaxial cable pictured

$$\begin{aligned} I_w &= I_2 \\ I_s &= I_1 + I_2 \end{aligned} \quad (3.5)$$

therefore

$$\begin{pmatrix} I_w \\ I_s \end{pmatrix} = \begin{bmatrix} 0 & 1 \\ 1 & 1 \end{bmatrix} \begin{pmatrix} I_1 \\ I_2 \end{pmatrix} \quad (3.6)$$

Figure 3.3 shows a complex cable bundle with multiple levels of shielding. In this case there are multiple local voltage references. The transformation matrices for these complex situations can be defined in a similar manner as for the coaxial cable.

The domain decomposition process is achieved by a matrix multiplication. This may be implemented in a Spice model using controlled voltage and current sources. In the example of the coaxial cable above a ground plane there are three conductors. We define the global voltage variables with respect to the ground plane as

$$V_1 = V_{shield} \quad (3.7)$$

$$V_2 = W_{wire}$$

The model is divided into two domains, the inner domain consisting of the inner wire and the shield (domain 1) and the external domain consisting of the outer shield and the ground (domain 2). Each of the domains has a single conductor in addition to its reference. The domain based voltage variables are

$$V_{d1.c1} = V_{wire} - V_{shield} = V_2 - V_1 \quad (3.8)$$

$$V_{d2.c1} = W_{shield} = V_1$$

The equation relating the global voltage variables and domain voltage variables is

$$\begin{pmatrix} V_{d1.c1} \\ V_{d2.c1} \end{pmatrix} = \begin{bmatrix} -1 & 1 \\ 1 & 0 \end{bmatrix} \begin{pmatrix} V_1 \\ V_2 \end{pmatrix} = [M_V] \begin{pmatrix} V_1 \\ V_2 \end{pmatrix} \quad (3.9)$$

Inverting this equation gives

$$\begin{pmatrix} V_1 \\ V_2 \end{pmatrix} = \begin{bmatrix} 1 & 1 \\ 1 & 0 \end{bmatrix} \begin{pmatrix} V_{d1.c1} \\ V_{d2.c1} \end{pmatrix} = [M_V]^{-1} \begin{pmatrix} V_{d1.c1} \\ V_{d2.c1} \end{pmatrix} \quad (3.10)$$

Similarly the equation relating the global current variables and domain current variables is

$$\begin{pmatrix} I_{d1.c1} \\ I_{d2.c1} \end{pmatrix} = \begin{bmatrix} 0 & 1 \\ 1 & 1 \end{bmatrix} \begin{pmatrix} I_1 \\ I_2 \end{pmatrix} = [M_I] \begin{pmatrix} I_1 \\ I_2 \end{pmatrix} \quad (3.11)$$

Figure 3.5 shows a Spice circuit model which implements equations 3.10 and 3.11. Note that the voltage sources on the left hand side of the figure have a value of zero volts, they are only required as Spice uses such voltage sources as current sensing elements for the current controlled voltage sources.

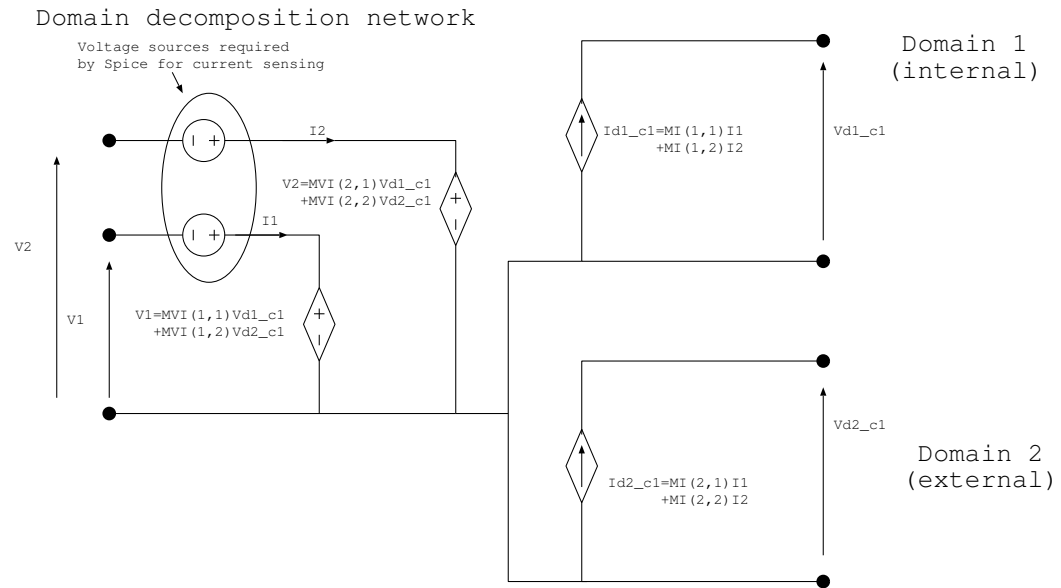


Figure 3.5 Spice circuit model which implements domain decomposition for a shielded cable

3.3 Twisted Pair Model

The twisted pair model assumes that any crosstalk or coupling in the cable bundle (as opposed to the terminations) will be to the common mode of the twisted pair. The differential mode propagates without any coupling to or from other conductors in the bundle. This twisted pair model behaves in a similar manner to a shielded cable with a perfect shield where the differential mode corresponds to the internal (shielded) mode which does not interact with its surrounding conductors and the common mode corresponds to the external propagation on the shield which does interact with the surrounding conductors. This correspondence allows a circuit model of a twisted pair to be constructed based on the domain decomposition method used for shielded cables. The model decomposes the twisted pair system into domains. The domains consist of a common mode domain which is exposed to the external EM environment and a differential mode domain which is perfectly shielded from the external environment. In an internal domain the natural reference conductor is the shield enclosing the domain. The model may be simply extended to the case of a shielded twisted pair. Note that for a twisted pair in isolation i.e. with no other return conductor then only the differential mode should be included in the model.

Figure 3.6 shows a twisted pair cable with an additional external conductor (ground plane). The external voltages and currents at the termination (LHS) are reference to ground plane (global reference) whilst the voltages and currents used in the model are the common and differential mode shown to the right.

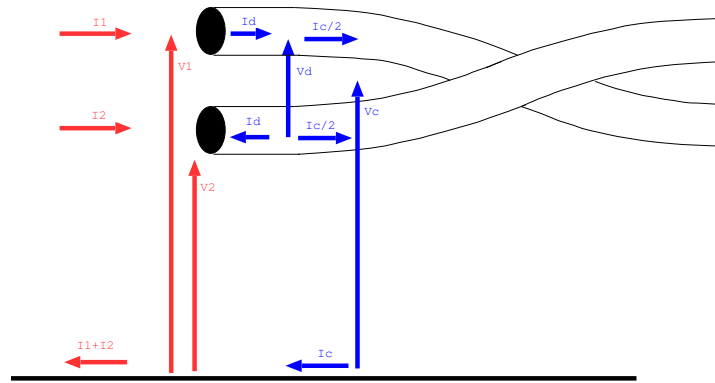


Figure 3.6 Domain decomposition for twisted pairs

For the twisted pair we can relate the differential mode and common mode voltages to the conductor voltages by

$$\begin{aligned} V_d &= V_1 - V_2 \\ V_c &= \frac{(V_1 + V_2)}{2} \end{aligned} \tag{3.12}$$

therefore the domain decomposition matrix M_V is given by

$$\begin{pmatrix} V_d \\ V_c \end{pmatrix} = [M_V] \begin{pmatrix} V_1 \\ V_2 \end{pmatrix} = \begin{bmatrix} 1 & -1 \\ \frac{1}{2} & \frac{1}{2} \end{bmatrix} \begin{pmatrix} V_1 \\ V_2 \end{pmatrix} \quad (3.13)$$

Similarly we can relate the differential mode and common mode currents to the conductor current by

$$\begin{aligned} I_d &= \frac{I_1 - I_2}{2} \\ I_c &= I_1 + I_2 \end{aligned} \quad (3.14)$$

therefore the domain decomposition matrix M_I is given by

$$\begin{pmatrix} I_d \\ I_c \end{pmatrix} = [M_I] \begin{pmatrix} I_1 \\ I_2 \end{pmatrix} = \begin{bmatrix} \frac{1}{2} & -\frac{1}{2} \\ 1 & 1 \end{bmatrix} \begin{pmatrix} I_1 \\ I_2 \end{pmatrix} \quad (3.15)$$

3.3.1 Per-unit-length parameters for the twisted pair model

The decomposition into the differential mode and the common mode for the twisted pair model requires the per-unit-length inductance and capacitance to be determined for these modes. The differential mode of a twisted pair in a bundle with other conductors and/ or a ground plane is assumed not to interact with the other conductors in the bundle, the differential mode inductance and capacitance are calculated for the two conductors in isolation i.e. with all other conductors removed. The differential mode inductance and capacitance are then independent of the orientation of the conductors in the analysis. The common mode inductance and capacitance are calculated by assuming that the common mode current is carried by an equivalent cylindrical conductor placed on the axis of the twisted pair. This equivalent conductor is then used in the analysis of the bundle cross section in the calculation of the twisted pair common mode contribution to the inductance and capacitance matrices. This process is illustrated in figure 3.7

3.3.2 Per-unit-length parameters for the shielded twisted pair model

The per-unit-length parameters for a shielded twisted pair are determined in a slightly different manner than for a twisted pair in a bundle with other conductors. In the case of a shielded twisted pair the orientation of the conductors is not of any significance due to the symmetry of the shield conductor. The inductance and capacitance of the three conductor system formed by the twisted pair and the shield can be calculated using the Laplace solver with the shield chosen as the reference conductor. This gives the conductor based transmission line equations of the following form

$$\frac{\partial}{\partial z} \begin{pmatrix} V_1 \\ V_2 \end{pmatrix} = -[L] \frac{\partial}{\partial t} \begin{pmatrix} I_1 \\ I_2 \end{pmatrix} \quad (3.16)$$

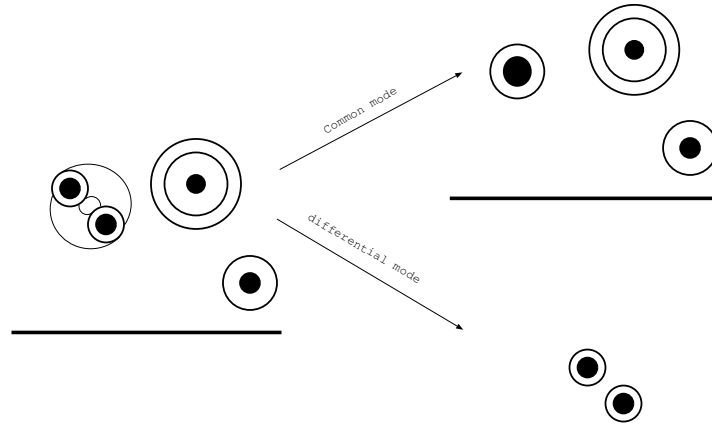


Figure 3.7 Twisted pair inductance and capacitance matrix calculation

where

$$[L] = \begin{bmatrix} L_A & L_B \\ L_B & L_A \end{bmatrix} \quad (3.17)$$

and

$$\frac{\partial}{\partial z} \begin{pmatrix} I_1 \\ I_2 \end{pmatrix} = -[C] \frac{\partial}{\partial t} \begin{pmatrix} V_1 \\ V_2 \end{pmatrix} \quad (3.18)$$

where

$$[C] = \begin{bmatrix} C_A & C_B \\ C_B & C_A \end{bmatrix} \quad (3.19)$$

The common and differential mode inductance and capacitance are then found by applying the domain decomposition matrices to transform the conductor based voltage and current variables to common and differential mode based voltages and currents i.e.

$$\frac{\partial}{\partial z} \begin{pmatrix} V_d \\ V_c \end{pmatrix} = -[M_V][L][M_I]^{-1} \frac{\partial}{\partial t} \begin{pmatrix} I_d \\ I_c \end{pmatrix}, [L] = \begin{bmatrix} 2(L_A - L_B) & 0 \\ 0 & \frac{1}{2}(L_A + L_B) \end{bmatrix} \quad (3.20)$$

and

$$\frac{\partial}{\partial z} \begin{pmatrix} I_d \\ I_c \end{pmatrix} = -[M_I][C][M_V]^{-1} \frac{\partial}{\partial t} \begin{pmatrix} V_d \\ V_c \end{pmatrix}, [C] = \begin{bmatrix} \frac{1}{2}(C_A + C_B) & 0 \\ 0 & 2(C_A - C_B) \end{bmatrix} \quad (3.21)$$

from which we identify the common and differential mode inductance and capacitances.

3.4 Modal decomposition

The multi-conductor frequency domain transmission line equations are given by

$$\begin{aligned}\frac{d}{dz} \left(\tilde{V}(z) \right) &= - \left[\tilde{Z} \right] \left(\tilde{I}(z) \right) \\ \frac{d}{dz} \left(\tilde{I}(z) \right) &= - \left[\tilde{Y} \right] \left(\tilde{V}(z) \right),\end{aligned}\tag{3.22}$$

where

$$\begin{aligned}\left[\tilde{Z} \right] &= [R] + j\omega [L] \\ \left[\tilde{Y} \right] &= [G] + j\omega [C].\end{aligned}\tag{3.23}$$

The frequency domain solution of these equations relied on a modal decomposition method as described in section 2 in which the $[Z][Y]$ product was diagonalised i.e. we must diagonalise the matrix

$$\left[\tilde{Z} \right] \left[\tilde{Y} \right] = [[R] + j\omega [L]] [[G] + j\omega [C]].\tag{3.24}$$

Even if we assume that the parameters of the cable are independent of frequency then the problems with the diagonalisation process can be seen by looking at the limits as $j\omega \rightarrow 0$ and $j\omega \rightarrow \text{inf}$. In the first case we have (if we assume that $[G] = 0$)

$$\left[\tilde{Z} \right] \left[\tilde{Y} \right] = [R] [j\omega [C]]\tag{3.25}$$

whereas at high frequency we can neglect $[R]$ and $[G]$ in comparison to to $j\omega[L]$ and $j\omega[C]$ and we have

$$\left[\tilde{Z} \right] \left[\tilde{Y} \right] = -\omega^2 [L] [C]\tag{3.26}$$

In the first case the $[Z][Y]$ matrix product is dominated by $[R]$ and $[C]$ whereas at high frequency it is dominated by $[L]$ and $[L]$. In the general case, we must therefore diagonalise the $[Z][Y]$ matrix product at every frequency.

A model which eliminates this problem may be found by lumping the d.c. resistances of the conductors at the conductor ends i.e. place a lumped resistance with value $R_{dc}/2$ at either end of the transmission line. Once this is done, the $[Z][Y]$ matrix product is again given by equation 3.26.

A justification for this is that the transmission line resistance may be attributed to the finite conductivity of the conductors. The resistance resulting from this is frequency dependent and increases as $\frac{1}{\sqrt{f}}$. Subtracting the d.c. resistance will result in a model which is still correct at d.c. and reasonably accurate provided the transmission line is short compared with the wavelength. The modal decomposition will be a weak function of frequency and the losses associated with the propagation of a mode on a lossy transmission line may be corrected by a frequency dependent loss term as described below.

It is interesting to observe that (if we consider a single mode transmission line), if there is a d.c. resistance present then the characteristic impedance of the lossy line is given by

$$Z_0 = \sqrt{\frac{R + j\omega L}{j\omega C}} \quad (3.27)$$

at low frequency

$$Z_0 \rightarrow \sqrt{\frac{R}{j\omega C}} \quad (3.28)$$

i.e. the characteristic impedance varies as $\frac{1}{\sqrt{j\omega}}$ i.e. $Z_0 \rightarrow \text{inf}$ as $\omega \rightarrow 0$.

The individual conductor currents and voltages within a domain are transformed into the modal currents and voltages. The conductor voltages and currents are solutions of the coupled first order equations

$$\begin{aligned} \frac{d}{dz} (\tilde{V}(z)) &= -[L] \frac{d}{dt} (\tilde{I}(z)) \\ \frac{d}{dz} (\tilde{I}(z)) &= -[C] \frac{d}{dt} (\tilde{V}(z)) \end{aligned} \quad (3.29)$$

Two uncoupled second order equations may be written:

$$\begin{aligned} \frac{d^2}{dz^2} (\tilde{V}(z)) &= [\tilde{L}] [\tilde{C}] \frac{d^2}{dt^2} (\tilde{V}(z)) \\ \frac{d^2}{dz^2} (\tilde{I}(z)) &= [\tilde{C}] [\tilde{L}] \frac{d^2}{dt^2} (\tilde{I}(z)). \end{aligned} \quad (3.30)$$

A change of variables via a similarity transformation to modal quantities allows the decoupling (diagonalisation) of the matrix system. The conductor voltages and currents are related to their corresponding modal quantities by voltage and current transformation matrices

$$\begin{aligned} (\tilde{V}(z)) &= [T_V] (\tilde{V}_m(z)) \\ (\tilde{I}(z)) &= [T_I] (\tilde{I}_m(z)) \end{aligned} \quad (3.31)$$

Thus the coupled first order equations 3.29 become

$$\begin{aligned} \frac{d}{dz} (\tilde{V}_m(z)) &= -[T_V]^{-1} [L] [T_I] \frac{d}{dt} (\tilde{I}_m(z)) \\ \frac{d}{dz} (\tilde{I}_m(z)) &= -[T_I]^{-1} [C] [T_V] \frac{d}{dt} (\tilde{V}_m(z)) \end{aligned} \quad (3.32)$$

and the uncoupled second order equations 3.30 become

$$\begin{aligned} \frac{d^2}{dz^2} (\tilde{V}_m(z)) &= [T_V]^{-1} [\tilde{L}] [\tilde{C}] [T_V] \frac{d^2}{dt^2} (\tilde{V}_m(z)) \\ \frac{d^2}{dz^2} (\tilde{I}_m(z)) &= [T_I]^{-1} [\tilde{C}] [\tilde{L}] [T_I] \frac{d^2}{dt^2} (\tilde{I}_m(z)). \end{aligned} \quad (3.33)$$

In the case of a lossless inhomogeneous transmission line it is possible to find matrices $[T_V]$ and $[T_I]$ which simultaneously diagonalise both $[L]$ and $[C]$ i.e.

$$\begin{aligned} [T_V]^{-1} [L] [T_I] &= [L_m] \\ [T_I]^{-1} [C] [T_V] &= [C_m] \end{aligned} \quad (3.34)$$

where $[L_m]$ and $[C_m]$ are diagonal matrices. Thus we have an uncoupled system for modal propagation where the mode characteristic impedance of the i th mode is

$$Z_{cmi} = \sqrt{\frac{l_{mi}}{c_{mi}}} \quad (3.35)$$

and the mode velocity is

$$V_{mi} = \frac{1}{\sqrt{l_{mi}c_{mi}}} \quad (3.36)$$

The matrices $[L]$ and $[C]$ are real, symmetric and positive definite and we may obtain the diagonalisation of these matrices as follows:

First diagonalise the real, symmetric matrix, $[C]$ with the orthogonal transformation matrix $[U]$

$$[U]^t [C] [U] = [\theta^2] \quad (3.37)$$

where

$$[U]^t = [U]^{-1} \quad (3.38)$$

The capacitance matrix, $[C]$ is positive definite so the square root of the diagonal eigenvalue matrix, $[\theta]$ is real.

Second form the product

$$[M] = [\theta] [U]^t [L] [U] [\theta] \quad (3.39)$$

$[M]$ is a real symmetric matrix which may again be diagonalised with an orthogonal matrix.

$$[S]^t [M] [S] = [\Gamma^2] \quad (3.40)$$

where

$$[S]^t = [S]^{-1} \quad (3.41)$$

Define the normalised matrix $[T_{norm}]$ as

$$[T_{norm}] = [U] [\theta] [S] [\alpha] \quad (3.42)$$

where the diagonal matrix $[\alpha]$ normalises the columns of $[T_{norm}]$ to length 1.

The matrices which diagonalise $[L]$ and $[C]$ are then

$$[T_V]^{-1} = [T_{norm}]^t \quad (3.43)$$

and

$$[T_I]^{-1} = [T_{norm}]^{-1} \quad (3.44)$$

Thus the voltage and current modal transformation matrices are related by

$$[\tilde{T}_I]^T = [\tilde{T}_V]^{-1} \quad (3.45)$$

The mode impedance and velocity for a mode i are

$$Z_{c_{mi}} = \sqrt{\frac{l_{mi}}{c_{mi}}} = \alpha_{ii}^2 \Gamma_i \quad (3.46)$$

$$V_{mi} = \frac{1}{\sqrt{l_{mi}c_{mi}}} = \frac{1}{\Gamma_i} \quad (3.47)$$

Mode propagation will underly the method of characteristics based propagation algorithm in the Spice model.

This leads to an efficient algorithm for both a.c. and transient models of multi-conductor propagation provided that the modal decomposition matrices are independent of frequency. Discussion of the incorporation of loss and frequency dependent properties will be discussed in sections 7.4 and 7.5.

For the example of a lossless 3 conductor cable the conductor currents are related to the modal currents by matrices of dimension 2:

$$\begin{pmatrix} I_1 \\ I_2 \end{pmatrix} = [\tilde{T}_I] \begin{pmatrix} I_{m1} \\ I_{m2} \end{pmatrix} \quad (3.48)$$

Hence the modal currents are related to the conductor currents by

$$\begin{pmatrix} I_{m1} \\ I_{m2} \end{pmatrix} = [\tilde{T}_I]^{-1} \begin{pmatrix} I_1 \\ I_2 \end{pmatrix} \quad (3.49)$$

And the conductor voltages are related to the modal voltages by

$$\begin{pmatrix} V_1 \\ V_2 \end{pmatrix} = [\tilde{T}_V] \begin{pmatrix} V_{m1} \\ V_{m2} \end{pmatrix} \quad (3.50)$$

A modal decomposition for a three conductor (two mode) transmission line is implemented by the network model in Figure 3.8. The model implements equations 3.49 and 3.50. As for the domain decomposition matrix implementation, the voltage sources on the left hand side of the figure have a value of zero volts, they are only required as Spice uses such voltage sources as current sensing elements for the current controlled voltage sources.

This model may be implemented in any of the Spice versions considered in this study and is suitable for a.c. and transient analysis. It may be extended to an arbitrary number of conductors under the assumption that the multi-conductor is lossless and non-dispersive.

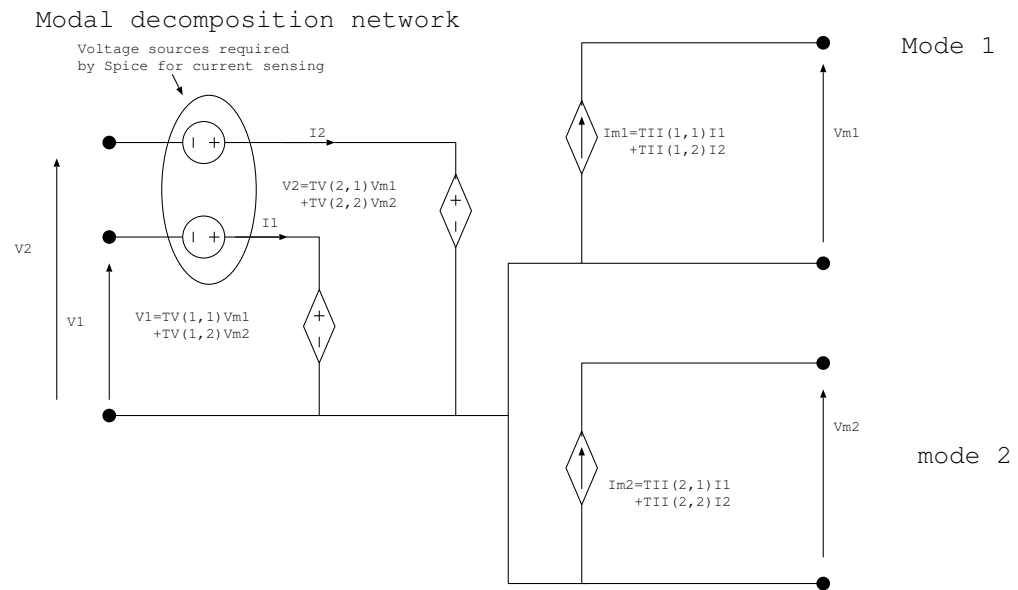


Figure 3.8 Spice circuit model which implements modal decomposition for a three conductor system

3.5 Method of characteristics

The propagation of modes is implemented using the method of characteristics [2] i.e. we identify modes propagating in the +z and -z directions at the terminations and propagate these separately. This has advantages for incorporating incident field excitation and transfer impedance coupling processes. In the derivation of the method of characteristics model we consider a lossless, dispersionless single mode transmission line of length L. This analysis generalizes to multi-mode transmission lines where each mode is treated separately and so is sufficient for the derivation of the proposed model. If we consider the propagation of a mode with modal current, I, modal voltage, V, and modal characteristic impedance Z_c then the voltage and current may be written as the sum of waves propagating in the +z and -z directions as

$$\begin{aligned} V &= V^+ + V^- \\ I &= I^+ - I^- \end{aligned} \quad (3.51)$$

The voltage and current for the +z and -z waves are related by

$$\begin{aligned} I^+ &= \frac{V^+}{Z_c} \\ I^- &= -\frac{V^-}{Z_c} \end{aligned} \quad (3.52)$$

We can work out the decomposition into +z and -z travelling modes from the voltage and current at any point, z, along the transmission line

$$\begin{aligned} 2V^+ &= V + Z_c I \\ 2V^- &= V - Z_c I \end{aligned} \quad (3.53)$$

Evaluating equation 3.53 at z=0 gives

$$V(0, t) = Z_c I(0, t) + 2V^-(0, t) \quad (3.54)$$

Similarly, at z=L we have

$$V(L, t) = -Z_c I(L, t) + 2V^+(L, t) \quad (3.55)$$

The -z travelling mode quantities at z=0 are the -z travelling mode quantities launched from the z=L termination at time t-T where T is the transmission line delay thus substituting equation 3.53 evaluated at time t-T, and z=L gives

$$V(0, t) = Z_c I(0, t) + V(L, t - T) - Z_c I(L, t - T) \quad (3.56)$$

A similar process leads to an equation for the z=L end of the transmission line

$$V(L, t) = -Z_c I(L, t) + V(0, t - T) + Z_c I(0, t - T) \quad (3.57)$$

Equations 3.54, 3.55 and 3.56, 3.57 are implemented in the spice compatible circuit shown in Figure 3.9 where the time delay is incorporated into the model by a perfectly matched ideal transmission line.

Method of characteristics network

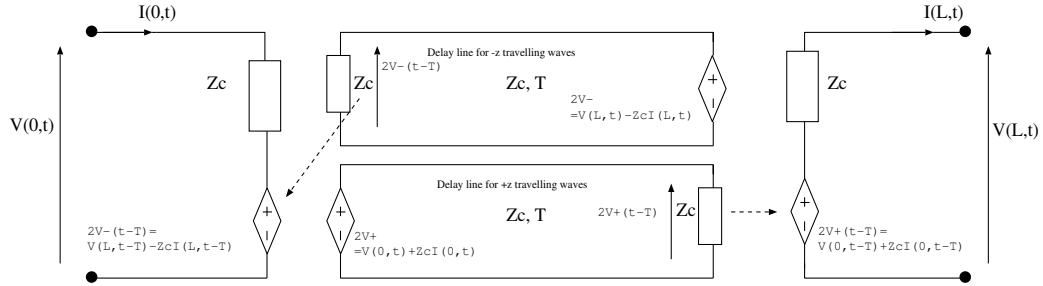


Figure 3.9 Spice compatible circuit implementing the method of characteristics

In practice the Spice circuit which implements the calculation of the characteristic variables in equations 3.53 uses voltage controlled voltage sources. The following expression allows for the calculation of the characteristic variables in the $+z$ direction from nodal voltage values at the $z = 0$ termination.

$$2V^+(0, t) = V(0, t) + Z_c I(0, t) = 2V(0, t) - (V(0, t) - Z_c I(0, t)) \quad (3.58)$$

Similarly, the following expression allows for the calculation of the characteristic variables in the $-z$ direction from nodal voltage values at the $z = L$ termination.

$$2V^-(L, t) = V(L, t) - Z_c I(L, t) = 2V(L, t) - (V(L, t) + Z_c I(L, t)) \quad (3.59)$$

3.6 Approximate model for frequency dependent transmission lines

The derivation of the model for frequency dependent transmission lines will be described in two stages. Firstly the model is described for single mode propagation. This model is subsequently generalised to multi-mode propagation. The frequency dependent properties in the models derived here arise from two mechanisms:

1. frequency dependent permittivity of dielectrics
2. finite conductivity of conductors.

3.6.1 Frequency dependent dielectric models

Frequency dependent cable properties (dielectric relative permittivity or transfer impedance) may be included in the model using the rational function form for the relative permittivity i.e.

$$\epsilon_r(j\omega) = \frac{a_0 + a_1 \left(\frac{j\omega}{\omega_0}\right) + a_2 \left(\frac{j\omega}{\omega_0}\right)^2 + \dots}{b_0 + b_1 \left(\frac{j\omega}{\omega_0}\right) + b_2 \left(\frac{j\omega}{\omega_0}\right)^2 + \dots} \quad (3.60)$$

For example the frequency dependent cable dielectric constant could be approximated by a Debye model [4] which has a relative permittivity (although in practice debye dielectrics would be too lossy to be used in transmission lines) described by

$$\epsilon_r = \epsilon_\infty + \frac{\epsilon_s - \epsilon_\infty}{1 + j\omega\tau} \quad (3.61)$$

where ϵ_∞ is the relative permittivity at the high frequency limit, ϵ_s is the relative permittivity at the low frequency limit and τ is the relaxation time of the material.

A frequency dependent dielectric model will then give rise to a frequency dependent admittance in the transmission line equations. We note however that the frequency dependent relative permittivity function in equation 3.60 will give rise to no admittance at d.c. The only mechanism which would give rise to a d.c. admittance would be a non-zero electrical conductivity in the dielectric.

3.6.2 Frequency dependent finite conductivity loss models

Cable losses arising from the finite conductivity of a conductor are incorporated into some of the cable models available. In these models the conductivity of the conductors are specified as parameters of the cable model. The cylindrical conductor loss models are based on reference [5] and the model for rectangular conductors is derived in [2] The models of finite conductivity of conductors include both a resistance and internal inductance (due to the magnetic field penetrating the conductor). These are frequency dependent and thus a complex internal impedance contributes to the impedance matrix of the idealised cable.

It is seen that the internal resistance due to finite conductivity increases as \sqrt{f} and the internal inductance decreases as $\frac{1}{\sqrt{f}}$. This is important to note for the derivation of the propagation correction.

Cylindrical Conductor

For a cylindrical conductor of radius, r , and conductivity, σ , the internal impedance due to the magnetic field penetrating the conductor at frequency f is given by [5], [2]

$$Z_{int} = \frac{1}{\sqrt{2\pi r \sigma \delta}} \left(\frac{ber(q) + jbei(q)}{bei'(q) - jber'(q)} \right) \quad (3.62)$$

where ber and bei are Kelvin functions, δ is the skin depth given by

$$\delta = \frac{1}{\sqrt{\pi f \mu \sigma}} \quad (3.63)$$

and q is

$$q = \sqrt{2} \frac{r}{\delta} \quad (3.64)$$

Cylindrical Shell

For a cylindrical shell i.e. a cable shield of radius, r , thickness, t , and conductivity, σ , the surface impedance (neglecting small terms related to the curvature of the conductor) may be evaluated as follows [5]

The d.c. resistance of a shell of radius, r , and thickness, t , is

$$R_{dc} = \frac{1}{\sqrt{2\pi \sigma r t}} \quad (3.65)$$

The complex propagation constant in the conductor is

$$\gamma = \frac{(1 + j)}{\delta} \quad (3.66)$$

Then the surface impedance of the cylindrical shell is

$$Z_{int_shell} = R_{dc} \gamma t \operatorname{cosech}(\gamma t) \quad (3.67)$$

It is important to note that at low frequency the surface impedance is equal to the d.c. resistance of the shield. and that the transfer impedance also takes this same value.

Rectangular Conductor

The loss model for rectangular conductors assumes that the internal impedance of the conductor takes the form [2]

$$Z_{int_rectangular} = R_{dc} + B \sqrt{j\omega} \quad (3.68)$$

where R_{dc} is the d.c. resistance of a rectangular wire of width w , and height t , is given by

$$R_{dc} = \frac{1}{\sigma wt} \quad (3.69)$$

and B is given by

$$B = \frac{1}{2(w+t)} \sqrt{\frac{\mu}{\sigma}} \quad (3.70)$$

3.6.3 Single mode propagation correction

Assume that the frequency dependence of the transmission line parameters takes the form

$$L(j\omega) = L_0 + L_{int}(j\omega)$$

$$R(j\omega) = R_{dc} + R_{int}(j\omega) \quad (3.71)$$

$$C(j\omega) = C_0 + C_{freq}(j\omega)$$

In the light of the models of the frequency dependence of the cable parameters discussed above, we emphasise the following points:

1. The internal inductance, $L_{int}(j\omega)$, decreases with frequency as $\frac{1}{\sqrt{f}}$.
2. The internal resistance, $R_{int}(j\omega)$, is equal to 0Ω at d.c.
3. The internal resistance, $R_{int}(j\omega)$, increases with frequency as \sqrt{f}
4. The capacitance, $C(j\omega) \rightarrow C_0$ as $\omega \rightarrow \inf$

thus as $\omega \rightarrow \inf$, we can assume that the inductance of the transmission line is L_0 and the capacitance of the transmission line is C_0 . The characteristic impedance of the transmission line is

$$Z_c(j\omega) = \sqrt{\frac{R(j\omega) + j\omega L(j\omega)}{j\omega C(j\omega)}} \quad (3.72)$$

The propagation factor of the transmission line is $e^{j\gamma L}$ where

$$\gamma(j\omega) = \sqrt{(R(j\omega) + j\omega L(j\omega))(j\omega C(j\omega))} \quad (3.73)$$

The method of characteristics outlined in section 3.5 above may be generalised for frequency dependent properties, including losses. Initially frequency domain expressions are obtained for the termination voltages as

$$V(0, j\omega) = Z_c(j\omega) I(0, j\omega) + e^{-\gamma L} (V(L, j\omega) - Z_c(j\omega) I(L, j\omega)) \quad (3.74)$$

A similar process leads to an equation for the $z=L$ end of the transmission line

$$V(L, j\omega) = Z_c(j\omega) I(L, j\omega) + e^{-\gamma L} (V(0, j\omega) + Z_c(j\omega) I(0, j\omega)) \quad (3.75)$$

Multiplication in the frequency domain implies a convolution in the time domain therefore the frequency dependent propagation and the frequency dependent impedance functions require convolution processes for time domain calculations. It has been found that a sufficiently accurate model across a wide frequency band down to d.c. and up into the GHz frequency range may be derived by a suitable extraction of the loss and dispersion effects to the terminations of the transmission line model. The first complication in equations 3.74 and 3.75 is the frequency dependent impedance. This is simplified firstly by assuming that the d.c. resistance of the transmission line, R_{dc} , can be lumped into two resistances $\frac{R_{dc}}{2}$ at either end of the line. The impedance of the transmission line with the d.c. resistance removed in this way is now

$$Z_c(j\omega) = \sqrt{\frac{R_{int}(j\omega) + j\omega L_0 + j\omega L_{int}(j\omega)}{j\omega C_0 + j\omega C_{freq}(j\omega)}} \quad (3.76)$$

R_{int} is 0 at d.c. and significantly less than the inductive impedance $j\omega L_0 + j\omega L_{int}(j\omega)$ at high frequency, we also observe that the internal inductance due to the skin effect decreases with frequency as \sqrt{f} therefore it appears to be an acceptable approximation that as far as the transmission line characteristic impedance is concerned we may calculate it using the high frequency inductance

$$Z_0 = \sqrt{\frac{L_0}{C_0}} \quad (3.77)$$

Therefore we can write

$$V'(0, j\omega) = Z_0 I(0, j\omega) + e^{\gamma'(j\omega)L} (V'(L, j\omega) - Z_0 I(L, j\omega)) \quad (3.78)$$

$$V'(L, j\omega) = -Z_0 I(L, j\omega) + e^{\gamma'(j\omega)L} (V'(0, j\omega) + Z_0 I(0, j\omega)) \quad (3.79)$$

where V' is the voltage across the modified (d.c. resistance removed) transmission line termination and the revised propagation factor γ' also takes account of the extraction of the d.c. resistance and is

$$\gamma'(j\omega) = \sqrt{(R_{int}(j\omega) + j\omega L(j\omega))(j\omega C(j\omega))} \quad (3.80)$$

The second complication is the frequency dependence of the propagation factor. This is treated as follows: We define γ_0 using the high frequency inductance value as

Then equations 3.78 and 3.79 may be written

$$V'(0, j\omega) = Z_0 I(0, j\omega) + e^{\gamma_0 L} e^{(\gamma'(j\omega) - \gamma_0)L} (V'(L, j\omega) - Z_0 I(L, j\omega)) \quad (3.81)$$

$$V'(L, j\omega) = -Z_0 I(L, j\omega) + e^{\gamma_0 L} e^{(\gamma'(j\omega) - \gamma_0)L} (V'(0, j\omega) + Z_0 I(0, j\omega)) \quad (3.82)$$

The $e^{j\gamma_0 l}$ propagation term is a simple delay of T seconds where

$$T = \sqrt{L_0 C_0} \quad (3.83)$$

The propagation factor $e^{j\gamma_0 L} e^{j(\gamma'(j\omega) - \gamma_0)L}$ can be thought of as a delay with a subsequent frequency dependent propagation correction applied.

The propagation of the characteristic variables can thus be implemented as a simple delay line in Spice followed by a frequency dependent correction factor $H(j\omega) = e^{j(\gamma'(j\omega) - \gamma_0)L}$ which may be implemented in Spice using the s-domain transfer function element. The corresponding time domain model equations are now

$$V'(0, t) = Z_0 I(0, t) + H(j\omega)^* (V'(L, t - T) - Z_0 I(L, t - T)) \quad (3.84)$$

$$V'(L, t) = -Z_0 I(L, t) + H(j\omega)^* (V'(0, t - T) + Z_0 I(L, t - T)) \quad (3.85)$$

where

$$H(j\omega) = e^{j(\gamma'(j\omega) - \gamma_0)L} \quad (3.86)$$

The Spice model for the method of characteristics propagation model with the propagation correction included is shown in Figure 3.10 The transmission line model may be

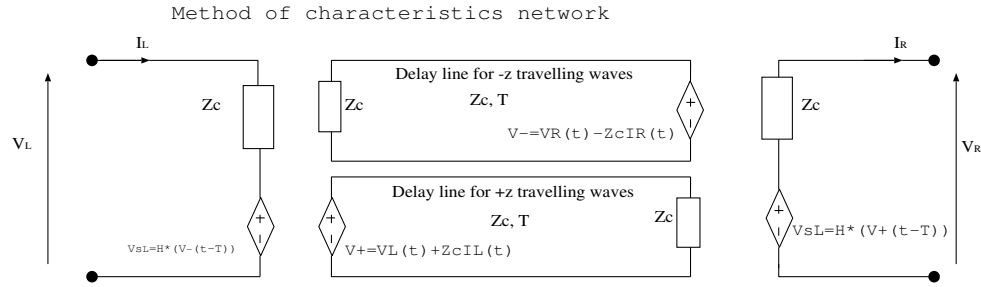


Figure 3.10 Method of characteristics Spice model with propagation correction

thought of as a lossless transmission line with a network at either end which models the effect of the frequency dependent line losses. It is found that the individual termination models implemented as shown in figure 3.10 is not reciprocal i.e. at the termination of the lossless line the propagation correction is applied to the wave in only one direction. The model can be made reciprocal by a termination network which applies half of the propagation correction $(\sqrt{H(j\omega)})$ at each end of the lossless transmission line as shown in Figure 3.11. Each part of the propagation correction corrects for propagation along half the length of the transmission line i.e. the propagation correction applied at each end of the method of characteristics delay line is

$$H'(j\omega) = e^{j(\gamma'(j\omega) - \gamma_0) \frac{L}{2}} \quad (3.87)$$

3.6.4 Multi-mode propagation correction

We follow the analysis of the frequency dependent single mode transmission line in our development of a frequency dependent multi-conductor transmission line model.

Reciprocal Frequency dependent method of characteristics network

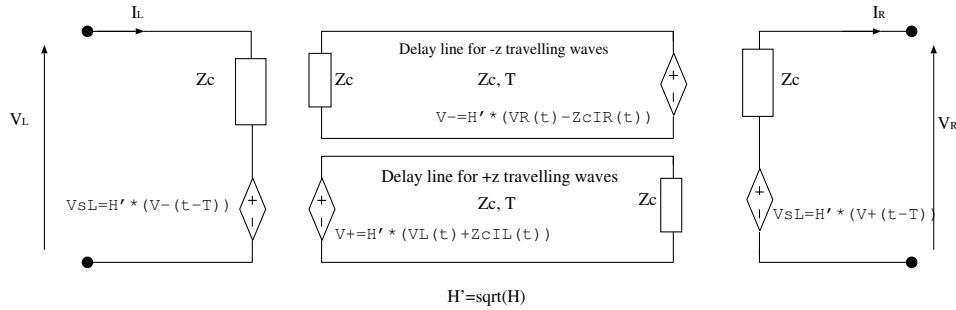


Figure 3.11 Reciprocal method of characteristics Spice model with propagation correction

Assume that the frequency dependence of the transmission line parameters takes the form

$$\begin{aligned}
 [L(j\omega)] &= [L_0] + [L_{int}(j\omega)] \\
 [R(j\omega)] &= [R_{dc}] + [R_{int}(j\omega)] \\
 [C(j\omega)] &= [C_0] + [C_{freq}(j\omega)]
 \end{aligned}
 \tag{3.88}$$

Where square brackets denote matrix quantities. We follow the same process as for the single mode model development i.e. firstly the d.c. resistance for each conductor is lumped at either end of the MTL.. The remaining transmission line is assumed to have the properties

$$\begin{aligned}
 [L(j\omega)] &= [L_0] + [L_{int}(j\omega)] \\
 [R(j\omega)] &= [R_{int}(j\omega)] \\
 [C(j\omega)] &= [C_0] + [C_{freq}(j\omega)]
 \end{aligned}
 \tag{3.89}$$

In deriving the modal decomposition and the mode impedances, the transmission line is approximated as a lossless line with the frequency independent properties

$$\begin{aligned}
 [L] &= [L_0] \\
 [C] &= [C_0]
 \end{aligned}
 \tag{3.90}$$

The transmission line impedance and admittance matrices are

$$\begin{aligned}
 [\tilde{Z}] &= j\omega [L_0] \\
 [\tilde{Y}] &= j\omega [C_0]
 \end{aligned}
 \tag{3.91}$$

In this lossless case we can derive a frequency domain solution to the transmission line equations using a modal analysis as outlined in section 2.3

The diagonal modal inductance and capacitance matrices on the lossless line are given by [2]

$$\begin{aligned} [L_m] &= [T_V]^{-1} [L_0] [T_I] \\ [C_m] &= [T_I]^{-1} [C_0] [T_V] \end{aligned} \quad (3.92)$$

The impedance of the i th mode is then

$$Z_{m,i} = \sqrt{\frac{L_{m,i}}{C_{m,i}}} \quad (3.93)$$

The modal transformation matrices and the modal impedances derived from the lossless line parameters are independent of frequency. It now remains to calculate the propagation correction which takes into account the frequency dependence of the transmission line losses. Taking into account the loss terms but excluding the d.c. resistance which has already been removed, the impedance and admittance matrices are

$$\begin{aligned} [\tilde{Z}'] &= [R_{int}(j\omega)] + j\omega [[L_0] + [L_{int}(j\omega)]] \\ [\tilde{Y}'] &= j\omega [[C_0] + [C_{freq}(j\omega)]] \end{aligned} \quad (3.94)$$

Having subtracted the d.c. resistance we know that $R_{int}(j\omega) = 0$ when $\omega = 0$. Also the contribution to the impedance due to the internal inductance (which is due to the field penetrating the conductors) becomes negligible compared to the inductance L_0 as $\omega \rightarrow \text{inf}$. The impedance matrix is assumed to be weakly varying with frequency which provides justification for the approximation that the modal decomposition and mode impedances are independent of frequency. In order to determine a propagation correction which incorporates the effects of loss we perform the modal decomposition on the product of the frequency dependent impedance and admittance i.e. diagonalise the matrix system

$$[\tilde{Z}'] [\tilde{Y}'] = [\tilde{T}_V] [\tilde{\gamma}^2] [\tilde{T}_V]^{-1} \quad (3.95)$$

As for the single mode transmission line the propagation correction for mode i is given by

$$H_i(j\omega) = e^{-(\gamma'_i(j\omega) - \gamma_{0,i})L} \quad (3.96)$$

Again, the propagation correction can be applied at both ends of the transmission line to give a reciprocal and symmetrical model. The propagation correction in this case is the square root of $H'(j\omega)$ i.e.

$$H'_i(j\omega) = e^{-(\gamma'_i(j\omega) - \gamma_{0,i})\frac{L}{2}} \quad (3.97)$$

The implementation of the propagation correction for each mode is identical to that described in the previous section. The derivation of the correction factor as described above relies on being able to uniquely identify each mode of the frequency dependent transmission line with a corresponding mode of the frequency independent

transmission line. The voltage transformation matrix $[T_v]$ which diagonalises the frequency dependent system in equation (7.57) has been found to be a weak function of frequency and hence the mode identification has been straightforward. We note that identifying the corresponding modes of the lossy transmission line and the lossless transmission line may require some care. In the implementation of this process we identify the modes on the lossy transmission line by identifying the closest mode of the lossless transmission line (using the vector norm as a distance measure). The propagation correction for the twisted pair model must take proper account of the domain decomposition. The propagation correction is developed as follows:

In the first stage the d.c. resistance of the conductors is lumped at the ends of the cable bundle model before the domain decomposition.

As derived in section 3.6 the propagation of the differential mode can be implemented as a simple delay line followed by a frequency dependent correction factor $H(j\omega) = e^{j(\gamma'(j\omega) - \gamma_0)L}$ where γ' takes account of the extraction of the d.c. resistance for the differential mode. The differential mode current sees the twice the impedance contribution of a single wire i.e. $(2R_{dc})$, twice the resistance of a single wires is subtracted.

$$\gamma'(j\omega) = \sqrt{(Z_{int}(j\omega) + j\omega L_{DM}(j\omega))(j\omega C_{DM}(j\omega))} \quad (3.98)$$

The common mode is slightly different in that the common mode current is distributed between the two twisted pair conductors in parallel so the contribution to the loss of the common mode is $(\frac{1}{2}R_{dc})$, i.e half the resistance of a single wires is subtracted (note that any resistance in the common mode return must be subtracted too).

3.7 Transfer Impedance Model

The spice model for transfer impedance coupling through cable shields uses a weak form of transfer impedance coupling i.e. the coupling is assumed to be in one direction only from source to victim domains. This requires identification of the source and victim domains by the user in each scenario. Transfer admittance is not included in the shield coupling model.

In this work the transfer impedance is assumed to take the form of a rational function in $j\omega$ i.e.

$$Z_T(j\omega) = \frac{a_0 + a_1 \left(\frac{j\omega}{\omega_0}\right) + a_2 \left(\frac{j\omega}{\omega_0}\right)^2 + \dots}{b_0 + b_1 \left(\frac{j\omega}{\omega_0}\right) + b_2 \left(\frac{j\omega}{\omega_0}\right)^2 + \dots} \quad (3.99)$$

where ω_0 is a normalisation constant to and the expansion can be taken up to any order required. Note that this model includes the common $Z_T = R_T + j\omega L_T$ model as a particular case. The transfer impedance of a shield is reciprocal thus the coupling through the shield is determined by the same transfer impedance for both coupling directions.

The model will be derived initially for a single mode in the source and victim domain before generalising to the multi-mode situation. In the derivation losses are assumed to be zero as we are using the 'propagation correction' model in which the effect of losses are lumped into the terminations as a lumped d.c. resistance and a propagation correction applied to the forward and backward modes on the transmission line.

The transfer impedance model derivation starts from the frequency domain equations for propagation in the victim domain.

$$\begin{aligned} \frac{\partial}{\partial z} \left(\tilde{V}_v(z) \right) + j\omega [L] \left(\tilde{I}_v(z) \right) &= \tilde{V}_{ZT,v}(z) \\ \frac{\partial}{\partial z} \left(\tilde{I}_v(z) \right) + j\omega [C] \left(\tilde{V}_v(z) \right) &= 0 \end{aligned} \quad (3.100)$$

in which the voltage source on the right hand side is due to transfer impedance coupling from source to victim domain and is given by the product of the frequency dependent transfer impedance and the shield current in the source domain.

$$\tilde{V}_{ZT,v}(z) = \tilde{Z}'_T(z) \tilde{I}_s(z) \quad (3.101)$$

We note here that for the transfer impedance in equation 3.101, \tilde{Z}'_T the d.c. part of the transfer impedance has been subtracted. This is a consequence of the extraction of the d.c. resistance of conductors being lumped at the transmission line terminations where we note that the transfer impedance of a shield is equal to the d.c. resistance of the shield and lumping this at the terminations of the transmission line means that the d.c. transfer impedance coupling is already included in the model (we also observe that the d.c. transfer impedance coupling will always be present in the model and is included in a self consistent manner in the model) thus

$$\tilde{Z}'_T(\omega) = \tilde{Z}_T(\omega) - \tilde{Z}_T(\omega = 0) \quad (3.102)$$

It has been found that this approximation can lead to errors at high frequency for shielded cables whose shields are terminated with very low (comparable with the shield resistance at d.c. or less). In this situation, improved results are obtained by excluding the R_{dc} value from the process of lumping the d.c. resistances at the terminations and keeping it in the transfer impedance model. A flag is available when running the software to use this alternative model. The price to be paid for this is accuracy of the model at low frequency. It is recommended that a suitable validation test be run to test which model is most appropriate in any given circumstance.

The voltage and current in the source domain are expressed using the sum and difference of forward and backward voltage waves (characteristic variables) as in equation 3.51 i.e.

$$\begin{aligned}\tilde{V}_s(z) &= \frac{1}{2} \left(\tilde{V}_s^+(0) e^{-j\beta_s z} + \tilde{V}_s^-(L) e^{j\beta_s(z-L)} \right) \\ \tilde{I}_s(z) &= \frac{1}{2Z_s} \left(\tilde{V}_s^+(0) e^{-j\beta_s z} - \tilde{V}_s^-(L) e^{j\beta_s(z-L)} \right)\end{aligned}\quad (3.103)$$

where the forward and backward voltage waves are

$$\begin{aligned}\tilde{V}_s^+(0) &= H'_s \left(\tilde{V}_s(0) + Z_s \tilde{I}_s(0) \right) \\ \tilde{V}_s^-(L) &= H'_s \left(\tilde{V}_s(L) - Z_s \tilde{I}_s(L) \right)\end{aligned}\quad (3.104)$$

where the propagation correction, H'_s has been applied in the source domain to determine the characteristics in the source domain.

In the victim domain the characteristics incident at the terminations, and subsequently corrected for the victim domain propagation by H'_v , are given by the sum of two contributions. The first comes from waves launched from the terminations in the victim domain and the second from the transfer impedance distributed sources i.e.

$$\begin{aligned}\tilde{V}_v^+(L) &= \tilde{V}_v(L) + Z_v \tilde{I}_v(L) = H'_v \tilde{V}_v^+(0) e^{-j\beta_v L} + H'_v \tilde{V}_{L,ZT,v}^+ \\ \tilde{V}_v^-(0) &= \tilde{V}_v(0) - Z_v \tilde{I}_v(0) = H'_v \tilde{V}_v^-(L) e^{-j\beta_v L} + H'_v \tilde{V}_{0,ZT,v}^-\end{aligned}\quad (3.105)$$

where the waves launched from the terminations are found as

$$\begin{aligned}\tilde{V}_v^+(0) &= H'_v \left(\tilde{V}_v(0) + Z_v \tilde{I}_v(0) \right) \\ \tilde{V}_v^-(L) &= H'_v \left(\tilde{V}_v(L) - Z_v \tilde{I}_v(L) \right)\end{aligned}\quad (3.106)$$

and where $\tilde{V}_{L,ZT,v}^+$ is the voltage wave in the $+z$ direction resulting from the transfer impedance coupling, received at the $z = L$ termination. Similarly, $\tilde{V}_{0,ZT,v}^-$ is the voltage wave in the $-z$ direction resulting from the transfer impedance coupling, received at the $z = 0$ termination. The current in the source domain transmission line is given by equation 3.103. The distributed voltage source on the victim transmission line is therefore given by

$$\tilde{V}_{ZT,v}(z) = \tilde{Z}'_T(z) \tilde{I}_s(z) = \frac{Z'_T(\omega)}{2Z_s} \left(\tilde{V}_s^+(0) e^{-j\beta_s z} - \tilde{V}_s^-(L) e^{j\beta_s(z-L)} \right)\quad (3.107)$$

At a point z on the victim transmission line, a voltage source $\tilde{V}_{ZT,v} dz$ launches waves in both the $-z$ and $+z$ directions. The waves in the $-z$ direction has amplitude

$$V^- dz = -\frac{\tilde{V}_{ZT,v} dz}{2} \quad (3.108)$$

and the wave in the $+z$ direction has amplitude

$$V^+ dz = +\frac{\tilde{V}_{ZT,v} dz}{2} \quad (3.109)$$

The currents associated with the waves are

$$I^- dz = \frac{\tilde{V}_{ZT,v} dz}{2Z_v} \quad (3.110)$$

and

$$I^+ dz = \frac{\tilde{V}_{ZT,v} dz}{2Z_v} \quad (3.111)$$

Therefore the characteristic variables (section 3.5) for the $-z$ travelling wave is

$$2V^- dz = \tilde{V} - Z_v \tilde{I} = -\tilde{V}_{ZT,v} dz \quad (3.112)$$

and for the $+z$ travelling wave it is

$$2V^+ dz = \tilde{V} + Z_v \tilde{I} = \tilde{V}_{ZT,v} dz \quad (3.113)$$

Thus the contribution to the $-z$ travelling wave arriving at the $z=0$ termination of the victim transmission line is found by integrating the distributed contributions to the $-z$ travelling wave from 0 to L i.e.

$$\begin{aligned} \tilde{V}_{0,ZT,v}^- &= \int_0^L 2V^-(z) dz \\ &= \int_0^L -\tilde{V}_{ZT,v}(z) dz \\ &= -\int_0^L \frac{Z'_T(\omega)}{2Z_s} \left(\tilde{V}_s^+(0) e^{-j\beta_s z} - \tilde{V}_s^-(L) e^{j\beta_s(z-L)} \right) e^{-j\beta_v z} dz \\ &= -\frac{Z'_T(\omega)}{2Z_s} \int_0^L \left(\tilde{V}_s^+(0) e^{-j(\beta_s+\beta_v)z} - \tilde{V}_s^-(L) e^{-j\beta_s L} e^{j(\beta_s-\beta_v)z} \right) dz \end{aligned} \quad (3.114)$$

The contribution to the $+z$ travelling wave at the $z=L$ termination is found by integrating the distributed contributions from $z=0$ to $z=L$

$$\begin{aligned} \tilde{V}_{L,ZT,v}^+ &= \int_0^L 2V^+(z) dz \\ &= \int_0^L \tilde{V}_{ZT,v}(z) dz \\ &= \int_0^L \frac{Z'_T(\omega)}{2Z_s} \left(\tilde{V}_s^+(0) e^{-j\beta_s z} - \tilde{V}_s^-(L) e^{j\beta_s(z-L)} \right) e^{-j\beta_v(L-z)} dz \\ &= \frac{Z'_T(\omega)}{2Z_s} \int_0^L \left(\tilde{V}_s^+(0) e^{-j\beta_v L} e^{-j(\beta_s-\beta_v)z} - \tilde{V}_s^-(L) e^{-j(\beta_s+\beta_v)(L-z)} \right) dz \end{aligned} \quad (3.115)$$

In the time domain these equations become

$$\begin{aligned}\tilde{V}_v^-(0) &= V_v(0, t) - Z_v I_v(0, t) \\ &= H'_v(t) * \tilde{V}_v^-(L, t - T_V) + H'_v(t) * V_{0,ZT,v}^-(t)\end{aligned}\quad (3.116)$$

where T_v is the time delay of the victim transmission line.

The first term in these equations are the method of characteristics propagation model already described in section 3.5.

The time domain source terms due to the transfer impedance coupling is described term by term as follows. Firstly the two terms contributing to the -z travelling wave arriving at the z=0 termination of the victim transmission line, $V_{0,ZT,v}^-$ in equation 3.114

-z propagation, term1: contribution to $V_{0,ZT,v}^-$ from the +z wave in the source transmission line:

$$\begin{aligned}-\frac{Z'_T(\omega)}{2Z_s} \int_0^L \tilde{V}_s^+(0) e^{-j(\beta_s + \beta_v)z} dz = \\ -\frac{1}{2Z_s} \left(-\frac{Z'_T(\omega)}{j\omega} \left(\frac{L}{T_z + T_v} \right) \left(1 - e^{-j(\beta_s + \beta_v)L} \right) \tilde{V}_s^+(0) \right)\end{aligned}\quad (3.117)$$

Transforming to the time domain gives

$$\begin{aligned}\frac{1}{2Z_s} \frac{Z'_T(\omega)}{j\omega} \left(\frac{L}{T_z + T_v} \right) \left(1 - e^{-j(\beta_s + \beta_v)L} \right) \tilde{V}_s^+(0) \leftrightarrow \\ \frac{1}{2Z_s} \left(\frac{L}{T_s + T_v} \right) H'_{ZT} * (V_s^+(0, t) - V_s^+(0, t - T_s - T_v))\end{aligned}\quad (3.118)$$

where the z-domain transfer function $H'_{ZT}(j\omega) = \frac{Z'_T(j\omega)}{j\omega}$ and $H'_{ZT}(t)$ is the impulse response of this transfer function.

-z propagation, Term2: contribution to $V_{0,ZT,v}^-$ from the -z wave in the source transmission line:

$$\begin{aligned}\frac{Z'_T(\omega)}{2Z_s} \int_0^L \tilde{V}_s^-(L) e^{-j(\beta_s L)} e^{j(\beta_s - \beta_v)z} dz \leftrightarrow \\ \frac{1}{2Z_s} \left(\frac{L}{T_s - T_v} \right) H'_{ZT} * (V_s^-(L, t - T_v) - V_s^-(L, t - T_s))\end{aligned}\quad (3.119)$$

In a similar manner, the characteristic variables incident at the +z termination are expressed in the time domain as

$$\begin{aligned}\tilde{V}_v^+(L) &= V_v(L, t) + Z_v I_v(L, t) \\ &= H'_v(t) * \tilde{V}_v^+(0, t - T_V) + H'_v(t) * V_{L,ZT,v}^+(t)\end{aligned}\quad (3.120)$$

Secondly the two terms contributing to the +z travelling wave arriving at the z=L termination of the victim transmission line, $V_{L,ZT,v}^+$ in equation 3.115.

+z propagation, term1: contribution to $V_{L,ZT,v}^+$ from the +z wave in the source transmission line:

$$\begin{aligned} \frac{Z'_T(\omega)}{2Z_s} \int_0^L \tilde{V}_s^+(0) e^{-j(\beta_v L)} e^{-j(\beta_s - \beta_v)z} dz \leftrightarrow \\ \frac{1}{2Z_s} \left(\frac{L}{T_s - T_v} \right) H'_{ZT} * (V_s^+(0, t - T_v) - V_s^+(0, t - T_s)) \end{aligned} \quad (3.121)$$

+z propagation, term2: contribution to $V_{L,ZT,v}^+$ from the -z wave in the source transmission line:

$$\begin{aligned} - \frac{Z'_T(\omega)}{2Z_s} \int_0^L \tilde{V}_s^-(L) e^{-j(\beta_s + \beta_v)(L-z)} dz \leftrightarrow \\ - \frac{1}{2Z_s} \left(\frac{L}{T_s + T_v} \right) H'_{ZT} * (V_s^-(L, t) - V_s^-(L, t - T_s - T_v)) \end{aligned} \quad (3.122)$$

3.7.1 Multiple mode propagation

The above theory is readily extended to the case of multi-mode systems, both in the source and victim domains. First we will discuss how to manage a multi-mode source domain before going on to derive the model for multi-mode victim domain.

multiple modes in the source domain

If there is more than one mode in the source domain then we must take into account that multiple modes can contribute to the shield current. There are two scenarios in which the shield is or is not the reference conductor for the source domain. These two scenarios must be treated separately.

If the shield is **not** the reference conductor in the source domain then the conductor currents are related to the mode currents by

$$\left(\tilde{I} \right) = \left[\tilde{T}_I \right] \left(\tilde{I}_m \right) \quad (3.123)$$

thus the shield current can be expressed in terms of the individual mode currents as

$$I_{shield} \sim = \sum_{i=1}^{N_m} T_{I,shield,i} \tilde{I}_{m,i} \quad (3.124)$$

If the shield is the reference conductor then the reference conductor current is found as minus the sum of the currents on all the other conductors in the domain i.e.

$$\begin{aligned} I_{shield} \sim &= - \sum_{j=1}^{N_m} \tilde{I}_j \\ &= - \sum_{j=1}^{N_m} \left(\sum_{i=1}^{N_m} T_{I,j,i} \tilde{I}_{m,i} \right) \\ &= \sum_{i=1}^{N_m} \left(- \sum_{j=1}^{N_m} T_{I,j,i} \right) \tilde{I}_{m,i} \end{aligned} \quad (3.125)$$

In either case the shield current is expressed as a linear combination of the individual mode currents in the source domain i.e.

$$I_{shield}^{\sim} = \sum_{i=1}^{N_m} P_{s,i} I_{m,i}^{\sim} \quad (3.126)$$

where $P_{s,i}$ is the coefficient of the i^{th} mode contribution.

multiple modes in the victim domain

The voltage source in the victim domain appears only on the shield conductor therefore each victim domain mode vm may receive a contribution from this source term . source and victim domains.

If there are multiple modes in the victim domain there are again two situations which need to be treated separately dependent on whether the shield is or is not the reference conductor of the domain. In the victim domain the weak transfer impedance coupling model gives a voltage source on the shield conductor $V_{s,ZT} = Z_T I_{shield}$.

If the shield is **not** the reference conductor then the modal voltage can be related to the individual conductor voltages by

$$\left(\tilde{V}_m \right) = \left[T_V^{-1} \right] \left(\tilde{V} \right) \quad (3.127)$$

thus the modal voltage source for mode i is found as

$$\left(\tilde{V}_{m,i} \right) = T_{V,i,shield}^{-1} \left(V_{s,ZT} \right) \quad (3.128)$$

If the shield **is** the reference conductor in the victim domain then all the other conductors have a source voltages $-V_{s,ZT}$ on them. The modal voltage source for mode i is found as

$$\left(\tilde{V}_{m,i} \right) = - \sum_{j=1}^{N_m} T_{V,i,j}^{-1} \left(V_{s,ZT} \right) \quad (3.129)$$

Again, in either case, the contribution to mode i has a weighting factor $P_{v,i}$

$$\left(\tilde{V}_{m,i} \right) = P_{v,i} V_{s,ZT} \quad (3.130)$$

multiple modes in the source domain and victim domains

In order to generalise the transfer impedance coupling model to multiple source and victim domains, equations 3.116 and 3.120 must be generalised. This is done by recognising that if there are ns source domain modes and nv victim domain modes then there are $ns \times nv$ contributions to the transfer impedance coupling i.e. there is a contribution relating to every combination of source and victim modes.

The contribution from source mode, s_i , to victim mode, v_j , is readily found using the weighted values in equations 3.126 and 3.130.

In this case equations 3.116 and 3.120 become:

$$\begin{aligned}
 \tilde{V}_{vj}^+(L, t) &= V_{vj}(L, t) + Z_{vj}I_{vj}(L, t) \\
 &= H'_{vj}(t) * \tilde{V}_{vj}^+(0, t - T_{Vj}) + \frac{P_{s,i}P_{v,j}}{2Z_{si}} H_{ZT} * H'_{vj}(t) * \\
 &\quad \left(\left(\frac{L}{T_{si} - T_{vj}} \right) (V_{si}^+(0, t - T_v) - V_{si}^+(0, t - T_{si})) \right. \\
 &\quad \left. - \left(\frac{L}{T_{si} + T_{vj}} \right) (V_{si}^-(L, t) - V_{si}^-(L, t - T_{si} - T_{vj})) \right)
 \end{aligned} \tag{3.131}$$

and

$$\begin{aligned}
 \tilde{V}_{vj}^-(0, t) &= V_{vj}(0, t) - Z_{vj}I_{vj}(0, t) \\
 &= H'_{vj}(t) * \tilde{V}_{vj}^-(L, t - T_v) - \frac{P_{s,i}P_{v,j}}{2Z_{si}} H_{ZT} * H'_{vj}(t) * \\
 &\quad \left(\left(\frac{L}{T_{si} + T_{vj}} \right) (V_{si}^+(0, t) - V_{si}^+(0, t - T_{si} - T_{vj})) \right. \\
 &\quad \left. - \left(\frac{L}{T_{si} - T_{vj}} \right) (V_{si}^-(L, t - T_{vj}) - V_{si}^-(L, t - T_{si})) \right)
 \end{aligned} \tag{3.132}$$

3.7.2 Spice circuit for Transfer Impedance model

The transfer impedance model equations may be implemented in spice using controlled sources, delay lines plus s-domain transfer functions to implement the frequency dependent transfer functions/ time domain convolutions. The Spice model for the main method of characteristics propagation model for source domain mode smi, and victim domain model, vmi are seen in figure 3.12

The following delay lines are also required in addition to the delay lines required to implement the method of characteristics in the source and victim domains:

1. Delay line for $V_{si}^+(0, t - T_{si} - T_{vi})$
2. Delay line for $V_{si}^+(0, t - T_{vi})$
3. Delay line for $V_{si}^-(0, t - T_{si} - T_{vi})$
4. Delay line for $V_{si}^-(0, t - T_{vi})$

The Spice model for these elements is shown in figure 3.13

When $T_s = T_v$ there is a problem implementing equations 3.119 and 3.121 in Spice. in this case it can be shown that as $T_s \rightarrow T_v$ equation 3.119 becomes

$$\begin{aligned}
 \frac{1}{2Z_s} \left(\frac{L}{T_s - T_v} \right) H_{ZT} * (V_s^-(L, t - T_v) - V_s^-(L, t - T_s)) \rightarrow \\
 \frac{L}{2Z_s} H_{ZT} * \frac{dV_s^-(0, t - T_v)}{dt}
 \end{aligned} \tag{3.133}$$

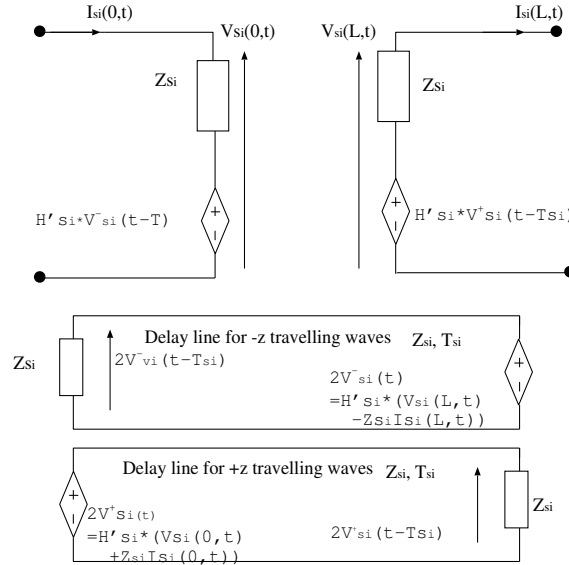
The time derivative may be implemented in Spice using a 1H inductor in parallel with a current source of value $V_s^+(0, t - T_v)$ whose voltage will provide the time derivative as shown in figure 3.14 Similarly, equation 3.121 becomes

$$\frac{1}{2Z_s} \left(\frac{L}{T_s - T_v} \right) H_{ZT} * (V_s^+(0, t - T_v) - V_s^+(0, t - T_s)) \rightarrow \frac{L}{2Z_s} \frac{dV_s^+(0, t - T_v)}{dt} \quad (3.134)$$

and the Spice circuit takes a similar form to that shown in figure 3.14

Controlled sources with s-domain transfer functions implement the convolutions in equations 3.118, 3.119, 3.121 and 3.122.

Source Domain method of characteristics circuit mode i



Victim Domain method of characteristics circuit, mode j

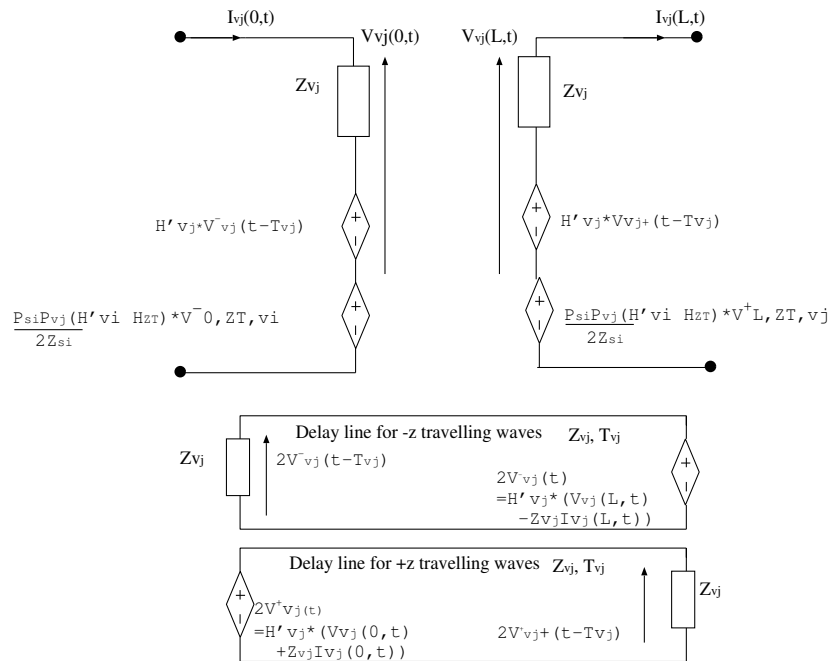


Figure 3.12 Spice circuit for the simulation of source and victim domain modes with the method of characteristics with additional source term for transfer impedance coupling

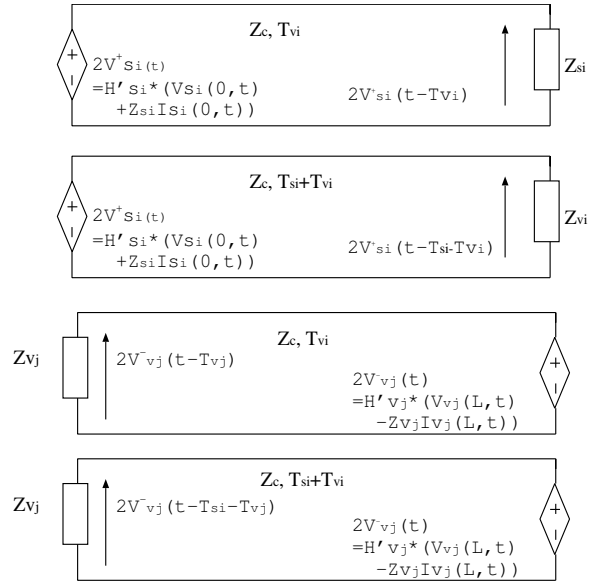


Figure 3.13 Spice circuit for the simulation of source and victim domain modes with the method of characteristics: Delay lines for transfer impedance course term

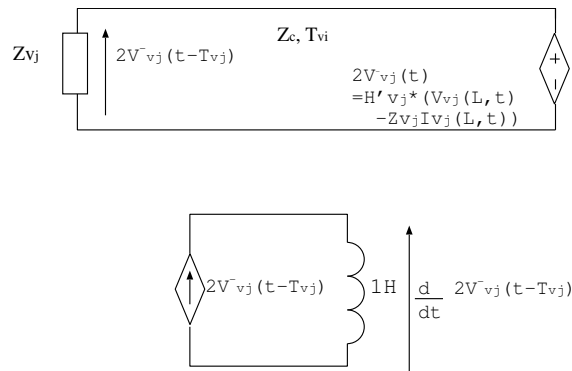


Figure 3.14 Spice circuit for the special case $T_s = T_v$

3.8 Spice Incident Field Excitation Model

The model for the incident field excitation is based on that described in reference [2]. For the purposes of incident field excitation analysis the axis of the cable bundle is assumed to be in the z direction. The direction of the incident field plane wave is specified by its wave vector in polar coordinates (figure 3.15)

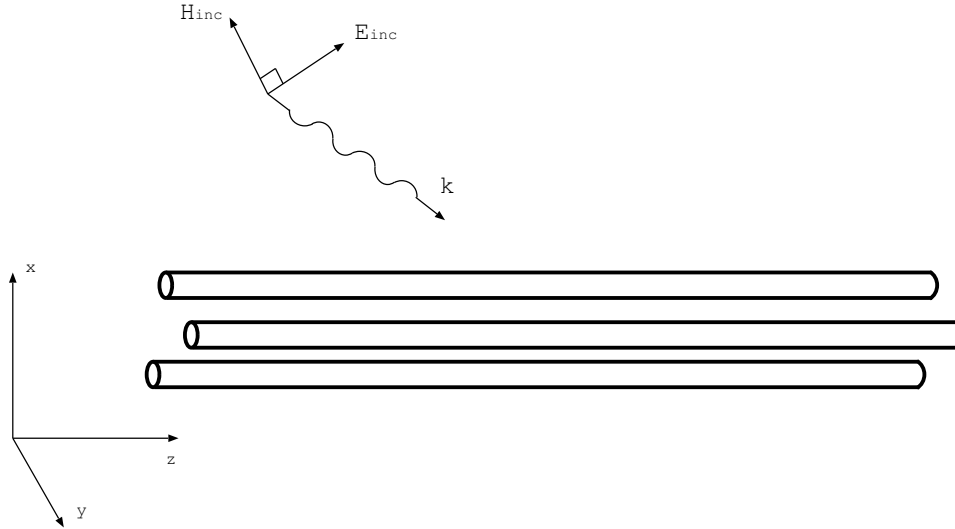


Figure 3.15 Specification of the incident field

The wave vector in cartesian coordinates is

$$\begin{aligned} k_x &= k_0 \sin(\theta) \cos(\phi) \\ k_y &= k_0 \sin(\theta) \sin(\phi) \\ k_z &= k_0 \cos(\theta) \end{aligned} \quad (3.135)$$

where $k_0 = \frac{\omega}{c}$ The wave velocity vector in cartesian coordinates is

$$\begin{aligned} v_x &= \frac{\omega}{k_x} \\ v_y &= \frac{\omega}{k_y} \\ v_z &= \frac{\omega}{k_z} \end{aligned} \quad (3.136)$$

Given this k vector unit vectors in the θ and ϕ directions can be defined. The Electric field polarisation direction is specified in terms of these vectors as shown in figure 3.16 Thus the θ and ϕ unit vectors are given by

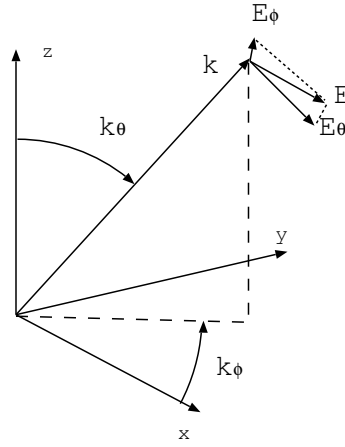


Figure 3.16 Specification of the incident field polarisation

$$\begin{aligned}\theta_x &= \cos(\theta) \cos(\phi) \\ \theta_y &= \cos(\theta) \sin(\phi)\end{aligned}\tag{3.137}$$

$$\theta_z = \sin(\theta)$$

$$\begin{aligned}\phi_x &= \sin(\phi) \\ \phi_y &= \cos(\phi)\end{aligned}\tag{3.138}$$

$$\phi_z = 0$$

and thus the polarisation vector is

$$\begin{aligned}e_x &= E_\theta \theta_x + E_\phi \phi_x \\ e_y &= E_\theta \theta_y + E_\phi \phi_y \\ e_z &= E_\theta \theta_z + E_\phi \phi_z\end{aligned}\tag{3.139}$$

The frequency domain electric field is given by

$$\begin{aligned}E_x &= E_0(\omega) e^{-j(k_x x + k_y y + k_z z)} e_x \\ E_y &= E_0(\omega) e^{-j(k_x x + k_y y + k_z z)} e_y \\ E_z &= E_0(\omega) e^{-j(k_x x + k_y y + k_z z)} e_z\end{aligned}\tag{3.140}$$

The time domain electric field is given by

$$\begin{aligned} E_x &= E_0 \left(t - \frac{x}{v_x} - \frac{y}{v_y} - \frac{z}{v_z} \right) e_x \\ E_y &= E_0 \left(t - \frac{x}{v_x} - \frac{y}{v_y} - \frac{z}{v_z} \right) e_y \\ E_z &= E_0 \left(t - \frac{x}{v_x} - \frac{y}{v_y} - \frac{z}{v_z} \right) e_z \end{aligned} \quad (3.141)$$

The magnetic field components are given by

$$H = \frac{(k \times E)}{Z_0} \quad (3.142)$$

where Z_0 is the impedance of free space.

Section 2.4 describes the solution for incident field excitation of a transmission line in the frequency domain. The starting point for the time domain spice model derivation for the external domain in which conductors are directly illuminated by the incident field are the frequency domain transmission line equations with distributed sources resulting from the incident field excitation

$$\begin{aligned} \frac{\partial}{\partial z} (V(z, j\omega)) + j\omega [L] (I(z, j\omega)) &= (V_F(z, j\omega)) \\ \frac{\partial}{\partial z} (I(z, j\omega)) + j\omega [C] (V(z, j\omega)) &= (I_F(z, j\omega)). \end{aligned} \quad (3.143)$$

We have assumed that the transmission line is lossless here however we will introduce the propagation correction to the incident field excitation terms in the method of characteristics solution so losses will be taken into account in the same manner as for the propagation model.

The voltages and currents at the ends of the transmission line can be related by the chain parameters

$$\begin{aligned} V(L) &= \Phi_{11}(L) V(0) + \Phi_{12}(L) I(0) + V_{FT}(L) \\ I(L) &= \Phi_{21}(L) V(0) + \Phi_{22}(L) I(0) + I_{FT}(L) \end{aligned} \quad (3.144)$$

where the incident field contribution appears as lumped voltage and current sources at the line termination $z = L$. The chain parameters, Φ_{11} , Φ_{12} , Φ_{21} and Φ_{22} are given by equation 2.58. The spice model will be constructed in this form with the effect of the incident field excitation being implemented using source terms at one end of the transmission line. These lumped source terms are given by the convolutions

$$\begin{aligned} V_{FT}(L) &= \int_0^L \Phi_{11}(L-z) V_F(z) + \Phi_{12}(L-z) I_F(z) dz \\ I_{FT}(L) &= \int_0^L \Phi_{21}(L-z) V_F(z) + \Phi_{22}(L-z) I_F(z) dz \end{aligned} \quad (3.145)$$

The spice multi-conductor propagation model is based on modal decomposition so we proceed by transforming equation 3.144 to modal quantities

$$\begin{aligned} V_m(L) &= \Phi_{m11}(L) V_m(0) + \Phi_{m12}(L) I_m(0) + V_{FTm}(L) \\ I_m(L) &= \Phi_{m21}(L) V_m(0) + \Phi_{m22}(L) I_m(0) + I_{FTm}(L) \end{aligned} \quad (3.146)$$

where the (diagonal) modal chain parameter matrices are given by

$$\begin{aligned}
 \Phi_{m11}(L) &= [T_V]^{-1} \Phi_{11}(L) [T_V] \\
 &= \cosh(\gamma_m L) \\
 \Phi_{m12}(L) &= [T_V]^{-1} \Phi_{12}(L) [T_I] \\
 &= -[Z_m] \sinh(\gamma_m L) \\
 \Phi_{m21}(L) &= [T_I]^{-1} \Phi_{21}(L) [T_V] \\
 &= -\sinh(\gamma_m L) [Z_m]^{-1} \\
 \Phi_{m22}(L) &= [T_I]^{-1} \Phi_{22}(L) [T_I] \\
 &= \cosh(\gamma_m L)
 \end{aligned} \tag{3.147}$$

and the modal forcing functions (using the properties of the modal decomposition matrices in equations 3.34) may be expressed as

$$\begin{aligned}
 V_{FTm}(L) &= [T_V]^{-1} V_{FT}(L) \\
 &= \int_0^L \cosh(\gamma_m L - z) V_{Fm}(z) \\
 &\quad - \sinh(\gamma_m L - z) [Z_{cm}] I_{Fm}(z) dz
 \end{aligned} \tag{3.148}$$

$$\begin{aligned}
 I_{FTm}(L) &= [T_I]^{-1} I_{FT}(L) \\
 &= \int_0^L -\sinh(\gamma_m L - z) [Z_{cm}]^{-1} V_{Fm}(z) \\
 &\quad + \cosh(\gamma_m L - z) I_{Fm}(z) dz
 \end{aligned} \tag{3.149}$$

where γ_m is the diagonal matrix of mode propagation constants and Z_{cm} is the diagonal matrix of mode impedances, $V_{Fm} = [T_V]^{-1} V_F$ and $I_{Fm} = [T_I]^{-1} I_F$.

The modal characteristic variables at $z = 0$ and $z = L$ are found by first substituting the modal chain parameters (equation 3.147) into the expressions for the modal voltage and current expressions (equation 3.146)

$$\begin{aligned}
 V_m(L) &= \cosh(\gamma_m L) V_m(0) - \sinh(\gamma_m L) [Z_m] I_m(0) + V_{FTm}(L) \\
 [Z_m] I_m(L) &= -\sinh(\gamma_m L) V_m(0) + \cosh(\gamma_m L) [Z_m] I_m(0) + [Z_m] I_{FTm}(L)
 \end{aligned} \tag{3.150}$$

The characteristic variables are found by adding and subtracting these equations to give

$$\begin{aligned}
 V_{m,0}^- &= V_m(0) - [Z_m] I_m(0) = e^{-\gamma_m L} [V_m(L) - [Z_m] I_m(L)] + E_{inc0}(L) \\
 V_{m,L}^+ &= V_m(L) + [Z_m] I_m(L) = e^{-\gamma_m L} [V_m(0) + [Z_m] I_m(0)] + E_{incL}(L)
 \end{aligned} \tag{3.151}$$

The incident field source terms are

$$\begin{aligned} E_{inc0}(L) &= -e^{-\gamma_m L} [V_{FTm}(L) - [Z_m] I_{FTm}(L)] \\ E_{incL}(L) &= [V_{FTm}(L) + [Z_m] I_{FTm}(L)] \end{aligned} \quad (3.152)$$

The exponential in equations 3.151 and 3.152 may be recognised as a time delay therefore equation 3.151 may be expressed in the time domain for mode i as

$$\begin{aligned} V_{m,0}^-(t) &= V_{mi}(0, t) - [Z_{mi}] I_{mi}(0, t) \\ &= [V_{mi}(L, t - T_{mi}) - [Z_{mi}] I_{mi}(L, t - T_{mi})] + E_{inc0,i}(L, t) \\ V_{m,0}^+(t) &= V_{mi}(L, t) + [Z_{mi}] I_{mi}(L, t) \\ &= [V_{mi}(0, t - T_{mi}) + [Z_{mi}] I_{mi}(0, t - T_{mi})] + E_{incL,i}(L, t) \end{aligned} \quad (3.153)$$

T_{mi} is the delay in mode i, propagating a distance L.

$$T_{mi} = \frac{L}{v_{mi}} = \frac{\gamma_{mi} L}{j\omega} \quad (3.154)$$

Equations 3.151 express the method of characteristics based model as described in section 3.5 with the addition of sources which model the effect of the incident field coupling. In order to develop a viable Spice model for incident field coupling, we need to develop a circuit model for the time domain source terms $E_{inc0,i}(L, t)$ and $E_{incL,i}(L, t)$

If the incident field takes the form of a plane wave then the source terms $E_{inc0,i}(L, t)$ and $E_{incL,i}(L, t)$ may be derived analytically to give a complete time domainspice model for incident field excitation of multi-conductor transmission lines which may be implemented using delay lines and controlled sources.

Substituting the expressions for the distributed incident field sources 2.53 and 2.56, transformed to the frequency domain, with the Electric field expressions for a plane wave (3.140) allows the evaluation of the modal forcing functions in equations 3.148 and 3.149. The modal incident field transmission line source functions may be written in terms of the transverse and longitudinal electric field contributions $E_T(z)$ and $E_L(z)$ respectively

$$\begin{aligned} E_{inc0}(L) &= -e^{-\gamma_m L} [V_{FTm}(L) - [Z_m] I_{FTm}(L)] \\ &= -\int_0^L e^{-\gamma_m z} [T_I]^t E_L(z) dz \\ &\quad - e^{-\gamma_m L} [T_I]^t E_T(L) - [T_I]^t E_T(0) \\ E_{incL}(L) &= [V_{FTm}(L) + [Z_m] I_{FTm}(L)] \\ &= \int_0^L e^{-\gamma_m(L-z)} [T_I]^t E_L(z) dz \\ &\quad - [T_I]^t E_T(L) + e^{-\gamma_m L} [T_I]^t E_T(0) \end{aligned} \quad (3.155)$$

where the transverse electric field contribution for the incident field expression given in equation 3.140 for conductor k is

$$\begin{aligned}
 E_T(z)_k &= \int_{ref}^{conductor i} E^{inc}(\omega) \cdot dl \\
 &= \int_0^{d_k} E_{inc}(\omega) \left(e_x \frac{x_k - x_0}{d_i} + e_y \frac{y_k - y_0}{d_k} \right) e^{-jk_z z} e^{-j \left(k_x \frac{x_s - x_0}{d_k} + k_y \frac{y_s - x_0}{d_k} \right)} dl \\
 &= E_{inc}(\omega) \left(e_x \frac{x_k - x_0}{d_k} + e_y \frac{y_k - y_0}{d_k} \right) e^{-jk_z z} e^{j \left(k_x \frac{x_0}{d_k} + k_y \frac{y_0}{d_k} \right)} \int_0^{d_k} e^{-j \left(k_x \frac{x}{d_k} + k_y \frac{y}{d_k} \right) s} ds \\
 &= E_{inc}(\omega) (e_x (x_k - x_0) + e_y (y_k - y_0)) e^{-jk_z z} e^{j \left(k_x \frac{x_0}{d_k} + k_y \frac{y_0}{d_k} \right)} e^{-j \psi_k} \frac{\sin(\psi_k)}{\psi_k}
 \end{aligned} \tag{3.156}$$

where (x_k, y_k) is the position of the kth conductor in the x-y plane, (x_0, y_0) is the position of the reference conductor in the x-y plane and d_k is the distance between these conductors and

$$\psi_k = \frac{k_x x_k + k_y y_k}{2} \tag{3.157}$$

If we assume that the origin in the x-y plane is at the position of the reference conductor then we can write

$$E_T(z)_k = E_{inc}(\omega) (e_x x_k + e_y y_k) e^{-jk_z z} e^{-j \psi_k} \frac{\sin(\psi_k)}{\psi_k} \tag{3.158}$$

The contribution from the longitudinal field is

$$\begin{aligned}
 E_L(z)_i &= E_0(\omega) (e^{-j(k_x x_k + k_y y_k + k_z z)} - e^{-j(k_z z)}) \\
 &= E_0(\omega) e^{-jk_z z} (e^{-j(k_x x_k + k_y y_k)} - 1) \\
 &= -j(k_x x_k + k_y y_k) E_0(\omega) e^{-j \psi_k} \frac{\sin(\psi_k)}{\psi_k} e^{-jk_z z}
 \end{aligned} \tag{3.159}$$

The shift of the origin of the cross section coordinate system will only have the effect of adding a timeshift to the incident field function.

The cross section time delay is defined for conductor k as

$$T_{xyk} = \frac{x_k - x_0}{v_x} + \frac{y_k - y_0}{v_y} \tag{3.160}$$

The time delay for the incident field to travel the length of the transmission line is denoted T_z and the delay for mode i is denoted T_i where

$$T_z = \frac{L}{v_z} \tag{3.161}$$

and

$$T_i = \frac{L}{v_i} = \frac{\gamma_i L}{j\omega} \quad (3.162)$$

Following [2] equations 3.152 can be expressed for each mode i as

$$E_{inc0}(L)_i = E_0(\omega) \sum_{k=1}^n \left\{ \left[\frac{\sin(\psi_k)}{\psi_k} \right] [T_I]_{i,k}^t \right. \\ \left. [e_z T_{xyk} L + (e_x x_k + e_y y_k) (T_i - T_z)] \left[\frac{e^{-j\omega(T_{xyk}/2)} - e^{-j\omega(T_i + T_z + T_{xyk}/2)}}{(T_i + T_z)} \right] \right\} \quad (3.163)$$

$$E_{incL}(L)_i = E_0(\omega) \sum_{k=1}^n \left\{ \left[\frac{\sin(\psi_k)}{\psi_k} \right] [T_I]_{i,k}^t \right. \\ \left. [e_z T_{xyk} L + (e_x x_k + e_y y_k) (T_i - T_z)] \left[\frac{e^{-j\omega(T_i + T_{xyk}/2)} - e^{-j\omega(T_z + T_{xyk}/2)}}{(T_i - T_z)} \right] \right\} \quad (3.164)$$

The transformation to the time domain is again achieved by recognising the $e^{-j\omega T}$ terms as time delays to give

$$E_{inc0}(t)_i = \sum_{k=1}^n \left\{ [e_z T_{xyk} L - (e_x x_k + e_y y_k) (T_i + T_z)] [T_I]_{i,k}^t \right. \\ \left. p_k(t) * \frac{E_0(t - T_{xyk}/2) - E_0(t - T_i - T_z - T_{xyk}/2)}{(T_i + T_z)} \right\} \\ E_{incL}(t)_i = \sum_{k=1}^n \left\{ [e_z T_{xyk} L + (e_x x_k + e_y y_k) (T_i - T_z)] [T_I]_{i,k}^t \right. \\ \left. p_k(t) * \frac{E_0(t - T_i - T_{xyk}/2) - E_0(t - T_z - T_{xyk}/2)}{(T_i - T_z)} \right\} \quad (3.165)$$

Where $p_k(t)$ is a pulse function for the k th conductor which is convolved with the delayed incident field functions. Provided that the transmission line cross section is small it may be assumed that the pulse function is approximately an impulse function, we

may also assume that the cross section delay time is negligible. Under this assumption the convolution is eliminated and the source terms are for mode i ,

$$\begin{aligned} E_{inc0}(t)_i &= \alpha_0 \left[\frac{E_0(t) - E_0(t - T_i - T_z)}{(T_i + T_z)} \right] \\ E_{incL}(t)_i &= \alpha_L \left[\frac{E_0(t - T_i) - E_0(t - T_z)}{(T_i - T_z)} \right] \end{aligned} \quad (3.166)$$

where the vectors α_0 and α_L are for mode i

$$\begin{aligned} \alpha_{0,i} &= \sum_{k=1}^n \left\{ [e_z T_{xyk} L - (e_x x_k + e_y y_k) (T_i + T_z)] [T_I]_{i,k}^t \right\} \\ \alpha_{L,i} &= \sum_{k=1}^n \left\{ [e_z T_{xyk} L + (e_x x_k + e_y y_k) (T_i - T_z)] [T_I]_{i,k}^t \right\} \end{aligned} \quad (3.167)$$

The characteristic based expression for the incident field model in equation 3.151 may be written as

$$\begin{aligned} V_{m,0}^-(t) &= V_{mi}(0, t) - [Z_{mi}] I_{mi}(0, t) \\ &= [V_{mi}(L, t - T_{mi}) - [Z_{mi}] I_{mi}(L, t - T_{mi})] + \alpha_{0,i} \left[\frac{E_0(t) - E_0(t - T_i - T_z)}{(T_i + T_z)} \right] \\ V_{m,0}^+(t) &= V_{mi}(L, t) + [Z_{mi}] I_{mi}(L, t) \\ &= [V_{mi}(0, t - T_{mi}) + [Z_{mi}] I_{mi}(0, t - T_{mi})] + \alpha_{L,i} \left[\frac{E_0(t - T_i) - E_0(t - T_z)}{(T_i - T_z)} \right] \end{aligned} \quad (3.168)$$

These incident field source terms in this model are seen to consist of the time domain incident field function, $E_0(t)$ and delayed versions of this, each scaled by appropriate constants which are found in terms of the angle of incidence and polarisation of the incident plane wave (equations 3.167).

3.8.1 Spice circuit for Incident field excitation

The equations 3.168 may be implemented in Spice using controlled sources and delay lines. Two delay lines are required for each transmission line mode for the propagation model (delay T_i). In addition, for each mode, two delay lines with delays T_i and $T_i + T_z$ are required for the incident field and a final delay line with delay T_z is required. The structure of the Spice circuit model is shown in figure 3.17.

If $T_i = T_z$ for any mode, the second term in equation 3.168 has a zero in the denominator in this case the last term in square brackets may be rewritten as

$$\left[\frac{E_0(t - T_i) - E_0(t - T_z)}{(T_i - T_z)} \right]_{T_i \Rightarrow T_z} = \frac{d}{dt} E_0(t - T_i) \quad (3.169)$$

The time derivative may be implemented by an inductor of 1H driven by a current source as shown in figure 3.18

A second practical issue is for the case when $Tz < 0$ i.e. if $k_z < 0$ in this case the model would require negative time delays. This case is simply dealt with by reversing the transmission line terminations and k_z .

The Spice model for incident field excitation provides the incident field equivalent source in the form of the characteristic variables incident on the terminations of the transmission line i.e. $V_m(0) - Z_m I_m(0)$ and $V_m(L) - Z_m I_m(L)$. These waves require correction for the propagation losses in the transmission line. In order to include the propagation correction into the model these characteristic variables are multiplied by (convolved with) the appropriate mode propagation correction $H'(j\omega)$ giving the source terms on the transmission line terminations for mode i as

$$\begin{aligned} V_{Einc}^-(0, t) &= H'_i(t) * (V_{mi}(0, t) - [Z_{mi}] I_{mi}(0, t)) \\ V_{Einc}^+(L, t) &= H'_i(t) * (V_{mi}(L, t) + [Z_{mi}] I_{mi}(L, t)) \end{aligned} \quad (3.170)$$

3.8.2 Incident field excitation with a ground plane

If there is a ground plane present then the incident field may be expressed as the superposition of a direct wave and the wave reflected from the ground. Working through the analysis above in this case shows [2] that the effect of a ground plane can be taken into account by simply doubling the α terms in equations 3.167.

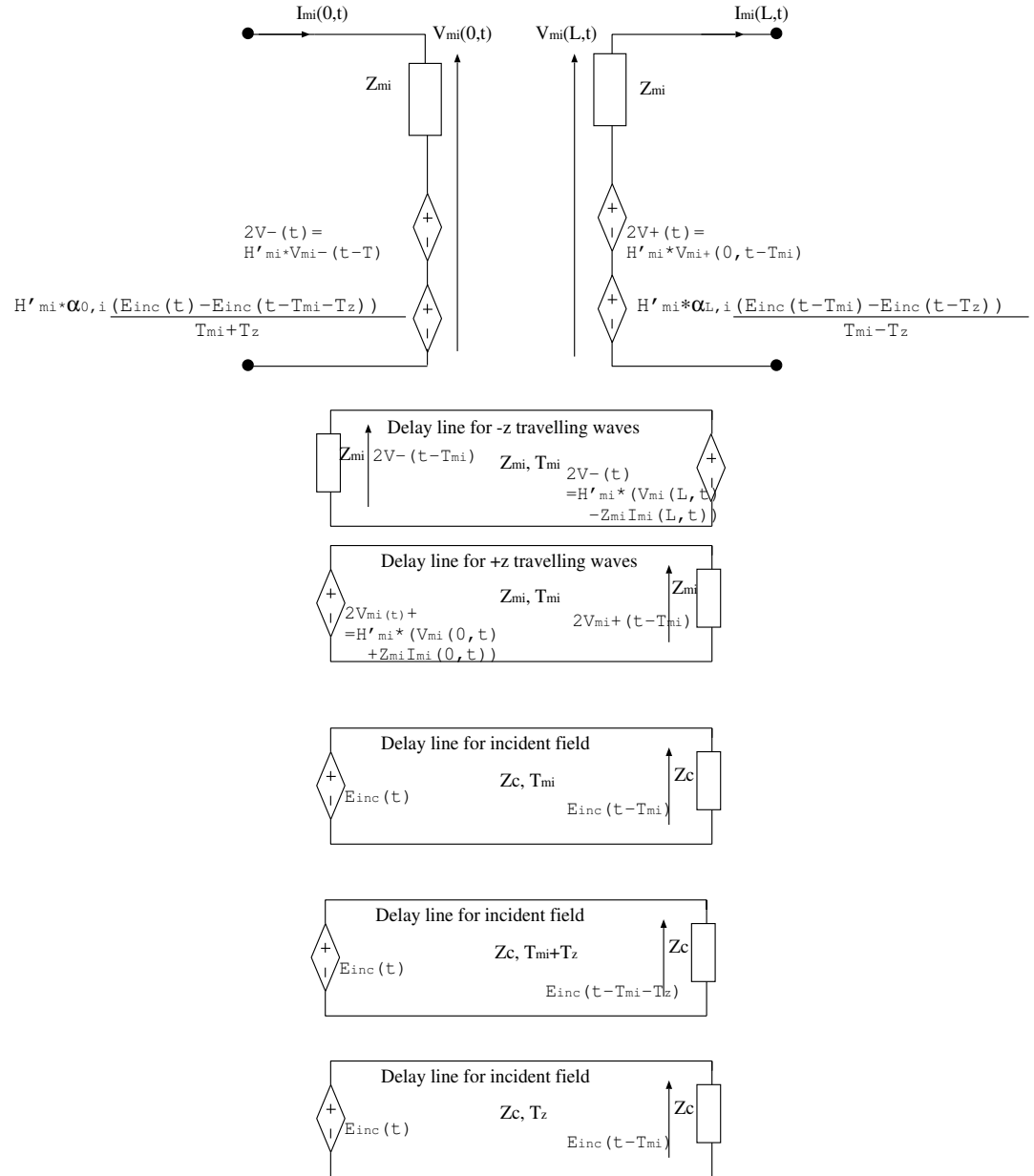


Figure 3.17 Spice circuit for the simulation of a multi-conductor transmission line illuminated by a plane wave

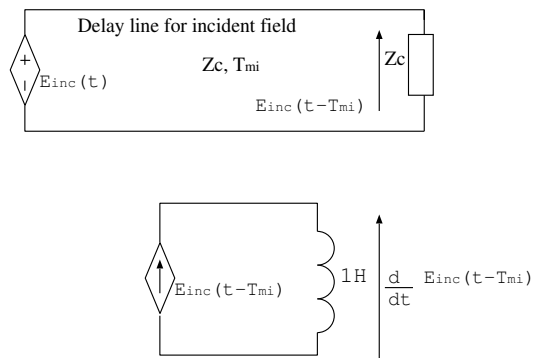


Figure 3.18 Spice circuit for the special case $T_i = T_z$

3.9 Spice Incident Field Excitation Model for shielded cables

The development of Spice models for incident field excitation and also for transfer impedance coupling have been described in sections 3.8 and 3.7. It has been shown in reference [7] that a rigorous model of incident field excitation of shielded cables can be derived. This section provides an outline of the analysis presented in reference [7] and gives the main results as implemented in the SACAMOS software.

The solution for the conductor voltage and current for a single mode, sm, in the external (source) domain may be expressed using the method of characteristics

$$V_{sm}(z) = \frac{1}{2} (V_{sm}^+(0) e^{-j\beta_{sm}z} + V_{sm}^-(L) e^{+j\beta_{sm}z} + V_{Eim}^+(z) + V_{Eim}^-(z)) \quad (3.171)$$

$$I_{sm}(z) = \frac{1}{2Z_{sm}} (V_{sm}^+(0) e^{-j\beta_{sm}z} - V_{sm}^-(L) e^{+j\beta_{sm}z} + V_{Eim}^+(z) - V_{Eim}^-(z)) \quad (3.172)$$

where:

V_{sm}^+ is the forward mode in the source domain launched from the $z = 0$ termination

V_{sm}^- is the backward mode in the source domain launched from the $z = L$ termination

$V_{Eim}^+(z)$ is the contribution to the $+z$ travelling wave due to the incident field excitation

$V_{Eim}^-(z)$ is the contribution to the $-z$ travelling wave due to the incident field excitation

and Z_{sm} and β_{sm} are the characteristic impedance and propagation constant of the mode on the lossless transmission line.

The forward mode launched from the termination at $z=0$, with the propagation correction for the mode applied is given by

$$V_{sm}^+(0) = H'_{sm} (V_{sm}(0) + Z_{sm}I_{sm}(0)) \quad (3.173)$$

the backward (-z) propagating mode launched from the termination at $z=L$ with the propagation correction for the mode applied is

$$V_{sm}^-(L) = H'_{sm} (V_{sm}(L) - Z_{sm}I_{sm}(L)) \quad (3.174)$$

The $+z$ propagating voltage wave due to the distributed incident field sources (V_F and I_F in equation 3.143) is found by integrating the contributions to this wave from 0 to z i.e.

$$V_{Eim}^+(z) = \int_0^z (V_F(\tau) + Z_{sm}I_F(\tau)) e^{-j\beta_{sm}(z-\tau)} d\tau \quad (3.175)$$

Similarly the $-z$ propagating voltage wave due to the distributed incident field sources is found as

$$V_{Eim}^-(z) = \int_L^z (V_F(\tau) - Z_{sm}I_F(\tau)) e^{+j\beta_{sm}(z-\tau)} d\tau \quad (3.176)$$

The response on the inner (victim) domain is again written in terms of the characteristic variables launched from the terminations plus an additional term related to the transfer impedance coupling from the external domain current thus the characteristic variables incident at the terminations (and with the propagation correction for the victim domain applied) are expressed as

$$\begin{aligned}\tilde{V}_{vm}^+(L) &= V_{vm}(L) + Z_{vm}I_{vm}(L) \\ &= H'_{vm}(V_{vm}(0) - Z_{vm}I_{vm}(0))e^{-j\beta_{vm}L} + H'_{vm}V_{L,Enc,ZT}^+ \\ &= H'_{vm}(\tilde{V}_{vm}^+(0))e^{-j\beta_{vm}L} + H'_{vm}V_{L,Enc,ZT}^+\end{aligned}\quad (3.177)$$

$$\begin{aligned}\tilde{V}_{vm}^-(0) &= V_{vm}(0) - Z_{vm}I_{vm}(0) \\ &= H'_{vm}(V_{vm}(L) - Z_{vm}I_{vm}(L))e^{-j\beta_{vm}L} + H'_{vm}V_{0,Enc,ZT}^- \\ &= H'_{vm}(\tilde{V}_{vm}^-(L))e^{-j\beta_{vm}L} + H'_{vm}V_{0,Enc,ZT}^-\end{aligned}\quad (3.178)$$

In the time domain, these equations become

$$\tilde{V}_{vm}^+(L,t) = H'_{vm} * (\tilde{V}_{vm}^+(0,t - T_{vm})) + H'_{vm} * V_{L,Enc,ZT}^+ \quad (3.179)$$

$$\tilde{V}_{vm}^-(0,t) = H'_{vm} * (\tilde{V}_{vm}^-(L,t - T_{vm})) + H'_{vm} * V_{0,Enc,ZT}^- \quad (3.180)$$

Where the transfer impedance coupling sources may be expressed as

$$V_{0,ZT}^- = \frac{H_{ZT}}{2Z_{sm}}(j\omega) [-V_{0,ext}^+ + V_{0,ext}^-] \quad (3.181)$$

$$V_{L,ZT}^+ = \frac{H_{ZT}}{2Z_{sm}}(j\omega) [V_{L,ext}^+ - V_{L,ext}^-] \quad (3.182)$$

Transforming equations 3.181 and 3.182 into the time domain gives

$$V_{0,ZT}^- = \frac{1}{2Z_{sm}}H_{ZT}(t) * [-V_{0,ext}^+(t) + V_{0,ext}^-(t)] \quad (3.183)$$

$$V_{L,ZT}^+ = \frac{1}{2Z_{sm}}H_{ZT}(t) * [V_{L,ext}^+(t) - V_{L,ext}^-(t)] \quad (3.184)$$

where $V_{0,ext}^+$ and $V_{0,ext}^-$ are the contributions to the source term at $z=0$ due to the +z and -z propagating characteristics on the external conductor and $V_{L,ext}^+$ and $V_{L,ext}^-$

are the contributions to the source term at $z=L$ due to the $+z$ and $-z$ propagating characteristics on the external conductor

$$V_{0,ext}^+ = \int_0^L V_{sm}^+(0) e^{-j(\beta_{sm}+\beta_{vm})z} dz + \int_0^L V_{Eim}^+(z) e^{-j(\beta_{vm})z} dz \quad (3.185)$$

$$V_{0,ext}^- = \int_0^L V_{sm}^-(L) e^{-j\beta_{sm}L} e^{j(\beta_{sm}-\beta_{vm})z} dz + \int_0^L V_{Eim}^-(z) e^{-j(\beta_{vm})z} dz \quad (3.186)$$

$$V_{L,ext}^+ = \int_0^L V_{sm}^+(0) e^{-j\beta_{vm}L} e^{j(\beta_{vm}-\beta_{sm})z} dz + \int_0^L V_{Eim}^+(z) e^{-j\beta_{vm}L} e^{j\beta_{vm}z} dz \quad (3.187)$$

$$V_{L,ext}^- = \int_0^L V_{sm}^-(L) e^{-j\beta_{vm}+smL} e^{j(\beta_{sm}+\beta_{vm})z} dz + \int_0^L V_{Eim}^-(z) e^{j\beta_{vm}(L-z)} dz \quad (3.188)$$

Each of these terms has a contribution from the characteristic variables scattered from the terminations (V_{sm} terms) and from characteristic variables directly launched by the incident field source terms (V_{Eim} terms) i.e. the source terms (including the propagation correction for the victim domain propagation in equations 3.177 and 3.178 may be expressed as

$$H'_{vm} * V_{0,ZT}^- = \frac{1}{2Z_{sm}} H'_{vm} H_{ZT} \left[V_{0,ZT,vm}^- + V_{0,Einc,ZT,sm,vm}^- \right] \quad (3.189)$$

$$H'_{vm} * V_{L,ZT}^+ = \frac{1}{2Z_{sm}} H'_{vm} H_{ZT} \left[V_{L,ZT,vm}^+ + V_{L,Einc,ZT,sm,vm}^+ \right] \quad (3.190)$$

The contributions from the characteristic variables scattered from the terminations $V_{0,ZT,v}^-$ and $V_{L,ZT,v}^+$ have already been described in section 3.7. Here we will describe how the additional terms related to the (V_{Eim} terms in equations 3.185 to 3.188) i.e. the direct coupling of the incident field through the shield before any interaction with the terminations, may be included in the Spice cable bundel model. It is worth noting here that the influence of the incident field will be allowed to couple through the shield via the transfer impedance once it has scattered from the terminations when it becomes a part of the V_{sm}^+ and V_{sm}^- terms. The additional terms discussed here are a refinement of the incident field coupling model and could be considered to be a 'direct transfer impedance incident field coupling' model.

The contributions due to the direct transfer impedance incident field coupling model are

$$\begin{aligned} H'_{vm} * V_{0,Einc,ZT}^- &= \frac{1}{2Z_{sm}} H'_{vm} H_{ZT} V_{0,Einc,ZT,sm,vm}^- \\ &= \frac{1}{2Z_{sm}} H'_{vm} H_{ZT} \left[-E_{0,Eim}^+ + E_{0,Eim}^- \right] \end{aligned} \quad (3.191)$$

where

$$\begin{aligned} V_{0_Eim}^+ &= \int_0^L V_{Eim}^+(z) e^{-j\beta_{vm}z} dz \\ V_{0_Eim}^- &= \int_0^L V_{Eim}^-(z) e^{-j\beta_{vm}z} dz \end{aligned} \quad (3.192)$$

and

$$\begin{aligned} H'_{vm} * V_{L_Einc,ZT}^+ &= \frac{1}{2Z_{sm}} H'_{vm} H_{ZT} V_{L_Einc,ZT,sm,vm}^+ \\ &= \frac{1}{2Z_{sm}} H'_{vm} H_{ZT} [V_{L_Eim}^+ - V_{L_Eim}^-] \end{aligned} \quad (3.193)$$

where

$$\begin{aligned} V_{L_Eim}^+ &= \int_0^L V_{Eim}^+(z) e^{-j\beta_{vm}L} e^{j(\beta_{vm})z} dz \\ V_{L_Eim}^- &= \int_0^L V_{Eim}^-(z) e^{-j\beta_{vm}L} e^{j(\beta_{vm})z} dz \end{aligned} \quad (3.194)$$

If we assume a plane wave excitation as defined in equation 3.140 in the time domain and 3.141 for the frequency domain and identify the distributed source terms in the external domain as in equation 2.53 and 2.56 then we can substitute 2.53 and 2.56 into 3.175 and 3.176.

Using the resulting expressions for $V_{Eim}^+(z)$ and $V_{Eim}^-(z)$ in equations 3.192 and 3.194 and evaluating the resulting double integrals leads to a frequency domain solution. Recognising the $e^{j\beta z}$ terms as representing time delays then leads to a time domain solution for the contributions to the terminations at $z=0$ and $z=l$ as

$$H'_{vm} * V_{0_Einc,ZT}^- = \frac{1}{2Z_{sm}} H'_{ZT,vm} * [-V_{0_Eim}^+(t) + V_{0_Eim}^-(t)] \quad (3.195)$$

$$H'_{vm} * V_{L_Einc,ZT}^+ = \frac{1}{2Z_{sm}} H'_{ZT,vm} * [V_{L_Eim}^+(t) - V_{L_Eim}^-(t)] \quad (3.196)$$

where $H'_{ZT,vm}$ is the impulse response of the transfer function $\frac{H'_{vm} H_{ZT}}{j\omega}$ and

$$\begin{aligned} V_{0_Eim}^+(t) &= 2dL \frac{e_t(T_z - T_{sm}) - e_z T_x}{T_z - T_{sm}} \left\{ \frac{E_0(t) - E_0(t - (T_{sm} + T_{vm}))}{T_{sm} + T_{vm}} \right. \\ &\quad \left. - \frac{E_0(t) - E_0(t - (T_z + T_{vm}))}{T_z + T_{vm}} \right\} \end{aligned} \quad (3.197)$$

$$\begin{aligned} V_{0_Eim}^-(t) &= 2dL \frac{e_t(T_z + T_{sm}) - e_z T_x}{T_z + T_{sm}} \left\{ -\frac{E_0(t) - E_0(t - (T_z + T_{vm}))}{T_z + T_{vm}} \right. \\ &\quad \left. - \frac{E_0(t - (T_z + T_{vm})) - E_0(t - (T_z + T_{sm}))}{T_{vm} - T_{sm}} \right\} \end{aligned} \quad (3.198)$$

$$V_{L.Eim}^+(t) = 2dL \frac{e_t(T_z - T_{sm}) - e_z T_x}{T_z - T_{sm}} \left\{ \frac{E_0(t - T_z) - E_0(t - T_{vm})}{T_z - T_{vm}} - \frac{E_0(t - T_{vm}) - E_0(t - T_{sm})}{T_{vm} - T_{sm}} \right\} \quad (3.199)$$

$$V_{L.Eim}^-(t) = 2dL \frac{e_t(T_z + T_{sm}) - e_z T_x}{T_z + T_{sm}} \left\{ \frac{E_0(t - T_z) - E_0(t - T_{vm})}{T_z - T_{vm}} + \frac{E_0(t - T_z) - E_0(t - (T_z + T_{vm} + T_{sm}))}{T_{vm} + T_{sm}} \right\} \quad (3.200)$$

where e_t and e_z are the components of the Electric field in the plane of the cable from reference to the conductor in question and the z directions respectively, d is the distance from the reference conductor to the conductor in question, $T_z = \frac{L}{v_z}$ and $T_x = \frac{L}{v_x}$ and v_z and v_x are the velocities of propagation of the incident field in the x and z directions.

3.9.1 Incident field excitation with a ground plane

If there is a ground plane present then the incident field may be expressed as the superposition of a direct wave and the wave reflected from the ground and the source terms are found as described in section 3.8.2.

3.9.2 Multiple mode propagation

As for the transfer impedance coupling model, the above theory is readily extended to the case of multi-mode systems, both in the external (source) domain and the shielded (victim) domain. The calculation of the contribution from each mode to the shield current is discussed in section 3.7.1, similarly the distribution of a voltage source (due to transfer impedance coupling) to the modes in the victim (shielded) domain is discussed in section 3.7.1. We can summarise these discussions by noting that:

1. The shield current is expressed as a linear combination of the individual mode currents in the source domain i.e.

$$I_{shield}^{\sim} = \sum_{i=1}^{N_m} P_{s,i} I_{m,i}^{\sim} \quad (3.201)$$

2. the voltage source contribution to victim mode i has a weighting factor $P_{v,i}$

$$(V_{m,i}^{\sim}) = P_{v,i} V_{s,ZT}^{\sim} \quad (3.202)$$

multiple modes in the source domain and victim domains

In order to generalise the direct transfer impedance incident field coupling model to multiple source and victim domains, equations 3.195 and 3.196 must be generalised. This is done by recognising that if there are ns source domain modes and nv victim domain modes then there are $ns \times nv$ contributions to the transfer impedance coupling i.e. there is a contribution relating to every combination of source and victim modes.

The contribution from source mode, smi , to victim mode, vmj , is readily found using the weighted values in equations 3.201 and 3.202.

In this case equations 3.195 and 3.196 become:

$$H'_{vmj} * V_{0,Einc,ZT,smi,vmj}^- = \frac{1}{2Z_{smi}} P_{s,i} P_{v,j} H'_{ZT_v,vmj} * \left[-E_{0,Eim,smi,vmj}^+(t) + E_{0,Eim,smi,vmj}^-(t) \right] \quad (3.203)$$

$$H'_{vmj} * V_{L,Einc,ZT,smi,vmj}^+ = \frac{1}{2Z_{smi}} P_{s,i} P_{v,j} H'_{ZT_v,vmj} * \left[E_{L,Eim,smi,vmj}^+(t) - E_{L,Eim,smi,vmj}^-(t) \right] \quad (3.204)$$

where the expressions for $E_{0,Eim,smi,vmj}^+(t)$, $E_{0,Eim,smi,vmj}^-(t)$, $E_{L,Eim,smi,vmj}^+(t)$ and $E_{L,Eim,smi,vmj}^-(t)$ are evaluated using equations 3.197 to 3.200 with delays $T_{vm} = T_{vmi}$ and $T_{sm} = T_{smi}$

3.9.3 Spice circuit for direct transfer impedance incident field coupling model

The Spice circuit for the direct transfer impedance incident field coupling model is a variation on the circuit for transfer impedance coupling seen in figures 3.12 and 3.13. The only change to the main circuit in figure 3.12 is that there is an additional source term in series with the usual transfer impedance csource term at the $z = 0$ and $z = L$ terminations of the victim transmission line as shown in figure 3.19.

The following delay lines are also required in addition to the delay lines required to implement the method of characteristics in the source and victim domains:

1. Delay line for $E_0(t - T_z - T_{si} - T_{vi})$
2. Delay line for $E_0(t - T_{si} - T_{vi})$
3. Delay line for $E_0(t - T_z - T_{vi})$
4. Delay line for $E_0(t - T_z - T_{si})$
5. Delay line for $E_0(t - T_{vi})$
6. Delay line for $E_0(t - T_{si})$
7. Delay line for $E_0(t - T_z)$

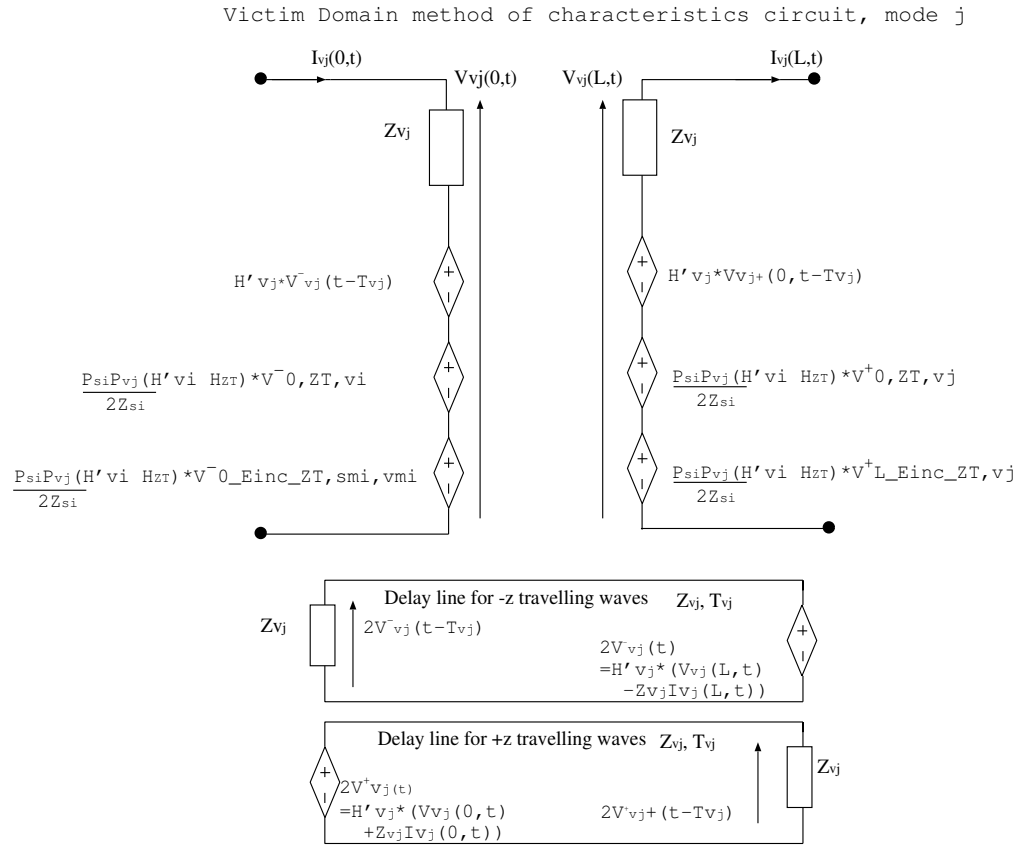


Figure 3.19 Spice circuit for the victim domain mode direct transfer impedance incident field coupling model

The Spice model for these elements is shown in figure 3.20

As for the incident field model and the transfer impedance model, there are circumstances in which terms in equations 3.197 to 3.200 need to be modified i.e. when $T_z - T_{sm} = 0$, $T_{vm} - T_{sm} = 0$ or $T_z - T_{vm} = 0$. In these cases the terms required are again (as in sections 3.8.1 and 3.7.2) shown to become time derivatives of the delayed incident field function which can be realised by circuits similar to that in figure 3.18 using a delay line and a 1H inductor in parallel with a controlled current source.

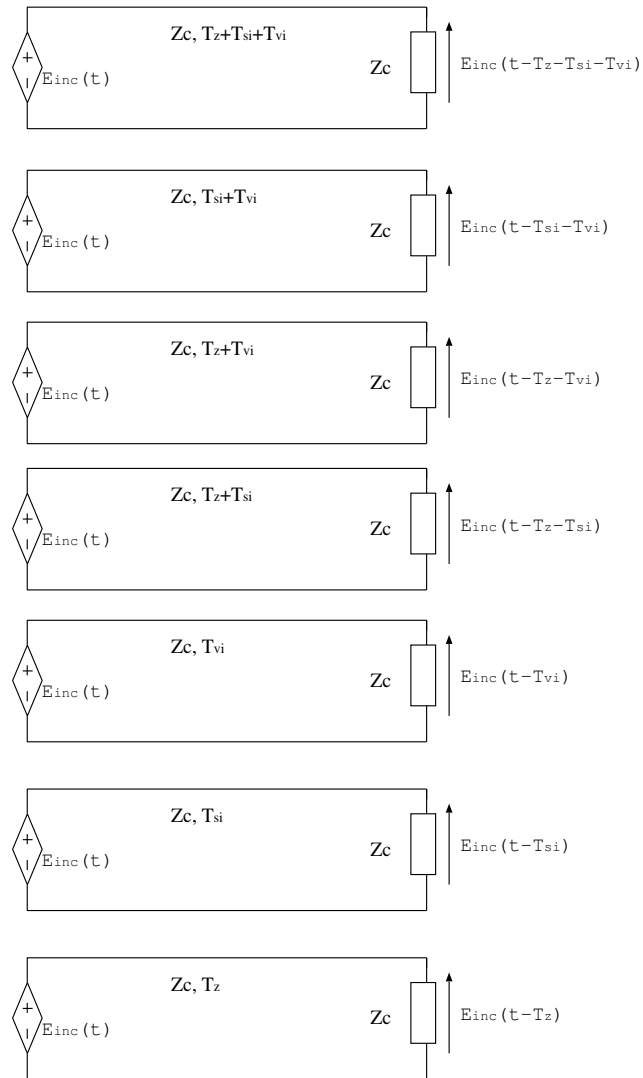


Figure 3.20 Delay lines required to implement the direct transfer impedance incident field coupling model

Chapter 4

Numerical computation of the per-unit-length MTL parameters using a FEM solver

Multiconductor Transmission Line (MTL) modelling is based on a set of coupled first order phasor MTL equations as discussed in chapter 2. In the set of coupled first-order MTL equations the impedance matrix $[\tilde{Z}(\omega)]$ and admittance matrix $[\tilde{Y}(\omega)]$ are given by

$$[\tilde{Z}(\omega)] = [\tilde{R}(\omega)] + j\omega [\tilde{L}(\omega)] \quad (4.1)$$

$$[\tilde{Y}(\omega)] = [\tilde{G}(\omega)] + j\omega [\tilde{C}(\omega)] \quad (4.2)$$

with $[\tilde{R}(\omega)]$ the per unit length resistance matrix, $[\tilde{L}(\omega)]$ the per unit length inductance matrix, $[\tilde{G}(\omega)]$ the per unit length conductance matrix and $[\tilde{C}(\omega)]$ the per unit length capacitance matrix. In order to be able to perform a propagation or crosstalk analysis using MTL modelling it is important to determine good approximations of these per-unit length parameter matrices.

It is assumed in the initial discussion that the inductance and capacitance matrix are independent of frequency and that dielectrics are loss-less and frequency independent. In section 4.2.2 frequency dependent capacitance is introduced by means of a complex relative permittivity. In this case the capacitance and conductance matrix may be evaluated at specific frequencies.

In the book by Paul,[2], chapter 5, a definition of the $[L]$, $[G]$ and $[C]$ matrices is given and it is explained that these matrices can be determined from static field solutions in

the transverse plane for perfect line conductors. Closed-form solutions for these static field problems however only exist for a small set of configurations and several approximate solutions have limited applicability. As a consequence approximate numerical methods must be used for the computation of the entries in the per-unit-length matrices. In the same book by Paul, chapter 5, it is also shown that in order to numerically determine the entries of the $[L]$, $[G]$ and $[C]$ matrices we only need a capacitance solver, that is, we only need a numerical solver that is able to compute a capacitance matrix $[C]$. The inductance matrix $[L]$ can be derived from the capacitance matrix solution $[C_0]$ for the static field problem in which we have replaced all dielectrics in the cross-section with free space, the per-unit-length inductance matrix can be obtained from

$$[L] = \mu_0 \varepsilon_0 [C_0]^{-1} \quad (4.3)$$

with μ_0 and ε_0 the permeability and permittivity of free space. The conductance matrix $[G]$ can be obtained by introducing a complex permittivity and solving for a complex valued capacitance matrix $[C]$.

Two dimensional electrostatic field problems are governed by the two-dimensional Poisson equation

$$-\frac{\partial}{\partial x} \left(\varepsilon_{r,x} \frac{\partial \phi}{\partial x} \right) - \frac{\partial}{\partial y} \left(\varepsilon_{r,y} \frac{\partial \phi}{\partial y} \right) = \frac{\rho_c}{\varepsilon_0} \quad (4.4)$$

with ϕ the potential, ρ_c the charge density, ε_0 the permittivity of free space, $\varepsilon_{r,x}$ and $\varepsilon_{r,y}$ the diagonal components of the relative permittivity tensor (we have assumed all off-diagonal terms are zero) of the materials in the configuration.

We can solve the capacitance matrix, $[C]$, by discretising the cross-section of the cable (MTL) and solving the Laplace equation for this cross section numerically.

The two-dimensional Poisson equation follows from Gauss's law,

$$\frac{\partial}{\partial x} D_x + \frac{\partial}{\partial y} D_y = \rho_c \quad (4.5)$$

the constitutive relation between the electric flux density and the electric field intensity for a linear axial medium

$$\begin{bmatrix} D_x \\ D_y \end{bmatrix} = \varepsilon_0 \begin{bmatrix} \varepsilon_{r,x} & 0 \\ 0 & \varepsilon_{r,y} \end{bmatrix} \begin{bmatrix} E_x \\ E_y \end{bmatrix} \quad (4.6)$$

and the definition of the scalar electric potential:

$$\begin{bmatrix} E_x \\ E_y \end{bmatrix} = - \begin{bmatrix} \frac{\partial \phi}{\partial x} \\ \frac{\partial \phi}{\partial y} \end{bmatrix} \quad (4.7)$$

In the static field problems that need to be solved in order to determine the entries of the capacitance matrix of a MTL, there is no free charge in the region between the conductors and the potential is prescribed on the conductors. As a result we have to solve the two dimensional field problem:

$$-\frac{\partial}{\partial x} \left(\epsilon_r \frac{\partial \phi}{\partial x} \right) - \frac{\partial}{\partial y} \left(\epsilon_r \frac{\partial \phi}{\partial y} \right) = 0 \quad (4.8)$$

with an appropriate boundary condition applied on the outer boundary of the domain.

In the SACAMOS project the capacitance (and conductance) matrices are calculated numerically using a Finite Element Method [8] as outlined in the rest of this chapter. Details of the implementation are not discussed here however the software closely follows the process described in chapter 4 of [8].

4.1 Solving the capacitance matrix based on energy

The capacitance matrix can be solved based on energy or based on charges. We will use the method based on energy.

The total electrostatic energy stored in the multi-conductor configuration can be computed from the static field solution as

$$W = \frac{1}{2} \iint_S \mathbf{D} \mathbf{E} dA \quad (4.9)$$

For this method we set the p th and q th conductor to 1V, that is, $V_p = V_q = 1$ and connect all other conductors to reference, that is, all other conductors are set to 0V which implies $V_i = 0$ for all $i \neq q$ or p , the electrostatic energy W_{pq} stored in the system equals

$$W_{pq} = W_p + W_q - c_{pq} \quad (4.10)$$

where c_{pq} is the coupling capacitance. As a result, in case we have determined W_p for

all $p = 1, \dots, n$ and W_{pq} for all combinations of $p = 1, \dots, n$ and $q = 1, \dots, n$ for which $p \neq q$ we can first compute all coupling capacitances c_{pq} , namely

$$c_{pq} = W_p + W_q - W_{pq} \quad (4.11)$$

Then we may compute the coupling capacitances c_{p0}

$$c_{p0} = 2W_p - \sum_{\substack{j=1 \\ j \neq p}}^n c_{pj} \quad (4.12)$$

We can also immediately compute the coefficients of capacitance C_{pq} for all combinations of $p = 1, \dots, n$ and $q = 1, \dots, n$ as we note that:

$$C_{pq} = -c_{pq} = W_{pq} - W_p - W_q \quad (4.13)$$

$$C_{pp} = \sum_{\substack{j=0 \\ j \neq p}}^n c_{pj} = 2W_p \quad (4.14)$$

So, with a static field solver available we are able to compute the entries in the capacitance matrix.

4.2 Procedure capacitance matrix computation based on energy analysis

The procedure for determining the capacitance matrix via computation of the energy storage is:

1. First select all n non-reference conductors one after another and each time compute the static field solution with the voltage of the conductor under consideration set to 1V and all other conductors set to the reference 0V. With the p th conductor set to 1V ($V_p = 1V$) and all other conductors to reference (0V), compute the electrostatic energy E_p stored in the configuration by using the surface integral (4.9). This requires that the static field problem and energy integral has to be determined a total of n times.

2. Second select all combinations of two different conductors from the n non-reference conductors one after another and each time compute the static field solution with the voltage of the two conductors under consideration set to 1V and all other conductors set to the reference 0V. With the p^{th} and q^{th} conductor set to 1V ($V_p = V_q = 1$) and all other conductors set to reference (0V), compute the electrostatic energy E_{pq} stored in the configuration by using the surface integral (4.9). This requires that the static field solution and energy integral has to be determined a total of $n(n-1)/2$ times.
3. Determine the entries of the capacitance matrix from the computed stored energies E_p and E_{pq} using expressions (4.13) and (4.14).

The reference conductor can be either a ground plane, a shield or a circular or rectangular conductor.

4.2.1 FEM Solver for the Open Boundary Electrostatic Field Problem

Without an outer shield the electrostatic field is no longer confined to a bounded domain while the FEM can only be used on a finite computational domain. In the course of time a number of techniques have been developed to circumvent this problem. A review of the most important finite element open boundary techniques is given by Chen and Konrad [10].

In unshielded conductor configurations a suitable boundary condition must be applied on the outer boundary of the problems space. The imposition of a boundary condition will necessarily have an effect on the fields within the Finite Element domain and hence the capacitance matrix to be calculated. Three possible boundary conditions are outlined here, the Dirichelet boundary condition ($\phi = 0$), the Neumann boundary condition $\frac{\partial\phi(r)}{\partial r} = 0$ and an asymptotic boundary condition, $\frac{\partial\phi(r)}{\partial r} = \frac{1}{r \ln(r)} \phi(r)$.

Dirichelet boundary conditions

The Dirichelet boundary condition imposes a $\phi = 0$ condition on the outer boundary. This implies that the outer boundary is another conductor which may store charge. In order to calculate the capacitance matrix with the Dirichelet boundary condition, the outer boundary must be included in the analysis as an additional conductor and a 'generalised capacitance' matrix calculated. The capacitance matrix for the interior conductors only may then be calculated from the generalised capacitance matrix via the procedure described in [2].

Neumann boundary conditions

The Neumann boundary condition is expressed as

$$\frac{\partial \phi(r)}{\partial r} = 0 \quad (4.15)$$

This boundary condition enforces a condition that the normal derivative of the potential is zero and hence the charge inside the boundary is zero (by application of the integral form of Gauss' law). The zero charge property is required by the capacitance matrix calculation and using the Neumann boundary condition leads to convergence of the capacitance matrix elements to the correct values as the boundary distance and the mesh density are increased.

Asymptotic boundary conditions

For 2D electrostatic problems, the potential in a point \mathbf{r} , can be written as

$$\phi(\mathbf{r}) = \iint_{\Omega} \rho(\mathbf{r}') G(\mathbf{r}, \mathbf{r}') d\mathbf{r}' \quad (4.16)$$

Where Ω is the charged region, $\rho(\mathbf{r}')$ is the charge distribution and $G(\mathbf{r}, \mathbf{r}')$ is the free space Greens function:

$$G(\mathbf{r}, \mathbf{r}') = \frac{1}{2\pi\epsilon_0} \ln |\mathbf{r} - \mathbf{r}'| \quad (4.17)$$

In the expression for the potential, the effect of dielectrics is taken into account by incorporating the polarization charge density in the charge distribution. Using polar coordinates (r, θ) the position vectors may be written as $\mathbf{r} = (r \cos \theta, r \sin \theta)$ and $\mathbf{r}' = (r' \cos \theta', r' \sin \theta')$ and the free space Green function equals

$$G(r, \theta, r', \theta') = \frac{1}{4\pi\epsilon_0} \ln (r^2 + r'^2 - 2rr' \cos(\theta - \theta')) \quad (4.18)$$

and hence

$$\frac{\partial}{\partial r} G(r, \theta, r', \theta') = \frac{1}{2\pi\epsilon_0} \frac{r - r' \cos(\theta - \theta')}{r^2 + r'^2 - 2rr' \cos(\theta - \theta')} \quad (4.19)$$

Expression immediately implies that the potential for $r \gg r'$, with r' the distances from the origin of the charges in the charged region, satisfies

$$\frac{\partial}{\partial r} \phi(r, \theta) = \frac{1}{r \ln(r)} \phi(r, \theta) \quad (4.20)$$

It has been observed that the use of the asymptotic boundary condition described here can have an effect on the convergence of the capacitance matrix calculation due to the total charge within the boundary not being null, which impacts the capacitance matrix calculation described in section 4.2. Currently it is not known whether a 'generalised capacitance matrix' type solution can be used along with this boundary condition as the outer boundary is not an equipotential (as it is in the Dirichelet case). As a consequence of this the Neumann boundary condition is recommended and used in the SACAMOS software as the default open boundary condition.

4.2.2 Computing the conductance matrix

The conductance matrix $[G]$ can be obtained by introducing a complex permittivity and solving for a complex valued capacitance matrix $[C]$. (reference [2] equation 3.6.1)

If the surrounding medium is homogeneous, G can be obtained from C or L by

$$G = \frac{\sigma}{\varepsilon} C = \mu\sigma L_e^{-1} \quad (4.21)$$

L_e is the external inductance matrix assuming perfect conductors.

Next we want to obtain G for inhomogeneous media. This can be the case for a conductor or shield that has a dielectric jacket (insulator). Actually, this is a simple modification of the calculation of the per-unit-length capacitance matrix C (also computed assuming perfect conductors). Losses in the medium are due to:

- Conductive losses (due to the conductance parameter σ).
- Polarization losses

Both of the losses can be represented by a complex permittivity.

$$\hat{\varepsilon} = \varepsilon' - j\varepsilon'' \quad (4.22)$$

$$\varepsilon' = \varepsilon \quad (4.23)$$

$$\varepsilon'' = \varepsilon_b + \frac{\sigma}{\omega} = \varepsilon' \tan(\delta) \quad (4.24)$$

where $\tan(\delta)$ is the loss tangent and ε_b are the polarization losses due to bound charges.

σ represents the conduction current losses.

We can include losses in the medium by solving for the capacitance matrix for a medium having a complex permittivity

$$\hat{\epsilon} = \epsilon' (1 - j \tan(\delta)) \quad (4.25)$$

and from that result directly obtain C and G.

$$\hat{Y} = G + j\omega C \quad (4.26)$$

$$\hat{Y} = j\omega \left(C - \frac{j}{\omega} G \right) = j\omega \hat{C} \quad (4.27)$$

From that we can obtain the capacitance matrix \hat{C}

$$C = \text{Re}(\hat{C}) \quad (4.28)$$

And the conductance matrix G

$$G = -\varpi \text{Im}(\hat{C}) \quad (4.29)$$

4.2.3 Iterative solution of the Finite Element matrix equations

The Finite Element method used to solve the Laplace equation for multi-conductor cable cross sections results in a matrix equation which must be solved for the unknown node potentials. The matrix is sparse however the V3 version of the SACAMOS software did not take advantage of this sparsity and a direct matrix inverse was used to solve the matrix equation. This approach is wasteful in that the sparsity of the matrix equation is not used to our advantage and the size of the Finite Element mesh which can be used is severely limited to systems of the order of 1000's of unknowns. Iterative matrix solutions have the potential to improve the efficiency of solution in terms of both storage (a full matrix never needs to be stored) and runtime for a solution. The method implemented here is described in reference [9]. A discussion of the use of conjugate gradient methods in Finite Element solutions may be found in reference [8].

The V4 version of the SACAMOS software addresses this issue by implementing the biconjugate gradient method, an iterative approach to the solution to the Finite Element matrix equations which is suitable for real and complex symmetric matrix systems as in equation 4.32.

$$[A](x) = (b) \quad (4.30)$$

The method is derived by writing a functional whose minimum corresponds to the solution of 4.32. Here we minimise the function

$$f(x) = \frac{1}{2} (x) [A](x) - (b)(x) \quad (4.31)$$

This function is minimised when it's gradient is zero i.e.

$$\nabla f = [A] (x) - (b) = 0 \quad (4.32)$$

The inner product is defined as follows: if we have two column vectors (a) and (b) each with n elements then

$$\langle a, b \rangle = \sum_{i=1}^n a_i b_i \quad (4.33)$$

The biconjugate gradient algorithm is described by the following process:
given an initial guess of the solution vector (x_1), calculate the residual

$$(r_1) = (b) - [A] (x_1) \quad (4.34)$$

then set

$$(r'_1) = [A] (r_1) \quad (4.35)$$

This choice of (r'_1) gives the so called 'minimum residual' algorithm which is suitable for non-positive definite matrices.

Also set the initial values of (p_1) and (p'_1) as

$$(p_1) = (r_1) \quad (4.36)$$

$$(p'_1) = (r'_1) \quad (4.37)$$

Then iterate the following process for $k = 1, 2, 3 \dots$ until the size of the residual is less than a specified tolerance (10^{-12})

$$a_k = \frac{\langle (r'_k), (r_k) \rangle}{\langle (p'_k) [A] (p_k) \rangle} \quad (4.38)$$

The improved estimate of the unknown solution vector is now

$$(x_{k+1}) = (x_k) + a_k (p_k) \quad (4.39)$$

The residual is given by

$$(r_k) = (b) - [A] (x_k) \quad (4.40)$$

Calculate the size (norm) of the residual

$$norm = \langle r_k, r_k^* \rangle = \sum_{i=1}^n r_{k,i} r_{k,i}^* \quad (4.41)$$

If norm is less than the specified tolerance then finish, otherwise calculate

$$(r_{k+1}) = (r_k) - a_k [A] (p_k) \quad (4.42)$$

$$(r'_{k+1}) = (r'_k) - a_k [A^T] (p'_k) \quad (4.43)$$

$$b_k = \frac{\langle (r'_{k+1}), (r_{k+1}) \rangle}{\langle (r'_k), (r_k) \rangle} \quad (4.44)$$

$$(p_{k+1}) = (r_{k+1}) + b_k (p_k) \quad (4.45)$$

$$(p'_{k+1}) = (r'_{k+1}) + b_k (p'_k) \quad (4.46)$$

Then return to the start of the iteration loop

Two implementations of the above iterative process have been developed, one for real matrices and one for complex matrices. The complex solution is only required if lossy dielectric materials are present in the cross section.

Chapter 5

Frequency dependent transfer functions

5.1 Introduction

Frequency dependent transfer functions are implemented in the Spice models using s-domain transfer functions, this includes the propagation corrections and transfer impedance terms. The coefficients of the s-domain transfer functions are required to provide the 'best fit' to a frequency dependent transfer function evaluated at a discrete set of frequencies. The software includes a process whereby the coefficients of an s-domain transfer function (taking the form of a rational function in s), which provides an approximation to a function, are determined.

5.2 Filter fitting process for s-domain transfer functions

The process implemented is based on that described in [13].

The starting point for the process is a set of complex transfer function values $H'(j\omega_i)$ at a set of discrete frequencies $i = 1..n$ and the aim is to find a rational function $H(j\omega)$ which best fits the available data points.

The transfer function takes the form:

$$H(j\omega) = \frac{a_0 + a_1 \left(\frac{j\omega}{\omega_0}\right) + a_2 \left(\frac{j\omega}{\omega_0}\right)^2 + \dots + a_{nn} \left(\frac{j\omega}{\omega_0}\right)^{nn}}{1 + b_1 \left(\frac{j\omega}{\omega_0}\right) + b_2 \left(\frac{j\omega}{\omega_0}\right)^2 + \dots + b_{nd} \left(\frac{j\omega}{\omega_0}\right)^{nd}} = \frac{A(j\omega)}{1 + B(j\omega)} \quad (5.1)$$

where the order of the numerator and the denominator are to be specified and the coefficients a_j and b_j are to be determined. If we assume that the numerator and denominator order are specified as nn and nd then we have unknown coefficients $a_j, j = 0..nn$ and $b_j, j = 1..nd$.

At a frequency w_i the error between the filter fit model and the transfer function value is

$$err(j\omega_i) = \text{frac}A(j\omega_i)1 + B(j\omega_i) - H'(j\omega_i) \quad (5.2)$$

multiplying equation 5.2 by $1 + B(j\omega_i)$ gives

$$(1 + B(j\omega_i)) err(j\omega_i) = err'(j\omega_i) = A(j\omega_i) - (1 + B(j\omega_i)) H'(j\omega_i) \quad (5.3)$$

The left hand side can be thought of as a weighted error function, err' .

Evaluating equation 5.3 for each frequency ω_i gives a set of n equations

$$\begin{pmatrix} err'(j\omega_1) \\ err'(j\omega_2) \\ \vdots \\ err'(j\omega_n) \end{pmatrix} = \begin{pmatrix} -H'(j\omega_1) \\ -H'(j\omega_2) \\ \vdots \\ -H'(j\omega_n) \end{pmatrix} + \begin{bmatrix} -(j\omega_1) H'(j\omega_1) & \dots & -(j\omega_1)^{nd} H'(j\omega_1) & 1 & (j\omega_1) & \dots & (j\omega_1)^{nn} \\ -(j\omega_2) H'(j\omega_2) & \dots & -(j\omega_2)^{nd} H'(j\omega_2) & 1 & (j\omega_2) & \dots & (j\omega_2)^{nn} \\ \vdots & \vdots & \vdots & \vdots & \vdots & \vdots & \vdots \\ -(j\omega_n) H'(j\omega_n) & \dots & -(j\omega_n)^{nd} H'(j\omega_n) & 1 & (j\omega_n) & \dots & (j\omega_n)^{nn} \end{bmatrix} \begin{pmatrix} b_1 \\ \vdots \\ b_{nd} \\ a_0 \\ a_1 \\ \vdots \\ a_{nn} \end{pmatrix} \quad (5.4)$$

The coefficients of the transfer function are required to be real. This can be enforced by augmenting the set of equations with an equal number of equations evaluated at negative frequency where we impose the condition $H(-j\omega) = H^*(j\omega)$.

$$\begin{pmatrix} err'(-j\omega_1) \\ err'(-j\omega_2) \\ \vdots \\ err'(-j\omega_n) \end{pmatrix} = \begin{pmatrix} -H'^*(j\omega_1) \\ -H'^*(j\omega_2) \\ \vdots \\ -H'^*(j\omega_n) \end{pmatrix} + \begin{bmatrix} -(-j\omega_1) H'^*(j\omega_1) & \dots & -(-j\omega_1)^{nd} H'^*(j\omega_1) & 1 & (-j\omega_1) & \dots & (-j\omega_1)^{nn} \\ -(-j\omega_2) H'^*(j\omega_2) & \dots & -(-j\omega_2)^{nd} H'^*(j\omega_2) & 1 & (-j\omega_2) & \dots & (-j\omega_2)^{nn} \\ \vdots & \vdots & \vdots & \vdots & \vdots & \vdots & \vdots \\ -(-j\omega_n) H'^*(j\omega_n) & \dots & -(-j\omega_n)^{nd} H'^*(j\omega_n) & 1 & (-j\omega_n) & \dots & (-j\omega_n)^{nn} \end{bmatrix} \begin{pmatrix} b_1 \\ \vdots \\ b_{nd} \\ a_0 \\ a_1 \\ \vdots \\ a_{nn} \end{pmatrix} \quad (5.5)$$

This combined set of equations is of the form

$$(err') (D) - [X] (W) \quad (5.6)$$

The mean square error is found as

$$\begin{aligned} \|err\|^2 &= \frac{1}{n} \Re \{ (err')^* (err') \} \\ &= \frac{1}{n} \Re \{ (D)^* (D) + (W)^T [X]^* [X] (W) - 2 (D) [X]^* (W) \} \end{aligned} \quad (5.7)$$

where * denotes the conjugate transpose and \Re denotes the real part
If we define

$$[R] = \Re \{ [X]^* [X] \} \quad (5.8)$$

and

$$(P) = [X]^* (D) \quad (5.9)$$

then

$$\|err\|^2 = \frac{1}{n} \Re \{ (D)^* (D) + (W)^T [R] (W) - 2 (P)^T (W) \} \quad (5.10)$$

This expression is minimised with respect to the vector (W) of unknown coefficients by differentiating with respect to (W) and equating the result to zero i.e.

$$\frac{\partial \|err\|^2}{\partial (W)} = \frac{1}{n} \Re \{ 2 [R] (W) - 2 (P)^T \} = 0 \quad (5.11)$$

This system of equations may be solved directly to give the unknown coefficient vector

$$(W) = [R]^{-1} (P) \quad (5.12)$$

An alternative approach to reaching equation 5.12 is to start from the set of equations 5.4 and 5.5. If we set the error on the left hand side to zero then we have the overdetermined set of equations

$$(D) = [X] (W) \quad (5.13)$$

A solution to this set of equations may be found by solving the 'normal equations' which are found by pre-multiplying equation 5.13 by $[X]^*$

$$[X]^* (D) = [X]^* [X] (W) \quad (5.14)$$

The matrix $[X]^* [X]$ is a square matrix which may be inverted to give the solution

$$(W) = [[X]^* [X]]^{-1} [X]^* (D) \quad (5.15)$$

The matrix $[[X]^* [X]]^{-1} [X]^*$ is the Moore Penrose pseudo inverse and solves the original overdetermined system of equation in a least squares sense.

Stability of the transfer function

The spice models are required to operate in the time domain which implies that all transfer functions in the model should be causal and that their impulse response should not diverge as $t \rightarrow \infty$. This implies that all poles of the transfer function $H(s)$ should lie in the left hand side of the s-plane. This condition is not naturally enforced by the method described above however experience has shown that if the function to be fitted is a physically reasonable then the filter fit process will produce a stable model.

Enforcing constraints on the transfer function

It may be the case that the transfer function is subject to constraints. If this is the case then the process may be adapted such that the constraints are naturally enforced. The filter fitting process is applied in a number of different aspects of the model. the filter fit required for the propagation correction function is subject to the constraint that $H(\omega = 0) = 1$. In this case we calculate a model fit to $H'(\omega) = H(\omega) - 1$ where $H'(\omega = 0) = 0$ thus $a'_0 = 0$ for the initial model. Once we have the coefficients for the initial model we can easily calculate the filter coefficients for $H(\omega) = 1 + H'(\omega)$.

Chapter 6

Cable models available

In this section each of the cable types available will be described and any assumptions regarding the specific cable models will be described.

The cable models available are

1. Frequency Dependent Cylindrical conductor with dielectric
2. Frequency Dependent Coaxial cable with transfer impedance and shield surface impedance loss
3. Frequency Dependent Twinax cable with transfer impedance and shield surface impedance loss
4. Frequency Dependent Twisted pair
5. Frequency Dependent Shielded twisted pair with transfer impedance and shield surface impedance loss
6. Frequency Dependent Spacewire with transfer impedance and shield surface impedance loss
7. Frequency Dependent Overshield with transfer impedance and surface impedance loss
8. Frequency Dependent flex cable
9. D connector

For each cable type the method of calculation for the inductance and capacitance matrices for any internal domains will be outlined. The domain decomposition matrices which relate local domain based voltages and currents to global conductor based voltages and currents will be shown. These domain decomposition matrices for cables will be augmented to include an external (reference) conductor which allows the cable to carry a common mode current.

6.1 Frequency Dependent Cylindrical conductor with dielectric

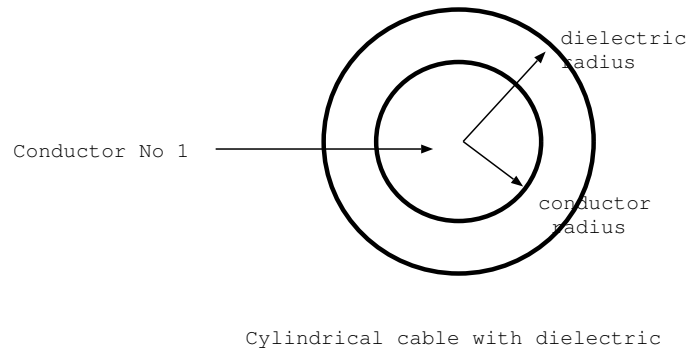


Figure 6.1 Frequency dependent cylindrical conductor with dielectric

The cylindrical conductor has no shielded conductors so no inductance/ capacitance matrix calculation has to be performed for internal domains.

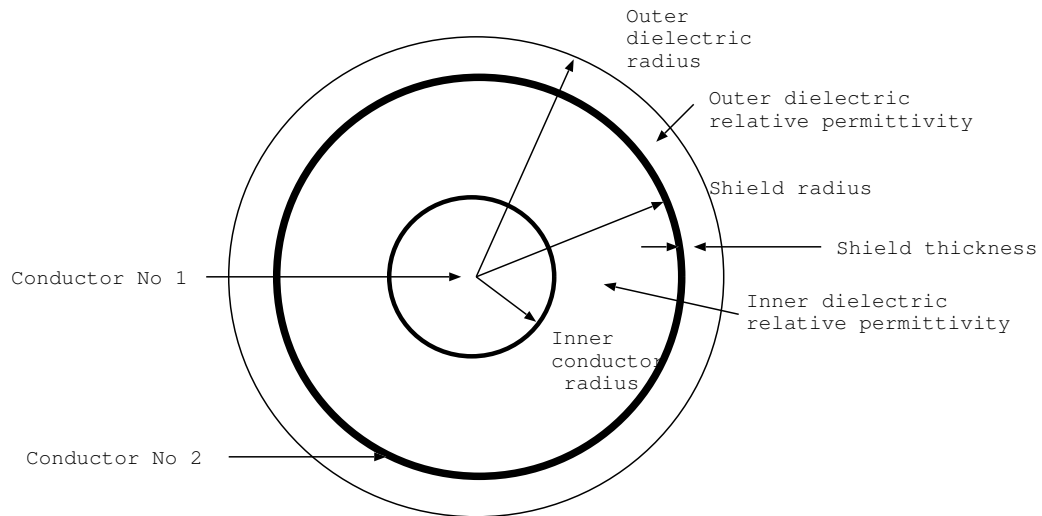
The domain decomposition voltage matrix, M_V for the single conductor is given by

$$\begin{pmatrix} V_{d1.c1} \\ V_{ref} \end{pmatrix} = \begin{bmatrix} 1 & -1 \\ 0 & 1 \end{bmatrix} \begin{pmatrix} V_1 \\ V_0 \end{pmatrix} \quad (6.1)$$

The domain decomposition current matrix, M_I for the single conductor is given by

$$\begin{pmatrix} I_{d1.c1} \\ I_{ref} \end{pmatrix} = \begin{bmatrix} 1 & 0 \\ 1 & 1 \end{bmatrix} \begin{pmatrix} I_1 \\ I_0 \end{pmatrix} \quad (6.2)$$

6.2 Frequency Dependent Coaxial cable with transfer impedance and shield surface impedance loss



Coaxial cable with surface impedance loss

Figure 6.2 Frequency Dependent Coaxial cable - high frequency model including shield surface impedance loss

The coaxial cable has a single internal domain in which a single mode propagates. The inductance and capacitance of the coaxial mode are calculated as

$$L = \frac{\mu_0}{2\pi} \ln \left(\frac{r_s}{r_w} \right) H/m \quad (6.3)$$

$$C(j\omega) = \frac{2\pi\epsilon(j\omega)}{\ln\left(\frac{r_s}{r_w}\right)} F/m \quad (6.4)$$

where r_s is the shield radius, r_w is the inner wire radius and $\epsilon(j\omega)$ is the permittivity of the dielectric filling the space between the shield and the inner wire. This dielectric may be frequency dependent and in this case the capacitance will also be frequency dependent.

The domain decomposition voltage matrix, M_V for the coaxial cable is given by

$$\begin{pmatrix} V_{d1.c1} \\ V_{d2.c1} \\ V_{ref} \end{pmatrix} = \begin{bmatrix} 1 & -1 & 0 \\ 0 & 1 & -1 \\ 0 & 0 & 1 \end{bmatrix} \begin{pmatrix} V_1 \\ V_2 \\ V_0 \end{pmatrix} \quad (6.5)$$

The domain decomposition current matrix, M_I for the coaxial cable is given by

$$\begin{pmatrix} I_{d1.c1} \\ I_{d2.c1} \\ I_{ref} \end{pmatrix} = \begin{bmatrix} 1 & 0 & 0 \\ 1 & 1 & 0 \\ 1 & 1 & 1 \end{bmatrix} \begin{pmatrix} I_1 \\ I_2 \\ I_0 \end{pmatrix} \quad (6.6)$$

6.3 Frequency Dependent Twinax cable with transfer impedance and shield surface impedance loss

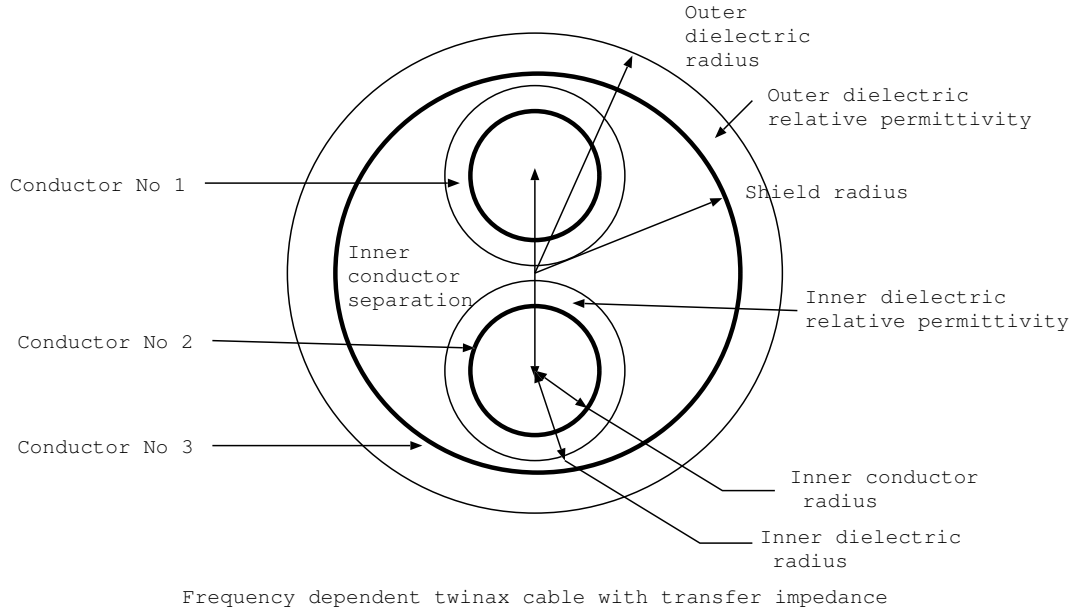


Figure 6.3 Frequency dependent twinaxial cable with transfer impedance - high frequency model including shield surface impedance loss

The twinax cable has a single internal domain in which two modes propagate. The inductance and capacitance matrices for the internal domain are calculated using the Laplace solver.

The domain decomposition voltage matrix, M_V for the twinax cable is given by

$$\begin{pmatrix} V_{d1.c1} \\ V_{d1.c2} \\ V_{d2.c1} \\ V_{ref} \end{pmatrix} = \begin{bmatrix} 1 & 0 & -1 & 0 \\ 0 & 1 & -1 & 0 \\ 0 & 0 & 1 & -1 \\ 0 & 0 & 0 & 1 \end{bmatrix} \begin{pmatrix} V_1 \\ V_2 \\ V_3 \\ V_0 \end{pmatrix} \quad (6.7)$$

The domain decomposition current matrix, M_I for the twinax cable is given by

$$\begin{pmatrix} I_{d1.c1} \\ I_{d1.c2} \\ I_{d2.c1} \\ I_{ref} \end{pmatrix} = \begin{bmatrix} 1 & 0 & 0 & 0 \\ 0 & 1 & 0 & 0 \\ 1 & 1 & 1 & 0 \\ 1 & 1 & 1 & 1 \end{bmatrix} \begin{pmatrix} I_1 \\ I_2 \\ I_3 \\ I_0 \end{pmatrix} \quad (6.8)$$

6.4 Frequency Dependent Twisted pair cable

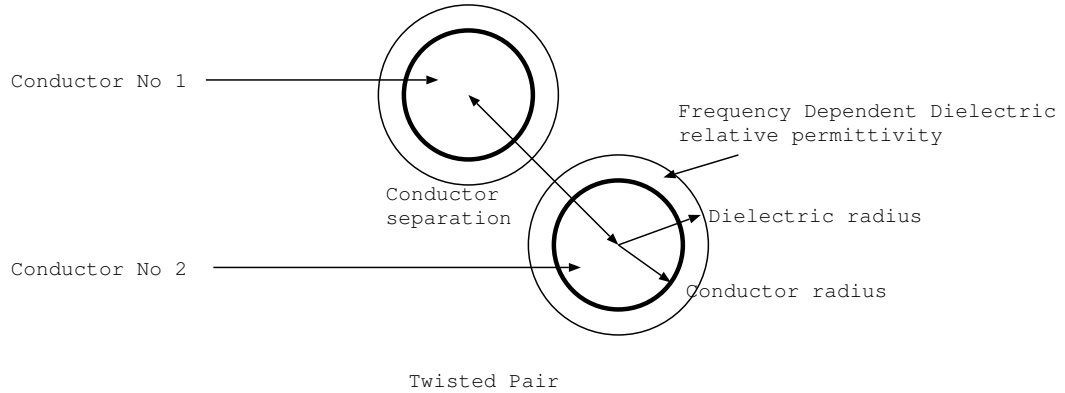


Figure 6.4 Frequency Dependent Twisted pair cable

The twisted pair cable model has a single internal domain in which the differential mode propagates. The inductance and capacitance of the differential mode is calculated for the two conductors in isolation as described in section 3.3.

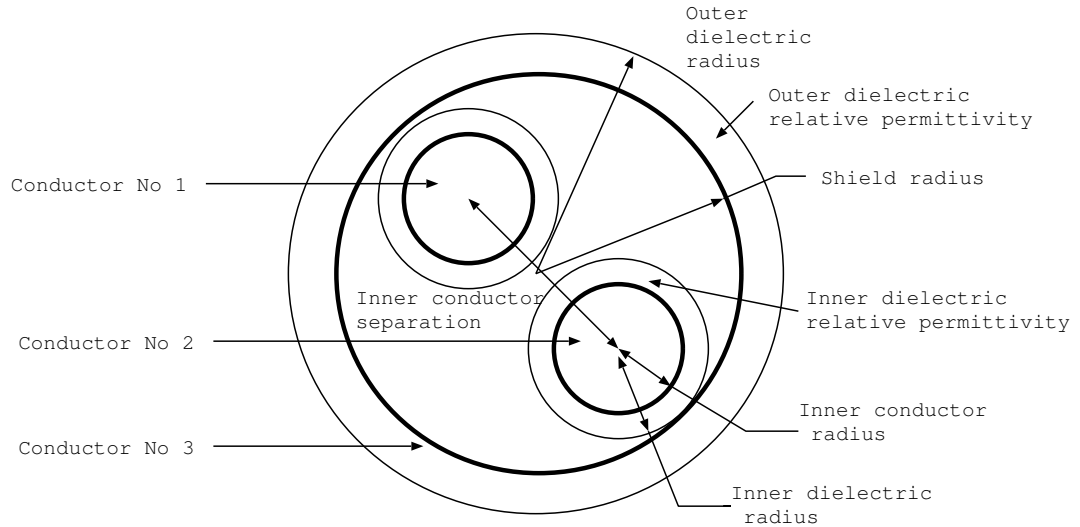
The domain decomposition voltage matrix, M_V for the twisted pair cable is given by

$$\begin{pmatrix} V_{d1.c1} \\ V_{d2.c1} \\ V_{ref} \end{pmatrix} = \begin{bmatrix} 1 & -1 & 0 \\ \frac{1}{2} & \frac{1}{2} & -1 \\ 0 & 0 & 1 \end{bmatrix} \begin{pmatrix} V_1 \\ V_2 \\ V_0 \end{pmatrix} \quad (6.9)$$

The domain decomposition current matrix, M_I for the twisted pair cable is given by

$$\begin{pmatrix} I_{d1.c1} \\ I_{d2.c1} \\ I_{ref} \end{pmatrix} = \begin{bmatrix} \frac{1}{2} & -\frac{1}{2} & 0 \\ 1 & 1 & 0 \\ 1 & 1 & 1 \end{bmatrix} \begin{pmatrix} I_1 \\ I_2 \\ I_0 \end{pmatrix} \quad (6.10)$$

6.5 Frequency Dependent Shielded twisted pair with transfer impedance and shield surface impedance loss



Frequency dependent shielded Twisted Pair with transfer impedance

Figure 6.5 Frequency dependent shielded twisted pair cable with transfer impedance - high frequency model including shield surface impedance loss

The shielded twisted pair cable model has two internal domains, one for the differential mode of the twisted pair and one for the common mode of the twisted pair with the shield as return conductor. The inductance and capacitance matrices for the internal domains are calculated using the Laplace solver as described in section 3.3.

The domain decomposition voltage matrix, M_V for the shielded twisted pair cable is given by

$$\begin{pmatrix} V_{d1.c1} \\ V_{d2.c1} \\ V_{d3.c1} \\ V_{ref} \end{pmatrix} = \begin{bmatrix} 1 & -1 & 0 & 0 \\ \frac{1}{2} & \frac{1}{2} & -1 & 0 \\ 0 & 0 & 1 & -1 \\ 0 & 0 & 0 & 1 \end{bmatrix} \begin{pmatrix} V_1 \\ V_2 \\ V_3 \\ V_0 \end{pmatrix} \quad (6.11)$$

The domain decomposition current matrix, M_I for the shielded twisted pair cable is given by

$$\begin{pmatrix} I_{d1.c1} \\ I_{d2.c1} \\ I_{d3.c1} \\ I_{ref} \end{pmatrix} = \begin{bmatrix} \frac{1}{2} & -\frac{1}{2} & 0 & 0 \\ 1 & 1 & 0 & 0 \\ 1 & 1 & 1 & 0 \\ 1 & 1 & 1 & 1 \end{bmatrix} \begin{pmatrix} I_1 \\ I_2 \\ I_3 \\ I_0 \end{pmatrix} \quad (6.12)$$

6.6 Frequency dependent spacewire with transfer impedance - high frequency model including shield surface impedance loss

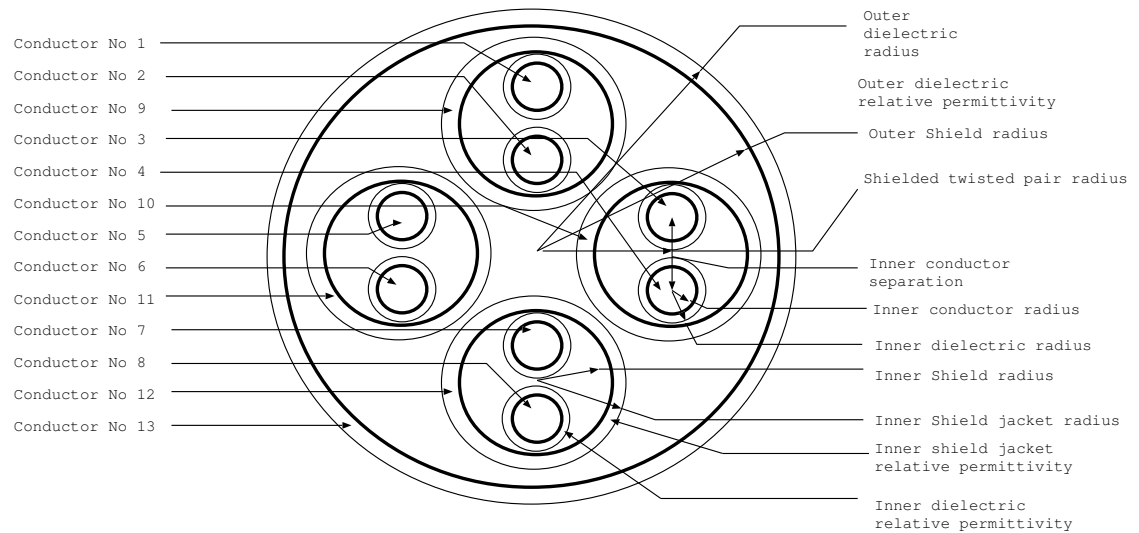


Figure 6.6 Spacewire

Spacewire consists of 13 conductors configured as four shielded twisted pairs within an overshield. There are 5 shields, four surrounding the twisted pairs and the domain consisting of the shields surrounding each of the twisted pairs and the overshield. As each of the shielded twisted pairs is modelled using two domains (differential and common mode for the twisted pair) then there is a total of 9 internal domains in the spacewire model.

The inductance and capacitance for the shielded twisted pair differential and common mode are calculated as for the shielded twisted pair model described in section 6.5. The 4×4 inductance and capacitance matrices for the domain consisting of the twisted pair shields and the overshield are calculated using the Laplace solver.

The domain decomposition voltage matrix, M_V for the spacewire cable is given by

$$\begin{pmatrix} V_{d1.c1} \\ V_{d2.c1} \\ V_{d3.c1} \\ V_{d4.c1} \\ V_{d5.c1} \\ V_{d6.c1} \\ V_{d7.c1} \\ V_{d8.c1} \\ V_{d9.c1} \\ V_{d9.c2} \\ V_{d9.c3} \\ V_{d9.c4} \\ V_{d10.c1} \\ V_{ref} \end{pmatrix} = \begin{bmatrix} 1 & -1 & 0 & 0 & 0 & 0 & 0 & 0 & 0 & 0 & 0 & 0 & 0 & 0 \\ \frac{1}{2} & \frac{1}{2} & 0 & 0 & 0 & 0 & 0 & 0 & -1 & 0 & 0 & 0 & 0 & 0 \\ 0 & 0 & 1 & -1 & 0 & 0 & 0 & 0 & 0 & 0 & 0 & 0 & 0 & 0 \\ 0 & 0 & \frac{1}{2} & \frac{1}{2} & 0 & 0 & 0 & 0 & 0 & -1 & 0 & 0 & 0 & 0 \\ 0 & 0 & 0 & 0 & 1 & -1 & 0 & 0 & 0 & 0 & 0 & 0 & 0 & 0 \\ 0 & 0 & 0 & 0 & \frac{1}{2} & \frac{1}{2} & 0 & 0 & 0 & 0 & -1 & 0 & 0 & 0 \\ 0 & 0 & 0 & 0 & 0 & 0 & 1 & -1 & 0 & 0 & 0 & 0 & 0 & 0 \\ 0 & 0 & 0 & 0 & 0 & 0 & \frac{1}{2} & \frac{1}{2} & 0 & 0 & 0 & -1 & 0 & 0 \\ 0 & 0 & 0 & 0 & 0 & 0 & 0 & 0 & 1 & 0 & 0 & 0 & -1 & 0 \\ 0 & 0 & 0 & 0 & 0 & 0 & 0 & 0 & 0 & 1 & 0 & 0 & -1 & 0 \\ 0 & 0 & 0 & 0 & 0 & 0 & 0 & 0 & 0 & 0 & 1 & 0 & -1 & 0 \\ 0 & 0 & 0 & 0 & 0 & 0 & 0 & 0 & 0 & 0 & 0 & 1 & -1 & 0 \\ 0 & 0 & 0 & 0 & 0 & 0 & 0 & 0 & 0 & 0 & 0 & 0 & 1 & -1 \\ 0 & 0 & 0 & 0 & 0 & 0 & 0 & 0 & 0 & 0 & 0 & 0 & 0 & 1 \end{bmatrix} \begin{pmatrix} V_1 \\ V_2 \\ V_3 \\ V_4 \\ V_5 \\ V_6 \\ V_7 \\ V_8 \\ V_9 \\ V_{10} \\ V_{11} \\ V_{12} \\ V_{13} \\ V_0 \end{pmatrix} \quad (6.13)$$

The domain decomposition voltage matrix, M_I for the spacewire cable is given by

$$\begin{pmatrix} I_{d1.c1} \\ I_{d2.c1} \\ I_{d3.c1} \\ I_{d4.c1} \\ I_{d5.c1} \\ I_{d6.c1} \\ I_{d7.c1} \\ I_{d8.c1} \\ I_{d9.c1} \\ I_{d9.c2} \\ I_{d9.c3} \\ I_{d9.c4} \\ I_{d10.c1} \\ I_{ref} \end{pmatrix} = \begin{bmatrix} \frac{1}{2} & -\frac{1}{2} & 0 & 0 & 0 & 0 & 0 & 0 & 0 & 0 & 0 & 0 & 0 & 0 \\ 1 & 1 & 0 & 0 & 0 & 0 & 0 & 0 & 0 & 0 & 0 & 0 & 0 & 0 \\ 0 & 0 & \frac{1}{2} & -\frac{1}{2} & 0 & 0 & 0 & 0 & 0 & 0 & 0 & 0 & 0 & 0 \\ 0 & 0 & 1 & 1 & 0 & 0 & 0 & 0 & 0 & 0 & 0 & 0 & 0 & 0 \\ 0 & 0 & 0 & 0 & \frac{1}{2} & -\frac{1}{2} & 0 & 0 & 0 & 0 & 0 & 0 & 0 & 0 \\ 0 & 0 & 0 & 0 & 1 & 1 & 0 & 0 & 0 & 0 & 0 & 0 & 0 & 0 \\ 0 & 0 & 0 & 0 & 0 & 0 & \frac{1}{2} & -\frac{1}{2} & 0 & 0 & 0 & 0 & 0 & 0 \\ 0 & 0 & 0 & 0 & 0 & 0 & 1 & 1 & 0 & 0 & 0 & 0 & 0 & 0 \\ 1 & 1 & 0 & 0 & 0 & 0 & 0 & 0 & 1 & 0 & 0 & 0 & 0 & 0 \\ 0 & 0 & 1 & 1 & 0 & 0 & 0 & 0 & 0 & 1 & 0 & 0 & 0 & 0 \\ 0 & 0 & 0 & 0 & 0 & 0 & 0 & 0 & 0 & 0 & 1 & 0 & 0 & 0 \\ 0 & 0 & 0 & 0 & 0 & 0 & 0 & 0 & 0 & 0 & 0 & 1 & 0 & 0 \\ 1 & 1 & 1 & 1 & 1 & 1 & 1 & 1 & 1 & 1 & 1 & 1 & 1 & 0 \\ 1 & 1 & 1 & 1 & 1 & 1 & 1 & 1 & 1 & 1 & 1 & 1 & 1 & 1 \end{bmatrix} \begin{pmatrix} I_1 \\ I_2 \\ I_3 \\ I_4 \\ I_5 \\ I_6 \\ I_7 \\ I_8 \\ I_9 \\ I_{10} \\ I_{11} \\ I_{12} \\ I_{13} \\ I_0 \end{pmatrix} \quad (6.14)$$

6.7 Frequency Dependent Overshield with transfer impedance and surface impedance loss

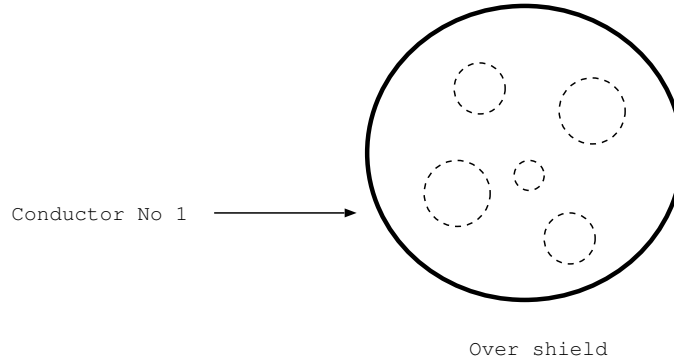


Figure 6.7 Over shield

The overshield is a single conductor which may enclose other conductors within a cable bundle. As the internal conductor structure is not known at the cable model building stage there is no internal domain information at this stage. For the same reason the domain decomposition matrices only describe the external domain. Information relating to any enclosed conductors will be built at the cable bundle building stage.

The domain decomposition voltage matrix, M_V for the overshield is given by

$$\begin{pmatrix} V_{d1.c1} \\ V_{ref} \end{pmatrix} = \begin{bmatrix} 1 & -1 \\ 0 & 1 \end{bmatrix} \begin{pmatrix} V_1 \\ V_0 \end{pmatrix} \quad (6.15)$$

The domain decomposition current matrix, M_I for the overshield is given by

$$\begin{pmatrix} I_{d1.c1} \\ I_{ref} \end{pmatrix} = \begin{bmatrix} 1 & 0 \\ 1 & 1 \end{bmatrix} \begin{pmatrix} I_1 \\ I_0 \end{pmatrix} \quad (6.16)$$

6.8 Flex cable

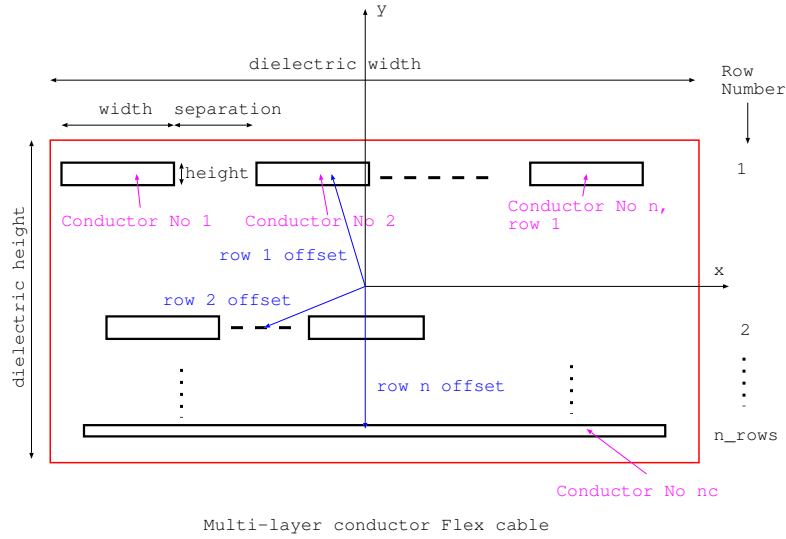


Figure 6.8 flex cable

A flex cable may have an arbitrary number of conductors, N_c . The dimension of the domain decomposition matrices is $N_c + 1$. The domain decomposition voltage matrix, M_V for a flex cable is given by

$$\begin{pmatrix} V_{d1.c1} \\ V_{d1.c2} \\ \vdots \\ V_{d1.cN_c} \\ V_{ref} \end{pmatrix} = \begin{bmatrix} 1 & 0 & \cdots & 0 & -1 \\ 0 & 1 & \cdots & 0 & -1 \\ \vdots & \vdots & \ddots & \vdots & \vdots \\ 0 & 0 & \cdots & 1 & -1 \\ 0 & 0 & \cdots & 0 & 1 \end{bmatrix} \begin{pmatrix} V_1 \\ V_2 \\ \vdots \\ V_{N_c} \\ V_0 \end{pmatrix} \quad (6.17)$$

The domain decomposition current matrix, M_I for a flex cable is given by

$$\begin{pmatrix} I_{d1.c1} \\ I_{d1.c2} \\ \vdots \\ I_{d1.cN_c} \\ I_{ref} \end{pmatrix} = \begin{bmatrix} 1 & 0 & \cdots & 0 & 0 \\ 0 & 1 & \cdots & 0 & 0 \\ \vdots & \vdots & \ddots & \vdots & \vdots \\ 0 & 0 & \cdots & 1 & 0 \\ 1 & 1 & \cdots & 1 & 1 \end{bmatrix} \begin{pmatrix} I_1 \\ I_2 \\ \vdots \\ I_{N_c} \\ I_0 \end{pmatrix} \quad (6.18)$$

6.9 D connector

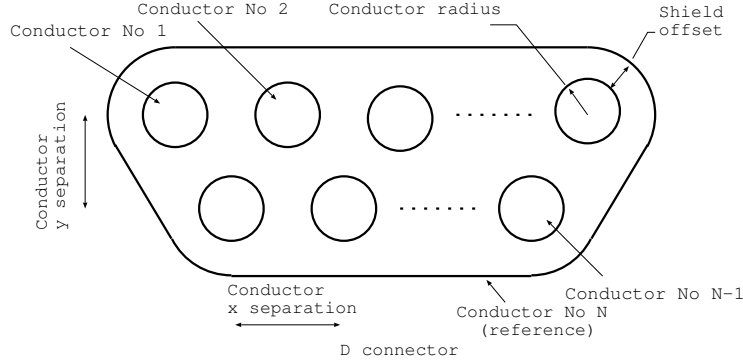


Figure 6.9 D connector

A D connector may have an arbitrary number of conductors, N_c consisting of $N_c - 1$ internal conductor pins and the outer shell.

The internal conductor pins are all shielded by the connector shell therefore there is a single internal domain. The inductance and capacitance matrices for the internal domain are calculated using the Laplace solver.

The dimension of the domain decomposition matrices is $N_c + 1$. The domain decomposition voltage matrix, M_V for a flex cable is given by

$$\begin{pmatrix} V_{d1.c1} \\ V_{d1.c2} \\ \vdots \\ V_{d1.cN_c-1} \\ V_{d2.c1} \\ V_{ref} \end{pmatrix} = \begin{bmatrix} 1 & 0 & \cdots & 0 & -1 & 0 \\ 0 & 1 & \cdots & 0 & -1 & 0 \\ \vdots & \vdots & \ddots & \vdots & \vdots & \vdots \\ 0 & 0 & \cdots & 1 & -1 & 0 \\ 0 & 0 & \cdots & 0 & 1 & -1 \\ 0 & 0 & \cdots & 0 & 0 & 1 \end{bmatrix} \begin{pmatrix} V_1 \\ V_2 \\ \vdots \\ V_{N_c-1} \\ V_{N_c} \\ V_0 \end{pmatrix} \quad (6.19)$$

The domain decomposition voltage matrix, M_I for a flex cable is given by

$$\begin{pmatrix} I_{d1.c1} \\ I_{d1.c2} \\ \vdots \\ I_{d1.cN_c-1} \\ I_{d2.c1} \\ I_{ref} \end{pmatrix} = \begin{bmatrix} 1 & 0 & \cdots & 0 & 0 & 0 \\ 0 & 1 & \cdots & 0 & 0 & 0 \\ \vdots & \vdots & \ddots & \vdots & \vdots & \vdots \\ 0 & 0 & \cdots & 1 & 0 & 0 \\ 0 & 0 & \cdots & 0 & 1 & 0 \\ 1 & 1 & \cdots & 1 & 1 & 1 \end{bmatrix} \begin{pmatrix} I_1 \\ I_2 \\ \vdots \\ I_{N_c-1} \\ I_{N_c} \\ I_0 \end{pmatrix} \quad (6.20)$$

Chapter 7

Network synthesis for specified frequency dependent transfer functions

7.1 Overview

It has been found from experience that Spice models making use of s-domain transfer functions to simulate frequency dependent transfer functions in Spice were susceptible to fail due to convergence problems, especially for transient analysis in Ngspice. An initial investigation of this issue showed that when the s-domain transfer functions were replaced by equivalent passive circuits which implemented the same transfer function, the convergence problems could be eliminated. This initial investigation was limited to first and second order rational functions only, however this observation has led to the development of a general implementation of s-domain transfer functions as passive circuits so that the convergence issues can be mitigated for the general case.

This chapter describes the theory which underlies the modelling of frequency dependent transfer functions as passive circuits in Spice. Frequency dependent transfer functions in this work are represented as rational functions in the laplace variable, s . It is assumed that the rational functions represent stable systems i.e. that their impulse response does not diverge as $t \rightarrow \infty$. This implies that the poles of the transfer function must lie in the left hand side of the s plane.

We consider two types of transfer functions according to their properties

1. Positive-real transfer functions which may be represented as a one port network (simple impedance)
2. non-positive-real transfer functions which may be represented as two port networks

The first type of transfer function arises in this work in the propagation correction functions. The second type may arise in transfer impedance models where the transfer

resistance and/or inductance may be negative at some frequencies.

The form of the transfer functions that we wish to implement as a passive circuit are rational functions as in equation 7.1

$$H(s) = \frac{a_0 + a_1 \left(\frac{s}{\omega_0}\right) + a_2 \left(\frac{s}{\omega_0}\right)^2 + \dots}{b_0 + b_1 \left(\frac{s}{\omega_0}\right) + b_2 \left(\frac{s}{\omega_0}\right)^2 + \dots} \quad (7.1)$$

where ω_0 is a frequency normalisation factor. The methods applied make use of the work of Foster Cauer [14], [15], and Brune [16]. The underlying theory and examples of the techniques outlined here are described in reference [17].

7.2 One port impedance models for positive-real transfer functions

A passive impedance function must be 'positive-real' to constitute a physical impedance which can be synthesised from a network of inductors, capacitors, resistors and transformers. A positive-real rational function is defined by the following conditions:

1. The real part of the function $Z(s)$ must be positive for all $s = \alpha + j\omega, \alpha > 0$
2. The imaginary part of the function $Z(s)$ must be zero for all $s = \alpha + j\omega, \omega = 0$

Positive real rational functions have the following properties:

1. The number of poles and zeros differ by at most 1
2. The coefficients of the rational function are all real and positive
3. The poles and zeros of the function must lie in the left hand side of the s-plane or on the $s = j\omega$ axis
4. If a function $Z(s)$ is positive-real then so is $Y(s) = \frac{1}{Z(s)}$

In this section we describe how an impedance represented as a rational function in s may be synthesised by a passive one port circuit consisting of resistors, inductors, capacitors and transformers i.e. Spice R, L, C and K elements.

Figure 7.1 shows a one port network driven by a current source $I(j\omega)$ whose port voltage is given by $V(j\omega) = Z(j\omega) I(j\omega)$. The impedance can be synthesised as a ladder network as shown in figure 7.2 The impedance of the ladder network may be expressed as the sum of the first series impedance, $Z_1(s)$ and a remainder, $Z_{r1}(s)$ i.e.

$$Z(s) = Z_1(s) + Z_{r1}(s) \quad (7.2)$$

The circuit is shown in figure 7.3 where $Z_1(s)$ is the impedance of a combination of R, L, C, K elements and $Z_{r1}(s)$ is a stable positive real function. The remainder

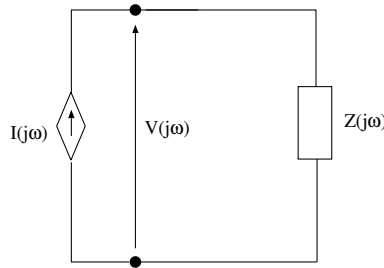


Figure 7.1 One port network model of a positive-real transfer function

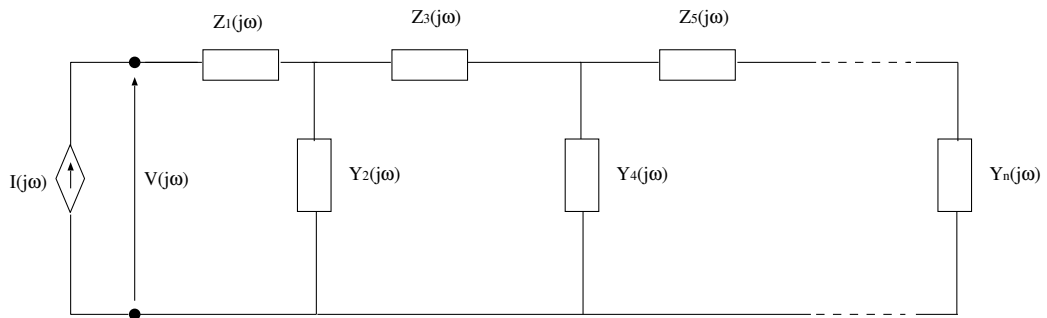


Figure 7.2 Ladder network synthesis of an impedance

impedance, $Z_{r1}(s)$, is then synthesised as the parallel combination of the admittance function $Y_2(s)$ and a remainder, $Y_{r2}(s)$ as seen in figure 7.4

$$Z_{r1}(s) = \frac{1}{Y_2(s) + Y_{r2}(s)} \quad (7.3)$$

thus

$$Z(s) = Z_1(s) + \frac{1}{Y_2(s) + Y_{r2}(s)} \quad (7.4)$$

The admittance $Y_{r2}(s)$ is then synthesised as the sum of two series impedances i.e.

$$Z(s) = Z_1(s) + \frac{1}{Y_2(s) + \frac{1}{Z_3(s) + Z_{r3}(s)}} \quad (7.5)$$

It is seen from this that the impedance function of the ladder network is expressed in a continued fraction form with alternating impedance and admittance terms. The circuit at this third stage is shown in figure 7.5. This synthesis procedure in which admittance and impedance elements of the ladder network are identified in turn continues until the remainder term is reduced to zero. This leads to a relatively straightforward synthesis process for impedance functions.

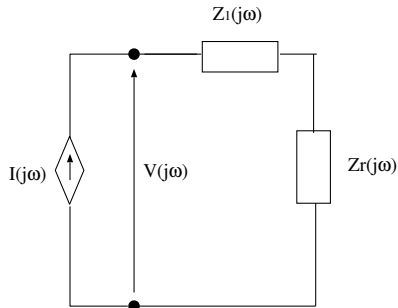


Figure 7.3 Initial stage of ladder network synthesis

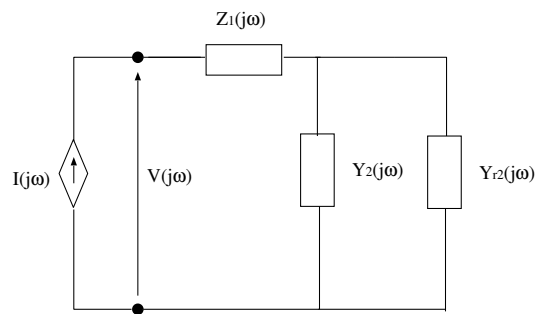


Figure 7.4 Second stage of ladder network synthesis

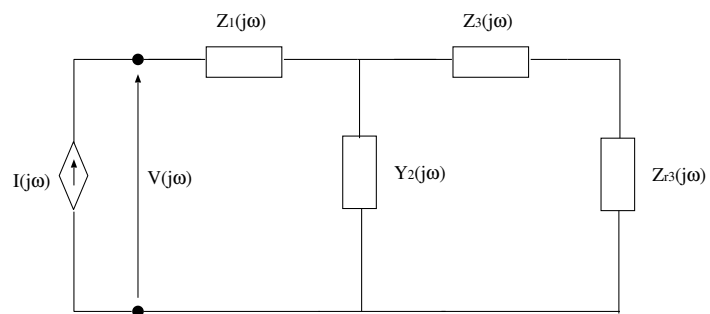


Figure 7.5 Third stage of ladder network synthesis

7.2.1 Algorithm for impedance synthesis

The starting point for the algorithm for impedance synthesis is a rational function in s which must be stable and positive-real. The impedance is synthesised by extracting series impedances and parallel admittances in turn until the remainder is zero. The impedance/ admittance extraction makes use of a pole-residue representation of the transfer function in order to identify branches which are combinations of R, L and C elements. This method can get stuck in that a viable branch cannot be identified while leaving a stable positive-real remainder function. In this case a technique developed by Brune [16] is used to continue the synthesis. Brune's method makes use of transformers (K elements in Spice).

An outline of the algorithm is as follows:

1. Attempt to identify a viable series impedance branch i.e. a branch which may be synthesised with R, L, and C elements and which leaves a remainder $Z_r(s)$ which is stable and positive-real. If a viable branch is found then this process can be repeated until no further viable series impedance branches can be found.
2. Once no further viable series impedance contributions can be found, calculate the admittance $Y_r(s) = 1/Z_r(s)$ and attempt to identify a viable parallel admittance branch i.e. a branch which may be synthesised with R, L, and C K elements and which leaves a remainder $Y_r(s)$ which is stable and positive-real. If a viable branch is found then this process can be repeated until no further viable parallel admittance branches can be found.
3. If no viable series impedance branches or parallel admittance branches can be found then use the Brune synthesis method and implement the resulting circuit with R, L, C and K elements
4. Return to step 1 and repeat until the remainder impedance/ admittance is zero.

7.2.2 Identification of series impedance branches

A viable series impedance branch can be one of the following:

1. RLC branch
2. LC branch
3. RC branch
4. RL branch
5. C branch
6. L branch
7. R branch (which may be identified in two different ways)

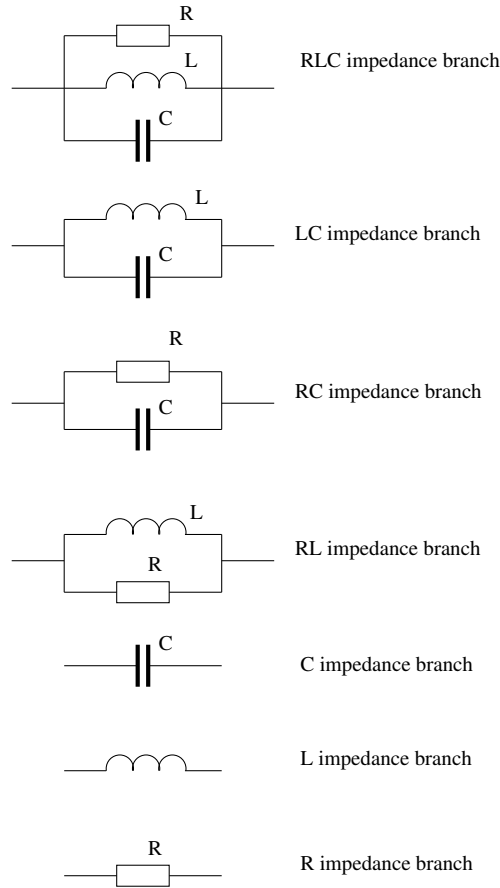


Figure 7.6 Series Impedance Branches

These branches are shown in figure 7.6

Viable branches are found by first forming a pole-residue expansion of the impedance function where poles and their corresponding residues may be real or may be complex conjugate pairs i.e.

$$Z(s) = R + sL + \sum_{i=1}^{n_real_poles} \frac{r_i}{s - p_i} + \sum_{i=1}^{n_complex_pole_pairs} \frac{r_i}{s - p_i} + \frac{r_i^*}{s - p_i^*} \quad (7.6)$$

Then each of the branch types is looked for in the pole-residue expansion in the order of the above list. Each of the following subsections shows how each of the above branch types may be identified from the pole-residue expansion.

RLC impedance branch

The RLC impedance branch has an impedance function which can be expressed in rational function as

$$Z(s) = \frac{\frac{s}{C}}{\frac{1}{LC} + \frac{s}{CR} + s^2} \quad (7.7)$$

This may be expressed in pole-residue form as the complex pole-residue pair

$$Z(s) = \frac{r}{s-p} + \frac{r^*}{s-p^*} = \frac{(rp^* - r^*p) + (r+r^*)s}{pp^* - (p+p^*)s + s^2} \quad (7.8)$$

Where the poles are complex (and not purely imaginary). Equating coefficients of the rational functions a requirement for a viable RLC branch can be established i.e. the numerator constant term is zero:

$$rp^* - r^*p = 0 \quad (7.9)$$

In addition we require that all the component values of the RLC circuit be positive i.e.

$$C = \frac{1}{r+r^*} > 0 \quad (7.10)$$

$$L = \frac{r+r^*}{pp^*} > 0 \quad (7.11)$$

$$R = \frac{r+r^*}{p+p^*} > 0 \quad (7.12)$$

The final requirement is that the remainder function be positive real i.e. the remaining terms of the impedance function describe a physical impedance. If these requirements are satisfied then a RLC branch can be extracted from the impedance function and implemented as an impedance branch in the ladder network.

LC impedance branch

The LC impedance branch has an impedance function which can be expressed in rational function as

$$Z(s) = \frac{\frac{s}{C}}{\frac{1}{LC} + s^2} \quad (7.13)$$

This is a special case of the RLC branch in which $R \rightarrow \infty$ may be expressed in pole-residue form as the complex pole-residue pair

$$Z(s) = \frac{r}{s-p} + \frac{r^*}{s-p^*} = \frac{(rp^* - r^*p) + (r+r^*)s}{pp^* - (p+p^*)s + s^2} \quad (7.14)$$

Where the poles are purely imaginary. Equating coefficients of the rational functions a requirement for a viable LC impedance branch can be established i.e. the poles are imaginary:

$$p^* + p = 0 \quad (7.15)$$

The numerator constant term is zero:

$$rp^* - r^*p = 0 \quad (7.16)$$

In addition we require that all the component values of the LC circuit be positive i.e.

$$C = \frac{1}{r + r^*} > 0 \quad (7.17)$$

$$L = \frac{r + r^*}{pp^*} > 0 \quad (7.18)$$

The final requirement is that the remainder function be positive real i.e. the remaining terms of the impedance function describe a physical impedance. If these requirements are satisfied then an LC branch can be extracted from the impedance function and implemented as an impedance branch in the ladder network.

RC impedance branch

The RC impedance branch has an impedance function which can be expressed in rational function as

$$Z(s) = \frac{\frac{1}{C}}{\frac{1}{RC} + s} \quad (7.19)$$

This may be expressed in pole-residue form as

$$Z(s) = \frac{r}{s - p} \quad (7.20)$$

Where the pole and residue are both real. By equating coefficients of the functions, values of R and C can be identified We require that all the component values of the RC circuit be positive i.e.

$$C = \frac{1}{r} > 0 \quad (7.21)$$

$$R = \frac{-r}{p} > 0 \quad (7.22)$$

The final requirement is that the remainder function be positive real i.e. the remaining terms of the impedance function describe a physical impedance. If these requirements are satisfied then an RC branch can be extracted from the impedance function and implemented as an impedance branch in the ladder network.

RL impedance branch

The RL impedance branch has an impedance function which can be expressed in rational function as

$$Z(s) = \frac{sR}{\frac{R}{L} + s} = R - \frac{\frac{R^2}{L}}{s + \frac{R}{L}} \quad (7.23)$$

This may be expressed in pole-residue form, including a constant term as

$$Z(s) = K + \frac{r}{s - p} \quad (7.24)$$

Where the pole and residue are both real. By equating coefficients of the functions, values of R and L can be identified. We require that all the component values of the RL circuit be positive i.e.

$$R = \frac{r}{p} > 0 \quad (7.25)$$

$$L = \frac{-r}{p^2} > 0 \quad (7.26)$$

The final requirement is that the remainder function be positive real i.e. the remaining terms of the impedance function describe a physical impedance. If these requirements are satisfied then an RL branch can be extracted from the impedance function and implemented as an impedance branch in the ladder network.

Capacitance branch

The capacitance branch has an impedance function which consists of a pole at zero i.e.

$$Z(s) = \frac{1}{sC} \quad (7.27)$$

Thus in the pole-residue expansion we require a pole at zero. In addition we require that capacitance be positive i.e.

$$C = \frac{1}{r} > 0 \quad (7.28)$$

The final requirement is that the remainder function be positive real i.e. the remaining terms of the impedance function describe a physical impedance. If these requirements are satisfied then a capacitance branch can be extracted from the impedance function and implemented as an impedance in the ladder network.

Inductance branch

The inductance branch has an impedance given by

$$Z(s) = sL \quad (7.29)$$

Thus in the pole-residue expansion we require a sL term (pole at infinity in the impedance function) with positive inductance, L. The final requirement is that the remainder function be positive real i.e. the remaining terms of the impedance function describe a physical impedance. If these requirements are satisfied then an inductance branch can be extracted from the impedance function and implemented as an impedance in the ladder network.

Resistance branch, type 1

The resistance branch of type 1 is identified by a positive constant term, R , in the pole-residue expansion of the impedance. If the remainder function is positive real i.e. the remaining terms of the impedance function describe a physical impedance then a resistance branch can be extracted from the impedance function and implemented as an impedance in the ladder network.

Resistance branch, type 2

The resistance branch of type 2 may be found from the rational function form of the impedance i.e. if

$$Z(s) = \frac{a_0 + a_1 \left(\frac{s}{\omega_0}\right) + a_2 \left(\frac{s}{\omega_0}\right)^2 + \dots}{b_0 + b_1 \left(\frac{s}{\omega_0}\right) + b_2 \left(\frac{s}{\omega_0}\right)^2 + \dots} \quad (7.30)$$

then we can calculate the resistance, R as

$$R = \frac{a_0}{b_0} \quad (7.31)$$

as opposed to the pole-residue form whose constant (resistance) term is found as the ratio of the numerator and denominator coefficients of the highest power of s subtracting the resistance as defined in 7.31 results in a remainder impedance function with a pole at infinity. As for all the other branch identification methods, this resistance branch can only be extracted if the remainder impedance is a stable physical impedance function.

7.2.3 Identification of admittance branches

A variable admittance branch can be one of the following combinations:

1. GLC branch
2. LC branch
3. GC branch
4. GL branch
5. C branch
6. L branch
7. G branch (which may be identified in two different ways)

These branches are shown in figure 7.7 and are seen to be the duals of the corresponding impedance branches in figure 7.6. The dual circuits are found by the transformations

$$\begin{aligned}
 Z &\leftrightarrow Y \\
 L &\leftrightarrow C \\
 \frac{1}{C} &\leftrightarrow \frac{1}{L} \\
 R &\leftrightarrow G
 \end{aligned}
 \tag{7.32}$$

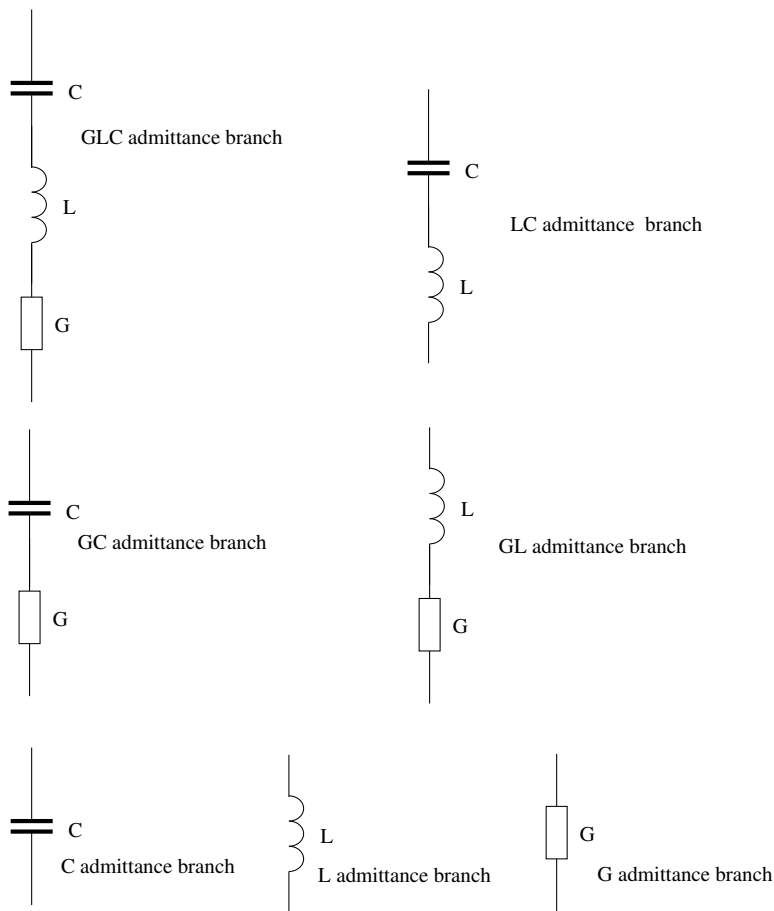


Figure 7.7 Parallel Admittance Branches

The admittance branches are found in the same way as for the series impedance branches i.e. viable branches are found by first forming a pole-residue expansion of the admittance function where poles and their corresponding residues may be real or

may be complex conjugate pairs i.e.

$$Y(s) = G + sC + \sum_{i=1}^{n_real_poles} \frac{r_i}{s - p_i} + \sum_{i=1}^{n_complex_pole_pairs} \frac{r_i}{s - p_i} + \frac{r_i^*}{s - p_i^*} \quad (7.33)$$

For completeness a brief summary of the admittance branch identification processes is given here. The admittances may have inductance, capacitance or conductance though a non-zero conductance is implemented as a resistance $R = \frac{1}{G}$ in Spice.

GCL admittance branch

The GCL admittance branch has an admittance function which can be expressed in rational function as

$$Y(s) = \frac{\frac{s}{L}}{\frac{1}{CL} + \frac{s}{LG} + s^2} \quad (7.34)$$

This may be expressed in pole-residue form as the complex pole-residue pair

$$Y(s) = \frac{r}{s - p} + \frac{r^*}{s - p^*} = \frac{(rp^* - r^*p) + (r + r^*)s}{pp^* - (p + p^*)s + s^2} \quad (7.35)$$

The poles are complex (and not purely imaginary). Equating coefficients of the rational functions a requirement for a viable GCL admittance branch can be established i.e. the numerator constant term is zero:

$$rp^* - r^*p = 0 \quad (7.36)$$

In addition we require that all the component values of the GCL circuit be positive i.e.

$$L = \frac{1}{r + r^*} > 0 \quad (7.37)$$

$$C = \frac{r + r^*}{pp^*} > 0 \quad (7.38)$$

$$G = \frac{r + r^*}{p + p^*} > 0 \quad (7.39)$$

The final requirement is that the remainder function be positive real i.e. the remaining terms of the admittance function describe a physical admittance. If these requirements are satisfied then a GCL branch can be extracted from the admittance function and implemented as an admittance branch in the ladder network.

LC admittance branch

The LC admittance branch has an admittance function which can be expressed in rational function as

$$Y(s) = \frac{\frac{s}{L}}{\frac{1}{CL} + s^2} \quad (7.40)$$

This is a special case of the GCL branch in which $G \rightarrow \infty$ ($R \rightarrow 0$) may be expressed in pole-residue form as the complex pole-residue pair

$$Y(s) = \frac{r}{s-p} + \frac{r^*}{s-p^*} = \frac{(rp^* - r^*p) + (r+r^*)s}{pp^* - (p+p^*)s + s^2} \quad (7.41)$$

Where the poles are purely imaginary. Equating coefficients of the rational functions a requirement for a viable LC admittance branch can be established i.e. the poles are imaginary:

$$p^* + p = 0 \quad (7.42)$$

The numerator constant term is zero:

$$rp^* - r^*p = 0 \quad (7.43)$$

In addition we require that all the component values of the LC circuit be positive i.e.

$$L = \frac{1}{r+r^*} > 0 \quad (7.44)$$

$$C = \frac{r+r^*}{pp^*} > 0 \quad (7.45)$$

The final requirement is that the remainder function be positive real i.e. the remaining terms of the admittance function describe a physical admittance. If these requirements are satisfied then an LC branch can be extracted from the admittance function and implemented as an admittance branch in the ladder network.

GL admittance branch

The GL admittance branch has an admittance function which can be expressed in rational function as

$$Y(s) = \frac{\frac{1}{L}}{\frac{1}{GL} + s} \quad (7.46)$$

This may be expressed in pole-residue form as

$$Y(s) = \frac{r}{s-p} \quad (7.47)$$

Where the pole and residue are both real. By equating coefficients of the functions, values of G and L can be identified We require that the component values of the GL circuit be positive i.e.

$$L = \frac{1}{r} > 0 \quad (7.48)$$

$$G = \frac{-r}{p} > 0 \quad (7.49)$$

The final requirement is that the remainder function be positive real i.e. the remaining terms of the admittance function describe a physical admittance. If these requirements are satisfied then a GL branch can be extracted from the admittance function and implemented as an admittance branch in the ladder network.

GC admittance branch

The GC admittance branch has an admittance function which can be expressed in rational function as

$$Y(s) = \frac{sG}{\frac{G}{C} + s} = G - \frac{\frac{G^2}{C}}{s + \frac{G}{C}} \quad (7.50)$$

This may be expressed in pole-residue form, including a constant term as

$$Y(s) = K + \frac{r}{s - p} \quad (7.51)$$

Where the pole and residue are both real. By equating coefficients of the functions, values of G and C can be identified. We require that all the component values of the series GC circuit be positive i.e.

$$G = \frac{r}{p} > 0 \quad (7.52)$$

$$C = \frac{-r}{p^2} > 0 \quad (7.53)$$

The final requirement is that the remainder function be positive real i.e. the remaining terms of the admittance function describe a physical admittance. If these requirements are satisfied then a GC branch can be extracted from the admittance function and implemented as an admittance branch in the ladder network.

Inductance branch

The inductance branch has an admittance function which consists of a pole at zero i.e.

$$Y(s) = \frac{1}{sL} \quad (7.54)$$

Thus in the pole-residue expansion we require a pole at zero. In addition we require that inductance be positive i.e.

$$L = \frac{1}{r} > 0 \quad (7.55)$$

The final requirement is that the remainder function be positive real i.e. the remaining terms of the admittance function describe a physical admittance. If these requirements are satisfied then an inductance branch can be extracted from the admittance function and implemented as an admittance in the ladder network.

Capacitance branch

The capacitance branch has an admittance given by

$$Y(s) = sC \quad (7.56)$$

Thus in the pole-residue expansion we require a sC term (pole at infinity in the admittance function) with positive capacitance, C. The final requirement is that the remainder

function be positive real i.e. the remaining terms of the admittance function describe a physical admittance. If these requirements are satisfied then a capacitance branch can be extracted from the admittance function and implemented as an admittance in the ladder network.

Conductance (Resistance) branch, type 1

The conductance branch of type 1 is identified by a positive constant term, G , in the pole-residue expansion of the admittance. If the remainder function is positive real i.e. the remaining terms of the admittance function describe a physical admittance then a resistance branch can be extracted from the admittance function and implemented as an admittance in the ladder network.

Conductance (Resistance) branch, type 2

The conductance branch of type 2 may be found from the rational function form of the admittance i.e. if

$$Y(s) = \frac{a_0 + a_1 \left(\frac{s}{\omega_0}\right) + a_2 \left(\frac{s}{\omega_0}\right)^2 + \dots}{b_0 + b_1 \left(\frac{s}{\omega_0}\right) + b_2 \left(\frac{s}{\omega_0}\right)^2 + \dots} \quad (7.57)$$

then we can calculate the conductance, G as

$$G = \frac{a_0}{b_0} \quad (7.58)$$

7.2.4 Brune Synthesis

There are circumstances when the ladder network synthesis procedure described above fails i.e. a physical impedance/ admittance function results for which no viable series impedance or parallel admittance branch can be found. In this case the method described by Brune [16] may be applied to allow the process to proceed. Brune's method involves the use of a transformer which can be included in Spice simulations using the K element. The basic process is described here however the associated proofs of the properties of the functions at each stage will not be given. For further details see references [16] and [17].

The ladder network synthesis procedure ensures that poles at zero, poles at infinity, zeros at infinity, zeros at zero, poles on the $s = \pm j\omega$ axis and zeros on the $s = \pm j\omega$ axis have been removed from the impedance function. Brune's method then operates on this remainder function, $Z_r(s)$, as follows:

Stage 1. Find ω_0 such that the real part of the impedance $Z_r(s = j\omega_0)$ is a minimum. The minimum resistance value at this frequency is R_{min} .

Stage 2. Subtract R_{min} from $Z_r(s)$ to give the minimum resistance impedance function

$$Z_1(s) = Z_r(s) - R_{min} \quad (7.59)$$

i.e. R_{min} is extracted as a series resistance.

The function $Z_1(s)$ is now purely reactive at ω_0 i.e. $Z_1(\omega_0) = jX$. This reactance is set to be the reactance of an inductor, L_A where $L_A = \frac{X}{\omega_0}$. Note that this inductance may be negative.

This series inductance is subtracted from $Z_1(s)$ to give

$$Z_2(s) = Z_1(s) - sL_A \quad (7.60)$$

$Z_2(s)$ has a zero of order 2 at $s = j\omega_0$ and we can write the admittance $Y_2(s) = \frac{1}{Z_2(s)}$ as

$$Y_2(s) = \frac{1}{Z_1(s) - sL_A} = \frac{\alpha}{s^2 + \omega_0^2} + Y_3(s) \quad (7.61)$$

From this we can identify a LC admittance branch where $L_B = \frac{1}{\alpha}$ and $C_B = \frac{1}{\omega_0^2 L_B}$

The remainder impedance $Z_3(s) = \frac{1}{Y_3(s)}$ after subtraction of the LC admittance branch has a first order pole at infinity and therefore a series inductance can be extracted i.e.

$$Z_r(s) = Z_3(s) - sL_C \quad (7.62)$$

where L_C is negative if L_A is positive and vice versa. In addition to this it can be shown that the remainder impedance, $Z_r(s)$ is positive-real.

This series of component identification leads to the circuit shown in figure 7.8 however this is not a physical circuit in that one of the series inductors L_A or L_B is negative.

The three inductances may be combined into two positive inductors with a mutual inductance term as seen in figure 7.9. In this circuit the component values can be shown to be

$$\begin{aligned} L_1 &= L_A + L_B \\ L_2 &= L_C + L_B \\ K &= 1 \end{aligned} \tag{7.63}$$

The inductances in the final Brune synthesis circuit are all positive and may therefore be simulated in Spice using L, C R and K elements. Since the remainder impedance is positive-real, the ladder network synthesis procedure can proceed.

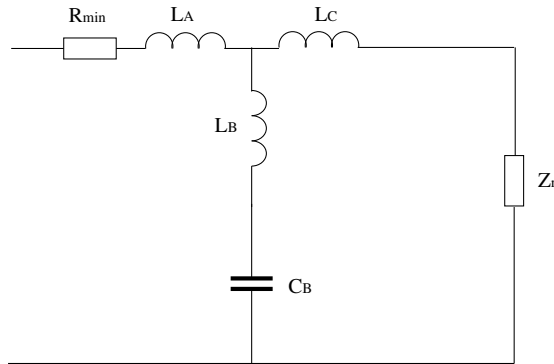


Figure 7.8 Initial Brune Synthesis Circuit

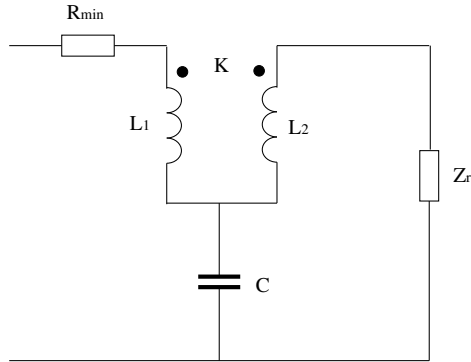


Figure 7.9 Final Brune Synthesis Circuit

7.3 Synthesis of non-positive real transfer functions

The process for one port synthesis requires that the impedance transfer function is a positive-real function. It may be the case that we need to synthesise a transfer function

which does not have this property. If this is the case then we can proceed by writing the transfer function as the difference between two positive real functions i.e.

$$Z_T(s) = Z_{T1} - Z_{T2} \quad (7.64)$$

Each of the positive-real impedances may be synthesised by using the one port network synthesis process described in the previous section. The final transfer function may then be implemented in spice as seen in figure 7.10. It can be seen that the non-positive-real function may be found as $V(j\omega)$ where

$$V(j\omega) = I(j\omega) (Z_{T1} - Z_{T2}) \quad (7.65)$$

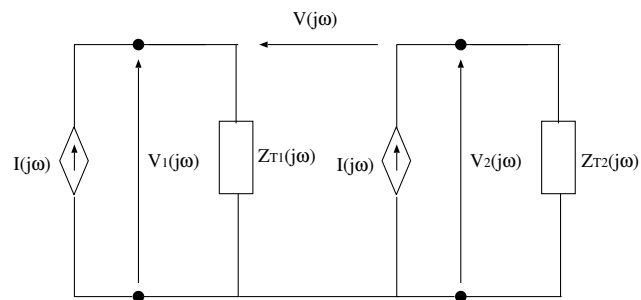


Figure 7.10 Synthesis of non-positive-real transfer functions

7.4 Application of the network synthesis in Spice cable bundle models

The Spice cable bundle models require the use of frequency domain transfer functions for the implementation of the propagation correction and for the transfer impedance coupling model. The propagation correction is expected to be a positive-real function as it represents the loss and dispersion in the modal propagation thus it will be implemented using a single port impedance. The transfer impedance functions however may have negative transfer resistance and/or inductance at certain frequencies and will therefore require a two port model for its implementation.

Bibliography

- [1] C. Smartt, D.W.P. Thomas, S. Greedy, J. Verpoorte, J. Lansink Rotgerink *SACAMOS User Guide*
- [2] C.R. Paul, *Analysis of Multi-conductor Transmission Lines*, Second edition, John Wiley & Sons, 2008, ISBN 978-0-470-13154-1.
- [3] A.K. Agrawal, H.J. Price, S.H. Gurbaxani, *Transient Response of Multiconductor Transmission Lines Excited by a Nonuniform Electromagnetic Field*, IEEE Trans EMC, Vol 22, No 2, pp 119-129, 1980.
- [4] B.K.P. Scaife, *Principles of Dielectrics*, Oxford University Press, 1998
- [5] S.A. Schelkunoff, *The Electromagnetic Theory of Coaxial Transmission Lines and Cylindrical Shields*, Bell System Technical Journal, Vol 13, No 4, pp 532-579, 1934.
- [6] C.R. Paul, *A SPICE Model for Multiconductor Transmission Lines Excited by an Incident Electromagnetic Field*, IEEE Trans EMC, Vol 36, No 4, pp 342-354, 1994.
- [7] H. Xie, J. Wang, R. Fan, Y. Liu, *SPICE Models to Analyze Radiated and Conducted Susceptibilities of Shielded Coaxial Cables*, IEEE Trans EMC, Vol 52, No 1, pp 215-222, 2010.
- [8] J-M Jin, *The Finite Element Method in Electromagnetics* 3rd Edition, John Wiley & sons 2014.
- [9] W.H. Press, S.A. Teukolsky, W. T. Vetterling, B. P. Flannery *Numerical Recipes in C* Second Edition, Cambridge University Press, 1992.
- [10] Q. Chen, A. Konrad, *A Review of Finite Element Open Boundary Techniques for Static and Quasi-Static Electromagnetic Field Problems*, IEEE Transactions on Magnetism, Vol.33, No 1, January 1997
- [11] E.O. Brigham, *The Fast Fourier Transform and its Applications*, Prentice Hall, 1988.
- [12] <http://www.netlib.org/eispack/>

- [13] J.F. Dawson, J.A. Cole, S.J. Porter, *Modelling of transmission and reflection of thin layers for EMC applications in TLM*. 10th international conference on EMC, 1997, pp65-70.
- [14] W. Cauer *Synthesis of Linear Communication Networks* vols 1 and 2, 2nd ed. McGraw-Hill New York, 1958.
- [15] R. M. Foster *A reactance Theorem* Bell System Tech. J, vol 3 1924, pp 259-267
- [16] O. Brune, *Synthesis of a finite two-terminal network whose driving-point impedance is a prescribed function of frequency* J. of Math. Phys., Vol 10, 1931, pp 191-236.
- [17] D. C. Youla *Theory and Synthesis of Linear Time-Invariant Networks* Cambridge University Press, 2015.